Università degli Studi di Padova
Dipartimento di Fisica e Astronomia
"Galileo Galilei"

Density instabilities in multi-layer dipolar Fermi gases

Studente:
Callegari Michele

Relatore:
Prof. L. Salasnich
(Università degli Studi di Padova)

Correlatore:
Prof.ssa F. M. Marchetti
(Universidad Autonoma de Madrid)

Anno Accademico 2013/2014

Fletto i muscoli e sono nel vuoto
(A. Plazzi, L. Ortolani)

Abstract

In this thesis we are going to study instabilities of the density in various geometries of a 2D single-component dipolar Fermi gas. Due to the anisotropic, partially repulsive and partially attractive interactions between dipoles, in order to describe appropriately the system instabilities it is strictly necessary to account for correct correlations between particles. The well-known Random Phase Approximation completely neglects exchange correlations, thus describing only partially the actually rich phase diagram of dipolar Fermi gases. After a critique to the RPA, we introduce local field corrections by mean of the local field factor $G(q)$, and then we present a scheme proposed in 1968 by Singwi, Tosi, Land and Sjölander (STLS) which is intended to compute the local field factor in a simple, self-consistent and physically motivated way. We focus here on the transition to what is known as stripe phase, precisely the one which is shown to be led by exchange interactions, thus completely neglected by the RPA. We study the properties of single- and bi-layers geometries, hence extending to multiple-layers geometries the previous framework. Finally, within a first neighbour approximation, we try and extend to $(N \to \infty)$-layers geometry our study.

Contents

Introduction

Extraordinary progresses in physics and technology of the last years have stimulated the investigation in ultracold gases, and in turn, the investigation has enhanced technology in this sense. In particular, experimental success in trapping and cooling polar atoms and molecules has attracted huge interest in the study of quantum gases of particles with high electric and magnetic dipolar moments. The dipole-dipole interaction is an anisotropic and long-range interaction, which exhibits both attractive and repulsive parts: All features that make new exotic phases have to be expected. Other fundamental steps forward have been achieved in the control of the short-range interactions via Feshbach resonances. Futhermore, the strength of the dipolar interaction itself can be modified and controlled as we will see in the secon chapter of this thesis.

If we examinate the dipolar potential, it is clear that two dipoles aligned head-to-toe feel an attractive force, whereas in the parallel side-by-side configurations they will repulse each other. It is not difficult to imagine that the attractive part of the interaction could lead to instabilities of the system. Moreover, many chemical polar species are highly reactive, thus leading to unstable system because of losses due to chemical reactions. A relatively simple way to stabilise dipolar quantum gases consists in lower their dimensionality by confining them into pancake-like geometries, and keep them aligned via external fields. This is why we are interested in 2D geometries.

Another relevant part of the discussion considers the quantum nature of interactions in ultracold gases, i.e. in this case we can no more take into account only the correlations due to the Coulomb or, specifically, dipolar potential, we need also to consider, in order to get a good description of the system, the exchange correlations. So that a fundamental role is played by the pair correlation function, which should enters the equations that describe e.g. the dielectric properties of the system or system instabilities. Decisive improvements in this direction have been given by Singwi, Tosi, Land and Sjölander in 1968 and 1970 by mean of a series of articles entitled "Electron correlations at metallic densities", in which the pair correlation function gives rise to an additional term in the effective field felt by a single electron embedded in an electron gas, hence introducing a new screened effective potential including exchange correlations. Their work provides a self-consistent set of equations that allow to estimate the local field factor, that not only goes far beyond the RPA, by including exchange in the expression of the susceptibility, but also refines the Hubbard approximation, which excludes from $G(q)$ the corrections to the correlation hole. The STLS method has been for a long time, till the advent of Quantum MonteCarlo simulations, one of the more accurate framework in condensed matter physics [1].

This thesis is articulated as follows: In Chapter 1 we recall schematically the linear response theory, thus introducing basic quantities such as the response function (or susceptibility), the static structure factor and so on, then we illustrate the RPA as a mean field theory, adducing some successful (or less) example of its results and a critique about its limits. Then, by mean of the stiffness theorem, we introduce the local field factor, and explain by the very same words of the STLS scheme authors, providing a comparison with other approximations.

In chapter 2 we analise in details the properties of the dipolar interactions and to some extent the scattering properties of fermions at low temperatures. We illustrate a significant method to control the scattering length, that is by using Feshbach resonances, and we underline a fundamental aspect of dipoles i.e. the tunability of the interaction strength. Finally, we present the properties of the dipole-dipole interaction in 2D geometries.

In chapter 3 the study of dipolar fermi gases begins. Actually, one must decide whether the simple RPA is sufficient or not in order to accurately describe the properties of such quantum fluids. A few calculations demonstrate that neither in the long wave length limit nor for small inter-particle separations (either taking into account of the natural cut-off provided by the thickness of the layer) the random phase approximation could lead to acceptable results. Then, we study the phase diagram of a dipolar quantum gas obtained for single-layer and bi-layers geometries as in Ref. [23] and [24] respectively, and we reproduce results for a particular phase transition, while showing that a simplified STLS scheme can describe the phase boundary in an equally effective way. Finally, we calculate for the first time the phase shift of the wave-density modulation between two layers in a classical background.

In chapter 4, finally, the study is extended to more complex systems, namely to many-layers geometries. We apply the simplified STLS scheme and show how the $\phi = 0$ stripe phase, the peculiar phase we are studying, for small layers separations overwhelms other phases by occupying almost all the phase diagram. Then we analise some asymptotic behaviour of the pancake-like system, especially as a function of the distance between layers and of their number. In the end, we try and diagonalise the inverse of the susceptibility matrix in the first neighbours approximation, in order to get a further simplified algorithm and therefore obtain the phase diagram for an infinity-layers geometry, which may be useful in the study of real systems having layered structures and anistotropic interactions.

CHAPTER 1

DENSITY MODULATIONS IN FERMIONIC SYSTEMS

In this first chapter we are going to illustrate the introductory material and basic tools that will be needed later. We first are going to introduce the basic concepts about the linear response theory, in general terms, and then focus more specifically on its application to the study of density instabilities. Later in this chapter we will introduce the Random Phase Approximation (RPA) scheme and further developments aimed at improving this approximation by adjusting the effects of interaction correlations. this scheme will be applied all the thesis wide, allowing us to obtain informations over the phase diagram of dipolar Fermi gases.

Let's have a insight about the linear response theory.

1.1. Linear response theory

What is a system's response to a small perturbation acting on it? In many cases it is possible to expand the perturbation and obtain the response to the *first*-order: The linear response theory describes the (linearized) response of a system to a small perturbation acting on it. Let us begin with an introductory example, by considering a system in his ground state; if, as a consequence of a perturbation, the unperturbed mean value of a quantity $\hat{B}$ is varying of an amount b, the foundamental energy results to be varied in this manner:

$$E(b) \simeq E_0 + \frac{\alpha_b}{2} b^2$$

where α_b stands for the second derivative of the enrergy with respect to b: this parameter is a measure of the stiffness provided by the system to small modifications of the average value of the quantity $\hat{B}$. The second term in this expression is referred to as "stifness energy". We now apply to the system an external field linearly coupled to the quantity $\hat{B}$ and such that the coupling energy is of the type εb, where ε is positive and can be made arbitrarily small. In this situation the energy acquires the form

$$E_\varepsilon \simeq E_0 + \frac{\alpha_b}{2} b^2 + \varepsilon b$$

so that at the equilibrium we have

$$b_{eq} = -\frac{\varepsilon}{\alpha_b}$$

which corresponds to the new ground-state energy:

$$E_\varepsilon(b_{eq}) \simeq E_0 + \frac{\varepsilon^2}{2\alpha_b}.$$

This implies that the linear coupling leads to a new ground-state of lower total energy, in which the average value of the quantity $\hat{B}$ deviates from its original

value by an amount directly proportional to the strength of the coupling (a linear response) and inversely proportional to the corresponding stiffness α_b. The *linear response function* is thus defined as the following limit:

$$\chi_{bb} = \lim_{\varepsilon \to 0} \frac{b_{eq}}{\varepsilon} = -\frac{1}{\alpha_b},$$

a relation showing the simple connection between the response function and the stifness. Also important is the expression for the stiffness energy, which can be written, in a quite general manner, as follows:

$$\delta E = -\frac{b_{eq}^2}{2\chi_{bb}}. \tag{1.1.1}$$

This last equation is the result of the *stiffness theorem*.

Even if very simple, this example leads to a fundamental property of the susceptibility, i.e. that it ought to be non positive, a condition more generally known as *foundamental condition of stability*:

$$\chi_{bb} \leq 0;$$

clearly this request is due to the fact that a system is stable only if it lays in an energy minimum, so that a perturbation whatever can only increase its energy.

1.1.1. Generalisations and response functions. In this section we will schematically show the foundamental definitions of the linear response theory. First of all we must discuss the meaning of *response* and then we must state what is *linear* and what is not. A system, when stimulated with an external perturbation $F(t)$, will react and emit, under an appropriate form, an observable output signal $R(t)$ that we will call *response*. A possible formulation of the conditions for $F(t)$ and $R(t)$ to suite the *linearity* is sketched below:

(1) *Stationarity:* Let $F(t) = f(t)$ and $R(t) = r(t)$. Then $F(t) = f(t + \delta t)$ implies $R(t) = r(t + \delta t)$. This condition is always valid if in the system hamiltonian there are no time dependent potentials, i.e. if the hamiltonian is conservative.

(2) *Linearity:* the following two conditions guarantee the linearity of the system response:

$$a) \qquad [F(t) \to R(t)] \Rightarrow [\lambda F(t) \to \lambda R(t)]$$

$$b) \qquad F(t) = \lambda_1 f_1(t) + \lambda_2 f_2(t) \to R(t) = \lambda_1 r_1(t) + \lambda_2 r_2(t)$$

(3) *Causality:* The implication

$$F(t) = 0 \Rightarrow R(t) = 0$$

defines the casuality of the response as a consequece of the perturbation.

The most general relationship between perturbation and response, that satisfies the above conditions (1-3), is given by:

$$R(t) = \int_{-\infty}^{t} \phi(t - t') F(t')\, dt'$$

which implicitly defines the *response function* $\phi(t-t')$. In the limit $t \to \infty$ this relation defines a convolution. Note that the stationarity requirement implies that the response function depends on time differences.

In general, if we are studying an observable $\hat{B}$, the response $R(t)$ is given by the ensemble average of the deviation $\langle \hat{\Delta B}(t) \rangle = \langle \hat{B}(t) \rangle - \langle \hat{B} \rangle$ of the observable $\hat{B}$ from the equilibrium value, and the perturbation $F(t)$ is the external force $f(t)$ which perturbs the system. In full generality, the external force is supposed to be coupled to a variable $\hat{A}$ that does not necessarily coincide with the observable $\hat{B}$ weare studying. The validity of the linear response theory is restricted, as stressed at the beginning of this section, to the range in which $f(t)$ is weak enough to ensure that $\langle \hat{B}(t) \rangle$ varies linearly with the force.

Under the influence of the perturbation, the full hamiltonian reads as:

$$H = H_0 + H_1$$

where[1]

$$H_1 = -\hat{A} f(t),$$

and H_0 is the unperturbed hamiltonian.

While the density operator of the unperturbed system reads as:

$$\rho_0 = \frac{1}{Z} e^{-\beta H_0}, \qquad Z = \mathrm{Tr}\left\{ e^{-\beta H_0} \right\}$$

we define the density operator of the full system as $\rho(t)$, and ensemble averages over an operator $\hat{B}$ read as

$$\langle \hat{B}(t) \rangle = \mathrm{Tr}\left\{ \rho(t) \hat{B} \right\}.$$

The linear response then can be rewritten as

$$\langle \hat{B}(t) \rangle - \langle \hat{B} \rangle = \int_{-\infty}^{t} \phi_{BA}(t-t') f(t')\, dt' \tag{1.1.2}$$

thus making it clear that $\rho(t \to -\infty) = \rho_0$ and that the causality can be included in the response function by requiring

$$\phi_{BA}(t-t') = 0 \qquad \text{for} \quad t' > t.$$

The latter condition allows the extension to the limit $t \to \infty$ of the above integral and, if

$$\lim_{\varepsilon \to 0^+} \int_0^{\infty} |\phi_{BA}(t)|\, e^{-\varepsilon t}\, dt < \infty$$

holds, the system is *stable* under the effect of the perturbation.

Let us consider a perturbation acting on a system during a time interval τ, and suppose that it is switched off at time t_1: Then, given $t > t_1$, if

$$\lim_{t \to \infty} \langle \hat{B}(t) \rangle - \langle \hat{B} \rangle = 0.$$

we can talk of *dissipation*, i.e. there are non-conservative forces in the system. Actually, dissipation implies a rapid decay of the response function with time, so the last statement immediatly requires the validity of the stability condition.

[1] In the following we let drop the obvious circumflex accents but for the two observables $\hat{A}$ and $\hat{B}$, in order to simplify notation and visualise immediately the perturbation-coupled variable and the response-coupled one.

Causality and stability prevents the Laplace transform of the response function to be ill-defined, and we can take some advantage from the frequency representation, in fact, let $z \in \mathbb{C}$: The function

$$\chi_{AB}(z) = \int_0^\infty \phi_{BA}(t) e^{izt}\, dt$$

is an analitic function in the upper complex plane. Then, if we define the Fourier transform

$$\left\langle \hat{B}(\omega) \right\rangle = \lim_{\varepsilon \to 0^+} \int_{-\infty}^{\infty} \left(\left\langle \hat{B}(t) \right\rangle - \left\langle \hat{B} \right\rangle \right) e^{-\varepsilon t} e^{i\omega t}\, dt,$$

where the factor $e^{-\varepsilon t}$ is needed in order to compensate the adiabatic switching on of the perturbation (which is necessary in order to obtain a uniquely determined evolution of the system), the equation (1.1.2) can be written

$$\left\langle \hat{B}(\omega) \right\rangle = \chi_{BA}(\omega) \tilde{f}(\omega)$$

where the *generalized susceptibility* $\chi_{BA}(\omega)$ is defined via

$$\chi_{BA}(\omega) = \lim_{\eta \to 0^+} \chi_{BA}(z = \omega + i\eta)$$

and $\tilde{f}(\omega)$ is the usual Fourier transform of the perturbation $f(t)$. Thus it is clearly convenient to work in the reciprocal (frequencies) space rather than in the direct space.

The same regularity in the upper complex plane allows to define a relation between the real and the imaginary part of the generalized susceptibility, called *Kramer-Kronig relation*

$$\chi_{BA}(\omega) = \frac{1}{i\pi} \mathcal{P} \int_{-\infty}^{\infty} \frac{\chi_{BA}(\omega')}{\omega' - \omega}\, d\omega'. \tag{1.1.3}$$

The real part χ' and the imaginary part χ'' of the response function are called respectively *reactive* and *absorptive* part, so that

$$\chi_{BA}(z) = \chi'_{BA}(z) + i\chi''_{BA}(z)$$

Static linear response. We are now looking for an answer to the question "how does the system react when perturbed?" in the contest of quantum sstatistical mechanics. Thus one can try and see whether the system reaches an equilibrium state when a perturbation $F(t)$ is acting on it or not, taking into account the time dependence of ρ due to the new term H_1 in the Hamiltonian. The partition function is the following:

$$Z = \mathrm{Tr}\left\{ e^{-\beta(H_0 + H_1)} \right\} = \mathrm{Tr}\left\{ e^{-\beta(H_0 - \hat{A} f(t))} \right\}$$

and the equilibrium density operator reads as:

$$\rho_{\mathrm{Eq}} = \frac{1}{Z} e^{-\beta(H_0 - \hat{A} f(t))}.$$

Actually in this specific case we can omit the time dependence in $f(t)$, and simply write f instead. In the classic limit, the above expression could be expanded till the first order in f, yelding

$$\rho_{\mathrm{Eq}} = \rho_0 \cdot \left(1 + \beta f \left(\hat{A} - \left\langle \hat{A} \right\rangle_0\right)\right) + \mathcal{O}(f^2)$$

and immediately

$$\left\langle \hat{B} \right\rangle_f = \mathrm{Tr}\left\{ \hat{B}\rho_{\mathrm{Eq}} \right\} = \left\langle \hat{B} \right\rangle_0 + \beta f \left[\left\langle \hat{A}\hat{B} \right\rangle_0 - \left\langle \hat{A} \right\rangle_0 \left\langle \hat{B} \right\rangle_0 \right] + \mathcal{O}(f^2),$$

where it is possible to recognize, once assumed $\left\langle \hat{A} \right\rangle_0 = 0$, the static susceptibility

$$\chi_{BA} = \beta \left\langle \hat{A}\hat{B} \right\rangle_0 .$$

Note that the circumflex accent has been preserved in order to have a direct comparison with the quantistic case; an observable in classical mechanic is not an operator, indeed; here it could possibly only suggest that the observable are thought as they were "acting" to a microscopic state of the system

In the quantistic case the expansion we have done is not possible if the two observables are not compatible. The Japanese physicist Kubo (in japanese 久保) has then find a way to escape from this problem, defining the Kubo transform of an observable $\hat{A}$ as

$$\hat{A}_K(\beta) = \frac{1}{\beta} \int_0^\beta \hat{A}_I(i\hbar\lambda)\, d\lambda$$

where $\hat{A}_I$ stands for the observable $\hat{A}$ in interaction picture. With this transform and thancks to the properties of the Laplace transform, the static response function writes identically in form as the classic, where the Kubo transform of $\hat{A}$:

$$\chi_{BA} = \beta \left\langle \hat{A}_K \hat{B} \right\rangle_0 .$$

Dynamic linear response. Here the dynamical evolution of the dendity operator has to be considered. A very effective way to find out the response function is to make use of the interaction picture. In this framework the equation of motion for the density operator is given by

$$\frac{d}{dt}\rho_I = -\frac{i}{\hbar} e^{iH_0 t/\hbar} \left[H_1, \rho(t) \right] e^{-iH_0 t/\hbar}$$

and because of the lineary of H_1 in $f(t)$, we may replace $\rho(t)$ by ρ_0, giving

$$\frac{d}{dt}\rho_I \simeq \frac{i}{\hbar} \left[\hat{A}_I(t), \rho_0 \right] f(t).$$

The solution of the equation of motion give us the time dependent density operator

$$\rho(t) = \rho_0 + \frac{i}{\hbar} \int_{-\infty}^{t} \left[\hat{A}_I(t-t'), \rho_0 \right] f(t')\, dt'$$

so, because we remind that the aspectation value of an observable is given by the trace over all the microscopic states of the system weigthed with the density operator, it is a simple substitution which finally lead to the expression

$$\left\langle \hat{B}(t) \right\rangle - \left\langle \hat{B} \right\rangle = \frac{i}{\hbar} \int_{-\infty}^{t} \left\langle \left[\hat{B}_I(t), \hat{A}_I \right] \right\rangle_0 f(t')\, dt'$$

and a comparison with equation (1.1.2) finally allows us to achieve the result named *the Kubo formula*:

$$\phi_{BA}(t-t') = \frac{i}{\hbar} \theta(t-t') \left\langle \left[\hat{B}(t), \hat{A}(t') \right] \right\rangle_0 ; \tag{1.1.4}$$

notice that the common notation suppresses the index 0, and we will adecuate our notation in the following.

The part

$$K_{BA}(t) = \frac{i}{\hbar}\left\langle\left[\hat{B}(t), \hat{A}\right]\right\rangle = \left\langle\left[\hat{B}, \hat{A}(-t)\right]\right\rangle$$

is also called a response function, and it is connected in an obvious way with $\phi_{BA}(t)$. The inverse of K_{BA} determines the response $\left\langle\hat{A}(t)\right\rangle$ caused by $H_1 = -f(t)\hat{B}$. The point is that K_{BA} and its inverse are in the following relationship:

$$K_{AB}(t) = \frac{i}{\hbar}\left\langle\left[\hat{A}(t), \hat{B}\right]\right\rangle = -K_{BA}(-t).$$

□ We open now a classical parenthesis in the discussion, in order to introduce some basic concept that will be useful later to better understand the fluctuation-dissipation theorem.

The Kubo formula express its relevance in the so called Onsager regression of fluctuation: The formula, in fact, is in relationship with the connected average which definition is

$$\langle XY\rangle_c = \langle XY\rangle - \langle X\rangle\langle Y\rangle .$$

Including this definition, one can express the response (1.1.2) as

$$\langle B(t)\rangle - \langle B\rangle \equiv \langle \Delta B(t)\rangle = \beta f \langle A(0)B(t)\rangle_{0c} .$$

In this last expression the *connected correlation function* appears

$$C_{AB}(t) = \langle A(0)B(t)\rangle_{0c} ,$$

which time derivative yields to the classical Kubo formula for the susceptibility:

$$\phi_{AB}(t) = -\beta\theta(t)\dot{C}_{AB}(t).$$

This result can be explicitly derived through a procedure called *regression protocol* (not demonstrated here), which consists in switching off abruptly the external perturbation, that was alive since $t = -\infty$, and then observe the system while it is allowed to relax back to equilibrium.

Let for a moment $B = A$: Then

$$\langle \Delta A(t)\rangle = \beta f \langle A(t)A(0)\rangle_{0c} = \beta f \langle \delta A(t)\delta A(0)\rangle_{0c}$$

where $\delta A(t)$ symbolise the fluctuation near the unperturbed average value of A at the time t. Then the connected correlation function is expected to give full correlation when $t = 0$, and zero correlation for $t \to \infty$, namely:

$$C_{AA}(0) = \left\langle \delta A^2(0)\right\rangle_0 \qquad C_{AA}(t\to\infty) = \langle\delta A(0)\rangle_0 \langle\delta A(t\to\infty)\rangle_0 .$$

The second expression is zero because we expect $\langle\delta A(0)\rangle_0 = \langle\delta A(t\to\infty)\rangle_0 = 0$. In general, the time law is

$$C_{AA}(t) \simeq C_{AA}(0)e^{-\frac{|t|}{\tau_A}},$$

where τ_A is the relaxation time of the observable A.

One can only conclude that *"if a system is, at time t_0 , out of equilibrium, it is impossible to know if this off-equilibrium state is the result of an external perturbation or of a spontanoues fluctuation. The relaxation of the system back to equilibrium will be the same for the two cases (assuming that the original deviation from equilibrium is small enough)."* (Onsager 1931)

The quantistic expression which include the connected average is obtained via the Kubo transform:

$$\left\langle \hat{\Delta B}(t) \right\rangle = f \int_{-\infty}^{\beta} \left\langle \hat{A}_I(i\hbar\lambda)\hat{B}(t) \right\rangle_{0c} d\lambda.$$

□

A further important relation is:

$$\kappa_{BA}(z) = 2i\chi''_{BA}(z) \tag{1.1.5}$$

in which appear the appropiate (i.e. such that it is analytic in the upper complex plane) Laplace transform $\kappa_{BA}(z)$ of $K_{BA}(t)$.

Before going on introducing other interesting and useful quantities, we should mention that the Kubo formula can be expressed in matrix form. The density operator will be expressed as

$$\hat{\rho}_0 = \sum_n |n\rangle \langle n| w_n$$

where the weigth w_n is the probability associated at the n^{th} state; in a canonical ensemble

$$w_n = \frac{1}{Z} e^{-\beta E_n}.$$

Some simple algebra will give

$$\phi_{BA}(t) = \frac{i}{\hbar}\theta(t) \sum_{n,l} (w_n - w_l) A_{nl} B_{ln} e^{i\frac{(E_n - E_l)}{\hbar}t}. \tag{1.1.6}$$

1.1.2. Structure factor and fluctuation-dissipation theorem. There is a strong relation between the time correlation of fluctuations and the absorption (or dissipation). In order to identify the relation, we define the dinamic correlation function

$$s_{BA}(t) \equiv \left\langle \hat{B}(t)\hat{A} \right\rangle - \left\langle \hat{B} \right\rangle \left\langle \hat{A} \right\rangle = \left\langle \hat{B}\hat{A}(-t) \right\rangle - \left\langle \hat{B} \right\rangle \left\langle \hat{A} \right\rangle.$$

Notice that it is identical to C_{BA} previously used, but here the average is *not* explicitly in the equilibrium state.

Thus it can be immediately identified the relation

$$K_{BA}(t) = \frac{i}{\hbar} \left[s_{AB}(t) - s_{AB}(-t) \right]. \tag{1.1.7}$$

A noticeable property of $s(t)$ is the following (it can be readily derived from the cyclic property of the trace and regarding $\hat{B}$ in the interaction picture):

$$s_{BA}(t) = s_{AB}(-t - i\hbar\beta).$$

As C_{BA} does, s_{BA} vanishes in the limit of infinite time and non-infinite temperature. From the Fourier transform of the above property we can extract the *condition of detailed balance*:

$$S_{BA}(\omega) = e^{\beta\hbar\omega} S_{AB}(-\omega).$$

Including the property (1.1.7) of K_{AB} and its Laplace transform (1.1.5) in the detailed balance condition, we finally get the *fluctuation-dissipation theorem*

$$S_{BA}(\omega) = 2\hbar \frac{1}{1 - e^{-\beta\hbar\omega}} \chi''_{BA}(\omega). \tag{1.1.8}$$

It is now self-evident the connection between the spontaneous fluctuations of the system and its power absorption. Moreover the fluctuation-dissipation theorem relates, even more evidenty, the relation between fluctuation and response function.

In perticular, let $B = A^\dagger$: For $\omega > 0$, $S_{A^\dagger A}(\omega)$ gives the absorption spectrum at a frequency ω, and for $\omega < 0$ it gives the stimulated emission spectrum (from which the name "detailed balance", that relates incoming and outgoing power in the system).

$S_{BA}(\omega)$ is known as *dinamical structure factor* as well, and take the attribute *static* in the $\omega \to 0$ limit. It strongly recalls the structure factor we know from optic: the dinamic correlation function can in fact describe the scattering properties of the system.

1.1.3. Multiple coupling. Since we are in a linear approximation, the perturbation(s) will appear in the hamiltonian as a sum of linear terms of coupling between the external perturbations and their associated observable:

$$H_1(t) = -\int \hat{\mathbf{A}}(\mathbf{r}) \cdot \mathbf{f}(\mathbf{r}, t)\, d\mathbf{r}.$$

From previous theory, we know that the response writes:

$$\left\langle \hat{A}_i(\mathbf{r}, t) \right\rangle = 2i \int_{-\infty}^{t} dt' \int \chi''_{A_i A_j}(\mathbf{r}, \mathbf{r}', t - t') f_j(\mathbf{r}', t')\, d\mathbf{r}'$$

where the sum over repeated indexes is understood and

$$\chi''_{A_i A_j}(\mathbf{r}, \mathbf{r}', t - t') = \frac{1}{2\hbar} \left\langle \left[\hat{A}_i(\mathbf{r}, t), \hat{A}_j(\mathbf{r}', t') \right] \right\rangle_0 .$$

A little work can demonstrate that the fluctuation dissipation theory is still valid in the identical form as the previous, and writes as follows:

$$\chi''_{A_i A_j}(\mathbf{k}, \omega) = \frac{1}{2\hbar} \left(1 - e^{-\beta\hbar\omega} \right) S_{A_i A_j},$$

so that the whole previous theory still applies even in this case. In particular a new feature arises, i.e. one can demonstrate that the response factor is a tensor (and this is the characteristic allowing us to extend in a such direct manner the theory from one observable to many coupled observables).

1.1.4. Sum-Rules. Sum-rules are identities that connect the moments of the absorption spectrum distribution to ground state averages of observables.

An example of application of a sum rule is the expression of the relationship between energy levels transitions and transition amplitudes: By meaning of this sum rule we can express in a simple form the sum of transition amplitudes *[Sanwu Wang, Generalization of the Thomas-Reiche-Kuhn and the Bethe sum rules, Physical Review A 60, 262 (1999). http://prola.aps.org/abstract/PRA/v60/i1/p262_1].*

Sum rules are derived from the Kramer Kronig relation, showed in equation (1.1.3): We start from expanding in series of ω powers the denominator in the integral in the high-frequency limit

$$\frac{1}{\omega' - \omega} = -\sum_{k=0}^{\infty} \frac{\omega'^k}{\omega^{k+1}}.$$

For hermitian observables, the integrals containing even powers vanish and the high-frequency expansion of Kramers-Kronig relation can be written

$$\chi'_{BA}(\omega) = \sum_k \frac{M^{(2k+1)}}{\omega^{2k+2}}$$

where

$$M^{(2k+1)} = -\frac{2}{\pi}\int_0^\infty \omega^{2k+1}\chi''_{BA}(\omega)\,d\omega.$$

The conclusion follows on-the-fly by including the Kubo formula (1.1.4) and the relation (1.1.5) in the series expansion, giving

$$\chi'_{BA}(\omega) = \frac{i}{\hbar}\sum_k (-1)^k \frac{\left\langle \left[\hat{A}^{(2k+1)}, \hat{B}\right]\right\rangle_0}{\omega^{2k+2}}$$

which connect any odd moment of the spectrum to the equilibrium expectation value of an equal-time Green function.

1.2. Density response

The linear response theory, previously formulated in general terms, is here applied to the case of density perturbations.

1.2.1. The density-density response function. The density-density response function describes the response of the expectation value of the number density operator

$$\hat{n}(\mathbf{r}) = \sum_i \delta(\mathbf{r} - \mathbf{r}'_i)$$

at a point $\mathbf{r}$ to a potential $V_{\text{ext}}(\mathbf{r}', t)$ that couples linearly to the density. We will look for the response of a system, actually its density modulation, to an external perturbation, in the context of the linear response theory. From the definition (1.1.2) one gets:

$$\delta n(\mathbf{r}, t) = \int_0^\infty d\tau \int d\mathbf{r}'\, \phi_{nn}(\mathbf{r}, \mathbf{r}', \tau) V_{\text{ext}}(\mathbf{r}', t - \tau).$$

Without loss of generality, we start considering the case of a perturbation periodic in time:

$$V_{\text{ext}}(\mathbf{r}', t) = \frac{1}{L^d}\tilde{V}_{\text{ext}}(\mathbf{q}', \omega)e^{i(\mathbf{q}'\cdot\mathbf{r}' - \omega t)} + c.c.;$$

a sostitution in the previous definition will give

$$\delta n(\mathbf{r}, t) = \frac{1}{L^d}\sum_{\mathbf{q}} \tilde{\delta n}(\mathbf{q}, \omega)e^{i(\mathbf{q}'\cdot\mathbf{r}' - \omega t)} + c.c. \tag{1.2.1}$$

with

$$\tilde{\delta n}(\mathbf{q}, \omega) = \chi_{nn}(\mathbf{q}, \mathbf{q}', \omega)\tilde{V}_{\text{ext}}(\mathbf{q}', \omega), \tag{1.2.2}$$

so obtaining as the response function the Fourier transform of ϕ_{nn}. Another completely equivalent way to write the response function in the reciprocal space is

$$\chi_{nn}(\mathbf{q}, \mathbf{q}', \omega) = \frac{1}{L^d}\chi_{n_{\mathbf{q}} n_{-\mathbf{q}'}}(\omega).$$

An important point which must be stressed is that in general a perturbation with wavevector $\mathbf{q}'$ induces a density modulation at all the wavevectors $\mathbf{q} \neq 0$ for which

$\chi_{nn}(\mathbf{q}, \mathbf{q}', \omega) \neq 0$. In the case of homogeneous systems this property simplifies and we are left with

$$\chi_{nn}(\mathbf{q}, \mathbf{q}', \omega) = \chi_{nn}(\mathbf{q}, \omega)\delta_{\mathbf{q},\mathbf{q}'}.$$

Finally if we are dealing with spatially periodic structures, the susceptibility is non zero only if the exited density fluctuations differs from the momentum of the incident perturbation by a reciprocal lattice vector $\mathbf{G}$, namely

$$\chi_{nn}(\mathbf{q}, \mathbf{q}', \omega) = \chi_{nn}(\mathbf{k} + \mathbf{G}, \mathbf{k} + \mathbf{G}', \omega).$$

1.2.2. The density structure factor. It is *the* structure factor. We have already talked about the role of the structure factor in the linear response theory.

First, let us talk about the dynamic structure factor: It can be defined in a slightly different - but completely equivalent - manner with respect to the definition we gave before in the chapter:

$$S_{AA^\dagger}(\omega) = \sum_{nm} w_m \left|A_{mn}\right|^2 \delta(\omega - \omega_{mn}),$$

this definition, for the observable density, reads

$$S(\mathbf{q}, \omega) = S_{n_\mathbf{q} n_{-\mathbf{q}}}(\omega) = \sum_{nm} w_m \left|(\hat{n}_\mathbf{q})_{mn}\right|^2 \delta(\omega - \omega_{mn}),$$

from which the symmetry properties immediatly follow:

$$S(-\mathbf{q}, \omega) = S(\mathbf{q}, \omega).$$

Both the detailed balance condition and the fluctuation dissipation theorem are valid, and in particular we underline that the detailed balance condition writes

$$S(\mathbf{q}, -\omega) = e^{-\beta\hbar\omega} S(\mathbf{q}, \omega).$$

The static structure factor, instead, is *not* the dynamic one in the limit $\omega \to 0$, but is defined as

$$S(\mathbf{q}) = \frac{1}{N} \int_{\mathbb{R}} S(\mathbf{q}, \omega)\, d\omega,$$

where N is the total number of particles in the system.

The static structure factor is in strong relationship with another important quantity, whose origin will be briefly discussed later (§ 1.3.2): the pair correlation function $\mathbf{g}(r)$. In an isotropic and homogeneous system of identical *fermions*, we define

$$\mathbf{g}\left(|\mathbf{r}_1 - \mathbf{r}_2|\right) = \frac{1}{n^2} \left\langle \psi^\dagger(\mathbf{r}_2)\psi^\dagger(\mathbf{r}_1)\psi(\mathbf{r}_1)\psi(\mathbf{r}_2) \right\rangle.$$

It is a matter of facts that the relation joining the two quantities is the following:

$$S(q) = 1 + n \int \left[\mathbf{g}(r) - 1\right] e^{-i\mathbf{r}\cdot\mathbf{q}}\, d\mathbf{r}$$

and this, together with the anticommutation rules for fermions, yield the following expression for the static structure factor:

$$S(q) = \frac{1}{N} \left\langle \hat{n}_\mathbf{q} \hat{n}_{-\mathbf{q}} \right\rangle - N\delta_{\mathbf{q},0}.$$

1.2.3. The compressibility sum rule. It is possible to draw out a fundamental relationship between the proper compressibility and the static density-density response function. From Kramer-Kronig relations (1.1.3) we note that the static density-density response function $\chi_{nn}(\mathbf{q},0)$ of an homogeneous fermion liquid in the long wavelength limit is associated with the first negative moment of $\chi''_{nn}(\mathbf{q},\omega)$: This is why we call (with a slight abuse: *see* § 1.1.4) a sum rule the connection between the susceptibility and the compressibility of the system.

In order to find the relation, consider an electron liquid which density reads as

$$n(\mathbf{r}) = n(1+\gamma\cos(\mathbf{q}\cdot\mathbf{r})),$$

where $\gamma \ll 1$. From equation (1.1.1) we can get the variation in the equilibrium energy when the system suffers the presence of a perturbation, in this case represented by the small periodic density inhomogeneity. Physical considerations indicate that the excess of energy in the long wavelength limit $q \to 0$ consists of two contributions: the electrostatic energy

$$\delta E_{\text{el}} = N\frac{nv_q}{4}\gamma^2$$

(actually valid for each q) and the kinetic plus exchange-correlation energy

$$\delta E_{\text{loc}} = \int [n(\mathbf{r})\varepsilon(n(\mathbf{r})) - n\varepsilon(n)]\, d\mathbf{r} \underset{q\to 0}{\simeq} N\frac{n\gamma^2}{4}\frac{\partial^2}{\partial n^2}n\varepsilon(n).$$

In the above expressions N is the total number of particles and $\varepsilon(n(\mathbf{r}))$ represents the energy of the homogeneous jellium model. The inverse of the sum of the two finally gives the relation we were looking for:

$$\lim_{q\to 0}\frac{\chi_{nn}(\mathbf{q},0)}{1+v_q\chi_{nn}(\mathbf{q},0)} = \frac{1}{\frac{\partial^2[n\varepsilon(n)]}{\partial n^2}} = -n^2K. \tag{1.2.3}$$

It makes sense now to define two *proper* quantities, which appear quietly in the previous expression: They are the proper density-density response function

$$\tilde{\chi}_{nn}(\mathbf{q},\omega) = \frac{\chi_{nn}(\mathbf{q},\omega)}{1+v_q\chi_{nn}(\mathbf{q},\omega)}$$

and the proper compressibility K. We use the attribute "proper" because, as a matter of fact, these quantities are concerned with an interacting system, i.e. the particles merged in the system feel interaction and external potentials as screened potentials, because of the presence of the other particles. So proper recalls that the system is properly described by a complete interaction. Indeed the proper susceptibility can be implicitly defined through

$$n_1(\mathbf{r},\omega) = \int \tilde{\chi}_{nn}(\mathbf{r},\mathbf{r}',\omega)V_{\text{sc}}(\mathbf{r}',\omega)\, d\mathbf{r}'$$

where n_1 is the response of the density to the screened potential V_{sc}.

1.3. Free electrons

In the last section we just mention the screened potential, talking about a proper response function. In fact, to calculate a response function of systems such as electron gases or more generally interacting fermion gases is extremely difficult. The only susceptibility one can calculate exactly is that of non-interacting fermions.

For the sake of simplicity and for concreteness we choose here to explain briefly what is known for a system of non-interacting electrons. We will use the second quantization formalism, i.e. each operator will be understood to be in the form

$$\hat{A} = \sum_{\alpha\beta} A_{\alpha\beta} \hat{a}^\dagger_\alpha \hat{a}_\beta$$

with $a^{(\dagger)}_\alpha$ distruction (creation) operators.

So the problem now is to find the response of a system of free electrons, which Hamiltonian writes

$$\hat{H}_0 = \sum_{\alpha\beta} \varepsilon_\alpha \hat{a}^\dagger_\alpha \hat{a}_\alpha,$$

to an external perturbation that coples linearly to an observable $\hat{B}$. So the perturbed Hamiltonian will reads as

$$\hat{H}_{0F} = \hat{H}_0 - F(t)\hat{B}.$$

Making use of equation (1.1.6) one readily gets for the response function (we will use the same symbol χ both for the response function and its Fourier transform):

$$\chi^{(0)}_{AB}(t) = -\frac{i}{\hbar}\theta(t) \sum_{\alpha\beta\gamma\delta} A_{\alpha\beta} B_{\gamma\delta} e^{i\frac{(\varepsilon_\alpha - \varepsilon_\beta)}{\hbar}t} \left\langle \left[\hat{a}^\dagger_\alpha \hat{a}_\beta, \hat{a}^\dagger_\gamma \hat{a}_\delta \right] \right\rangle_0,$$

and by mean of the Wick's theorem, introducing the Fermi-Dirac average occupation number n_λ of the λ^{th}-state.

$$\chi^{(0)}_{AB}(t) = -\frac{i}{\hbar}\theta(t) \sum_{\alpha\beta\gamma\delta} A_{\alpha\beta} B_{\gamma\delta} e^{i\frac{(\varepsilon_\alpha - \varepsilon_\beta)}{\hbar}t} (n_\alpha - n_\beta)$$

which Fourier transform with respect to time is

$$\chi^{(0)}_{AB}(\omega) = \sum_{\alpha\beta} \frac{A_{\alpha\beta} B_{\gamma\delta} (n_\alpha - n_\beta)}{\hbar\omega + \varepsilon_\alpha - \varepsilon_\beta + i\hbar\eta}.$$

We have demonstrated that it is possible to obtain straightforwardly an expression for the susceptibility of a non-interacting system of fermions. Now, we are interestred in the response of the system to density fluctuations, then we want to calculate the density-density response function. All we need is the explicit expression of the numeric density operator, but this is not a real difficulty, because we can assume that the particles are point-like and the density then is expressed like a delta:

$$\hat{n}(\mathbf{r}) = \sum_i \delta(\mathbf{r} - \mathbf{r}_i)$$

whose Fourier transform is

$$n_{\mathbf{q}} = \sum_i e^{-i\mathbf{q}\cdot\mathbf{r}_i}.$$

Using the Kubo formula Eqn. (1.1.4), we see that the only components we are interested in are

$$\left(n_{\pm\mathbf{q}}\right)_{\mathbf{k}\sigma,\mathbf{k}'\sigma'} = \delta_{\mathbf{k},\mathbf{k}'-\mathbf{q}}\delta_{\sigma\sigma'},$$

and a simple substitution will yield the required expression:

$$\chi^{(0)}_{nn}(\mathbf{q},\omega) = \frac{1}{L^d}\sum_{\mathbf{k},\sigma}\frac{(n_{\mathbf{k},\sigma} - n_{\mathbf{k}+\mathbf{q},\sigma})}{\hbar\omega + \varepsilon_{\mathbf{k},\sigma} - \varepsilon_{\mathbf{k}+\mathbf{q},\sigma} + i\hbar\eta} \tag{1.3.1}$$

where L^d is the volume of the system (and d its dimension). This function is actually a function of the modulus q. What we have obtained is known as *Lindhard function* $\chi_0(q,\omega)$.

1.3.1. The Lindhard function. The Lindhard function can be calculated analitically, at least in the zero temperature limit, in each dimension. Here our aim is to find an analytic expression for the Lindhard function relative to a 2D system. The main difficulty is to solve the sum that appears in Eqn. (1.3.1), but this difficulty vanishes in the zero temperature limit. We are going to neglect the spin in the discussion, but the generalisaton is trivial: Indeed, the complete result is given by the sum

$$\chi_0 = \chi_{0\uparrow} + \chi_{0\downarrow},$$

so we choose arbitrarily one of the two spin-dependent parts and write $\chi_{0\sigma} \equiv \chi_0$ (*one-spin* Lindhard function).

Let us rewrite (1.3.1) as

$$\chi_0(\mathbf{q},\omega) = \frac{1}{L^d}\sum_{\mathbf{k}}\frac{n_{\mathbf{k}}}{\hbar\omega + \varepsilon_{\mathbf{k}} - \varepsilon_{\mathbf{k}+\mathbf{q}} + i\hbar\eta} + \frac{1}{L^d}\sum_{\mathbf{k}}\frac{n_{\mathbf{k}+\mathbf{q}}}{-\hbar\omega + \varepsilon_{\mathbf{k}} - \varepsilon_{\mathbf{k}+\mathbf{q}} - i\hbar\eta},$$

then, once called ϑ the angle between $\mathbf{k}$ and $\mathbf{k}+\mathbf{q}$, k_F the Fermi wavevector modulus and $v_F = \frac{\hbar k_F}{m}$ the Fermi velocity, in the thermodinamic limit the sum can be regarded as an integral and above formula is transformed into the following:

$$\chi_0(q,\omega) = \frac{m k_F^{d-1}}{q(2\pi)^d\hbar^2}\int_0^1 dx \int \frac{x^{d-1}\, d\Omega_d}{\frac{\omega}{q v_F} - \frac{q}{2k_F} - x\cos\vartheta + i\eta} + (\omega^+ \to -\omega^+)$$

where Δ is the dimension of the system, $x = k/k_F$, $d\Omega_d$ is the solid angle element in dimension d and the shorthand $(\omega^+ \to -\omega^+)$ indicates the same term as the one completely explicited but for the substitution $\hbar\omega + i\eta \mapsto -(\hbar\omega + i\eta)$. After further appropriate substitutions of variables, according to the dimension of the system, the integral can be analytically resolved. Notice that the solution is a complex function of ω with a real and an imaginary part which express, respectively, the in-phase response of the system and its power absorption, as stressed when introducing the linear response theory. The Lindhard function for a bi-dimensional gas of (spinless) fermions reads as:

$$\chi_0(\mathbf{q}, i\omega) = \frac{m^2}{2\pi q^2}\left\{\sqrt{2}\sqrt{a + \sqrt{a^2 + \left(\frac{\omega q^2}{m}\right)^2} - \frac{q^2}{m}}\right\} \qquad a = \frac{q^4}{4m^2} - \frac{q^2 k_F^2}{m^2} - \omega^2,$$

In the static limit ($\omega = 0$) the Lindhard function is purely real, for the 2D case in the $T = 0$ limit it is easily obtained

$$\chi_0(q,0) = \frac{m}{2\pi\hbar}\left[\frac{\sqrt{q^2-4}}{q}\Theta(q-2) - 1\right].$$

In the conclusion of this section we address a comment to the Fourier transform of the Lindhard function. In fact, it is interesting to note that it physically represents

the response of the density to an impurity (charged with the same sign) located at the origin of the system; at large distances $\chi_0\left(r \gg k_F^{-1}, 0\right)$ oscillates and decays slowly. This phenomenon is known as *Friedel oscillations*, and — as it is clear from the direct calculation of the Fourier transform — it is a direct consequence of the existence of the Fermi surface. We refer the readers to the bibliography of this chapter for further information.

1.3.2. A picture of the origin of the pair correlation function. The kinetic and interaction energies are not the unique contributing to the total energy of a Fermionic system. For example, suppose we have a (eventually spinless) jellium model: The antisymmetric nature of the wave function make "holes" arise around each electron, in which any other electron cannot stay. At the same time, this local "vacuum" allows stronger interactions between positive background and electrons, and makes the well-known exchange energy originate. Analogous processes exist in general in any Fermionic system, and generates a depletion region called the *exchange-hole*.

This energy contribution can be formalised via the *pair correlation function*, defined as the joint probability of finding a fermion in $\mathbf{r}_2$ given the presence of another identical fermion in $\mathbf{r}_1$:

$$\mathbf{g}(\mathbf{r}_1, \mathbf{r}_2) = \frac{\left\langle \sum_{i \neq j} \delta\left(\mathbf{r}_2 - \mathbf{r}_j\right) \delta\left(\mathbf{r}_1 - \mathbf{r}_i\right) \right\rangle}{n(\mathbf{r}_1) n(\mathbf{r}_2)}$$

or equivalently, in terms of field operators

$$\mathbf{g}(\mathbf{r}_1, \mathbf{r}_2) = \sum_{\sigma_1 \sigma_2} \frac{\langle \hat{\psi}^\dagger_{\sigma_2}(\mathbf{r}_2) \hat{\psi}^\dagger_{\sigma_1}(\mathbf{r}_1) \hat{\psi}_{\sigma_1}(\mathbf{r}_1) \hat{\psi}_{\sigma_2}(\mathbf{r}_2) \rangle}{n(\mathbf{r}_1) n(\mathbf{r}_2)},$$

whereas in the homogeneous case $\mathbf{g}(\mathbf{r}_1, \mathbf{r}_2) = \mathbf{g}(|\mathbf{r}_1 - \mathbf{r}_2|)$.

Thus the fermion-fermion interaction energy can be expressed using $\mathbf{g}$. For example, in the jellium model the *total* potential energy writes

$$\frac{U}{N} = \frac{n}{2} \int v(\mathbf{r}) \left[\mathbf{g}(\mathbf{r}) - 1\right] d\mathbf{r} \tag{1.3.2}$$

It is important to notice that exchange hole always exists in Fermionic systems, even in the non-interacting case, in particular for spinless fermions in uniform systems we expect

$$\mathbf{g}(r = 0) = 0, \quad \mathbf{g}(r \to \infty) \to 1.$$

In conclusion, $\mathbf{g}$ describes the depletion region (*see* Figure 1.3.1) and therefore the total amount of the exchange energy of the system.

1.4. The interacting electron liquid

We can now ampliate the frame we are working in by including interaction in our system, thus better comprehending the meaning of screening potential. The first and perhaps the most famous approximation that allows the extension of previous studies to an interacting system is the Hartree-Fock approximation. We are not intentioned to give explanations about it, and we just remind that it is a self-consistent mean-field theory, in which the non local exchange potential appears to be intrinsically included. Historically, the first attempt to go beyond the HF approximation is the random phase approximation (RPA). We will show here the

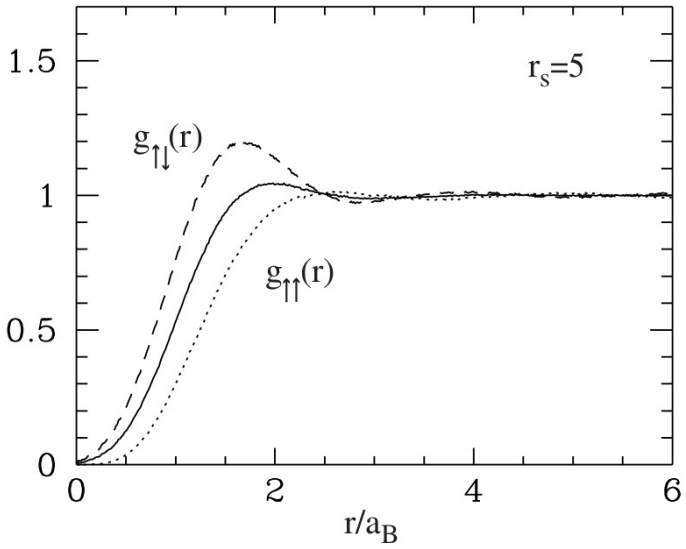

FIGURE 1.3.1. The pair correlation functions $\mathbf{g}_{\uparrow\uparrow}$, $\mathbf{g}_{\uparrow\downarrow}$ and their average (solid line) in paramagnetic uniform 2D electron gases at the density corresponding to $r_s = 5$, a_B is the Bohr radius. Image from *G. F. Giuliani, G. Vignale, Quantum Theory of the Electron Liquid.*

Hartree mean-field approximation and its link to the RPA, then we will furnish a more detailed analysis of the RPA with its advantages and limits.

Let us begin by considering a "wider" response theory, i.e. including dynamical mean field approximations: we will present a method based on the independent electron model that will turn out to be useful to calculate the response of interacting electron gas.

Consider a time-dependent perturbation so that the hamiltonian reads as

$$\hat{H}(t) = \hat{H} + F(t)\hat{B}$$

where we approximate the ground state hamiltonian $\hat{H}$ with a *single-particle* mean field hamiltonian:

$$\hat{H} \sim \hat{H}^{MF} = \hat{H}_0 + \hat{V}^{MF}.$$

In the above expression $\hat{V}^{MF}$ can be any mean field potential, for example we can choose the ground state part of Hartree Fock potential, or more simply the classical Hartree potential $\hat{V}^H$. So in this picture each operator can be expressed in second quantization as a single particle operator, and thus the potential writes

$$\hat{V}^{MF} = \sum_{ij} V_{ij}^{MF} \hat{a}_i^\dagger \hat{a}_j.$$

It actually can be rewritten as a functional of the density matrix which elements are $\rho_{uy} = \langle \hat{a}_u^\dagger \hat{a}_y \rangle$, so that $V_{ij}^{MF} = V_{ij}^{MF}\left[\rho_{uy}\right]$. Clearly this is valid for *each* single particle operator. Now we can apply the linear response theory, which tell us that the linear

response for any observable $\hat{A}$ that couples linearly to $\hat{B}$ reads as

$$\chi^f_{AB}(\omega) = \sum_{ij} \frac{n_i - n_j}{\hbar\omega + \varepsilon_i - \varepsilon_j + i\hbar\eta} A_{ij} B_{ji}.$$

But we must pay attention, because this is the response function of a *fictitious* non-interacting system (the potential is of single-particle) which hamiltonian is $\hat{H}^{MF}$. Then it is not the actual response function: The response of the system to the external perturbation modifies the mean field potential, which now shows a new time-dependent part.

Thus the way is traced: we can determine the true response function via a self-consistent path.

Precisely, the new potential has become

$$\hat{V}^{MF}(t) = \hat{V}^{MF}_0 + \hat{V}^{MF}_1(t),$$

and thanks to its expression as a functional of the density matrix, the time dependent part can be regarded as

$$\begin{aligned} \hat{V}^{MF}_1(t) &= \sum_{ij} \hat{V}^{MF}_{1,ij}(t) \hat{a}^\dagger_i \hat{a}_j \\ &= \sum_{ij} \left(\sum_{uy} \frac{\delta}{\delta \rho_{uy}} V^{MF}_{ij}\left[\rho_{uy}\right] \Big|_{\text{g.s.}} \rho_{1,uy}(t) \right) \hat{a}^\dagger_i \hat{a}_j \end{aligned}$$

(the subscript "g.s." indicates that the variation must be calculated in the ground state — thus at the 0^{th} order). Here the only quantity we have to calculate is $\rho_{1,uy}(t)$, that can be derived from

$$\rho_{1,uy}(\omega) = \chi^{MF}_{\rho_{uy}B}(\omega) F(\omega)$$

in a self-consistent way: In fact, now we can say that $-F(t)\hat{B} + \hat{V}^{MF}_1(t)$ is the term in the hamiltonian that stems for the perturbation, so that χ^f_{AB} describes only the 0^{th} order of the total response function, and the response of $\hat{A}$ up to the first order is given by

$$\left\langle \hat{A} \right\rangle_1 (\omega) = \chi^f_{AB}(\omega) F(\omega) + \sum_{ij,uy} \chi^f_{A\rho_{ij}} \frac{\delta}{\delta \rho_{uy}} V^{MF}_{ij}\left[\rho_{uy}\right] \Big|_{\text{g.s.}} \chi^{MF}_{\rho_{uy}B} F(\omega)$$

which can be resolved with respect to $\chi^{MF}_{\rho_{uy}B}$ (the quantity we are interested in) by choosing $\hat{A} = \hat{\rho}_{ij}$.

In this way we have achieved our aim to express the self-consistent response function in the picture of a mean field theory as a function of the only χ^f_{AB} of the fictitious non-interacting systems.

1.4.1. The RPA approximation. The mean field response theory can now be used in order to define the random phase approximation in a physically appealing way, choosing the Hartree field as the static mean field $\hat{V}^{MF}_0$. The Hartree potential is local in space, and it represents the average electrostatic potential created by the electronic charge density (then it does *not* include the exchange potential).

Let us consider as usual a gas of electron, and let $V(\mathbf{r})$ be a static potential acting on it. Then each electron, according to the Hartree approximation feels the

self-consistent potential

$$V_H(\mathbf{r}) = V(\mathbf{r}) + \int \frac{e^2 n(\mathbf{r}')}{|\mathbf{r} - \mathbf{r}'|}\, d\mathbf{r}',$$

with $n(\mathbf{r})$ the ground-state density. Such a system is called a Hartree system, and its susceptibility is given by $\chi^H_{nn}(\mathbf{r}, \mathbf{r}'; \omega)$. The following assumption is that the physical system will respond as the Hartree system would to perturbating potentials $V_1(\mathbf{r}, t)$ and to the electrostatic potentials created by the induced density modulations $n_1(\mathbf{r}, t)$:

$$n_1(\mathbf{r}, \omega) = \int \chi^H_{nn}(\mathbf{r}, \mathbf{r}'; \omega) V_{\text{sc}}(\mathbf{r}', \omega)\, d\mathbf{r}'$$

(already introduced in § 1.2.3) where

$$V_{\text{sc}}(\mathbf{r}', \omega) = V_{\text{ext}}(\mathbf{r}', \omega) + \int \frac{e^2}{|\mathbf{r}' - \mathbf{r}''|} \chi^{RPA}_{nn}(\mathbf{r}', \mathbf{r}'', \omega) V_{\text{ext}}(\mathbf{r}'', \omega)\, d\mathbf{r}''$$

is the screened potential. Thus if one compares this expression to those of the proper response function, immediately gets

$$\tilde{\chi}^{RPA}_{nn}(\mathbf{r}, \mathbf{r}', \omega) = \chi^H_{nn}(\mathbf{r}, \mathbf{r}', \omega)$$

i.e. in the RPA the proper susceptibility is given by the Hartree response function.

The whole discussion is valid in full generality, but a little simplification can be done in the homogeneous case by identificating the proper response function to the Lindhard function:

$$\tilde{\chi}^{RPA}_{nn}(q, \omega) = \chi_0(q, \omega),$$

indeed the Hartree system for a homogeneous electron system coincides with the non interacting electron gas.

In conclusion, directly from the compressibility sum rule and the definition of proper response function one gets:

$$\chi^{RPA}_{nn}(q, \omega) = \frac{\chi_0(q, \omega)}{1 - v_q \chi_0(q, \omega)}.$$

Before proceeding, we define the *dielectric function*

$$\varepsilon^{RPA}(q, \omega) = 1 - v_q \chi_0(q, \omega)$$

which, note, coincides with the denominator of χ^{RPA}_{nn}.

1.4.2. Properties from χ^{RPA}_{nn}. In this section we refer to the 3D jellium model, because it shows clearly observable features of the RPA in few simple calculations which can be readily extended to many systems. We will focus on the screening effects and to the poles of χ^{RPA}_{nn}, and finally on the correlation energy.

Static limit. The screening properties of the electron gas is controlled by the static dielectric function $\varepsilon^{RPA}(q, 0)$ which for a 3D electron gas in the long wavelength limit is given approximatively by

$$\varepsilon^{RPA}(q, 0) \sim 1 + \frac{q^2_{TF}}{q^2}, \qquad q \ll k_F,$$

where $q_{TF} = \sqrt{6\pi n e^2 / \epsilon^0_F}$ is the Thomas Fermi wavevector, with ϵ^0_F the non-interacting Fermi energy of the system. Notice that the divergence of ε^{RPA} at small wavevectors perfectly reflects the complete screening property of metals.

Hence the physical meaning of the Thomas Fermi wavevector is better understood if one consider the screened potential produced by an impurity in the electron gas:

$$V_{sc}(\mathbf{r}) \simeq \mathscr{F}\left[\frac{v_{\mathbf{q}}}{\varepsilon(q,0)}\right] = e^2\frac{e^{-q_{TF}r}}{r}$$

which is a Yukawa-like potential, i.e.: by mean of the dielectric function we have obtained a rapidly decaying potential, thanks to which impurities are completely screened after a distance of $\sim 1/q_{TF}$. This is a simplified approximation, in facts the true RPA screened potential shows the Friedel oscillations — associated with the singularity of $\varepsilon^{RPA}(q,0)$ in $q = 2k_F$ —, whereas the obtained Yukawa-like screened potential does not predict them. Nevertheless we have obtained correct predictions at least for $q \to 0$.

Dynamical limit. The poles of the density density response function are in correspondence of the excitation energies of collective modes of many body systems. In our jellium model, such collective modes are called *plasmons*. It is convenient to study the zeroes of the dielectric function.

In the limit $q \to 0, \omega \gg v_F q$, the RPA dielectric function for a 3D electron gas writes

$$\varepsilon^{RPA}(0,\omega) \sim 1 - \frac{4\pi n e^2}{m}\frac{1}{\omega^2} = 1 - \frac{\omega_p^2}{\omega^2}$$

where ω_p is referred to as the *electron plasma frequency*. Then RPA predicts the existence of a pole at the frequency $\omega = \omega_p$, a result experimentally confirmed. The value of ω_p varies with the dimensionality of the system (a result which can be found classically):

$$\omega_p(q) = \begin{cases} \sqrt{\frac{2\pi n e^2}{m}q} & \text{2D} \\ \sqrt{\frac{4\pi n e^2}{m}} & \text{3D} \end{cases}$$

and the following dispersion relation is found within the RPA:

$$\Omega_p^2(q) \simeq \omega_p^2(q) + c_d q^2 v_F^2 + \dots$$

where the Fermi velocity can be expressed in terms of the Thomas-Ferm wave vector and $c_2 = 3/4$ in dimension $d = 2$ whereas $c_3 = 3/5$ in the 3D case.

Correlation energy. The correlation energy is defined as the difference between the total energy and the sum (E_1) of kinetic energy (E_0) of the non-interacting gas and exchange energy of the system. From the Fourier transform of Eqn. (1.3.2) which reads

$$\frac{U}{N} = \frac{1}{2L^d}\sum_{\mathbf{q}\neq 0} v_q\left[S(q) - 1\right]$$

it can be shown that

$$\frac{E_1}{N} = \frac{E_0}{N} + \frac{1}{2L^d}\sum_{\mathbf{q}} v_q\left(-\frac{\hbar}{n\pi}\int_0^1 d\lambda \int_0^{+\infty}\chi_0(q,i\omega;\lambda)\,d\omega - 1\right)$$

where λ is a coupling constant. The RPA correlation energy reads as

$$\epsilon_c^{RPA} = \frac{E^{RPA} - E_1}{N} = \frac{1}{2L^d}\sum_{\mathbf{q}}\left(-\frac{\hbar}{n\pi}\int_0^1 d\lambda\int_0^{+\infty}\lambda v_q^2\chi_0(q,i\omega;\lambda)\frac{\chi_0(q,i\omega)}{1-\lambda v_q\chi_0(q,i\omega)}\,d\omega\right),$$

which can be carried out easily in λ whereas numerical calculations are often needed for the remaining part.

The correlation energy is an interesting quantity through which we can "test" the RPA, in facts it involves the susceptibility, the structure factor and the pair correlation function: Illnesses of these functions may indicate issues in the RPA.

1.4.3. RPA limits of validity. The most intriguing advantage of the RPA is its simplicity, leading in many cases to very good results. It provides substantially exact results for the total energy of an electron gas in the high density limit, gives good descriptions for plasmon oscillations, and the screening effects are derived in details.

Nevertheless, most details are lost out of the long wave length limit: For example, in the case of the jellium model to which is widely applied, the RPA strongly relies on the uniformity of the electron gas, thanks to which the Hartree term is identically zero. At finite wave lengths, even small density fluctuations become non-negligible, therefore the Hartree term does not cancel exactly. In real metals, this rapidly becomes a serious issue. Furthermore, at tipical metallic densities and small separations, the correlation function becomes unphysically negative. Another problem is that the RPA does not consider exchange correlations at all, as will be shown later on. At low densities (in the specific case of the jellium model) those problems are accentuated. Finally, it is important to notice the systematic violation of the compressility sum rule: while the compressibiliy calculated as the second derivative of the energy with respect to the density yields essentially correct results, the limit $\lim_{\mathbf{q}\to 0} \tilde{\chi}^{RPA}_{nn}(\mathbf{q}, 0)$ yields the compressibility of a non interacting system, a clear violation of the compressibility sum rule.

1.5. Beyond RPA: Local Field Factors

The preceding critique to the RPA indicates what problems have to be considered in order to improve the description of interacting fermion gases.

Let us preliminarly discuss the stiffness energy δE of a fermionic system: we can make the physically reasonable hypothesis that it is composed by the sum of two terms, the first due to the electrostatic energy associated with the density modulation, the second related to the kinetic stiffness energy of a non interacting fermions:

$$\delta E = \delta E_C + \delta E_T.$$

It appears clearly that the exchange and correlation energy are completely excluded from the calculations. A very simple and effective method to fix this issue is to introduce the non local exchange potential "by hands", by postulating the existence of an additional stiffness-energy term of the type

$$\delta E_{XC} = -\frac{v_q G(q) n^2_{\mathbf{q}}}{L^d} \tag{1.5.1}$$

where $G(q)$ represents a fractional modification of the Coulomb energy associated with the exchange-correlation hole. Expliciting term by term one gets

$$-\frac{n^2_{\mathbf{q}}}{\chi_{nn}(q,0)L^d} = \frac{v_q n^2_{\mathbf{q}}}{L^d} - \frac{n^2_{\mathbf{q}}}{\chi_0(q,0)L^d} - \frac{v_q G(q) n^2_{\mathbf{q}}}{L^d}, \tag{1.5.2}$$

and a simple rearrangement of terms in the complete stiffness energy (1.5.2) will lead to the Hubbard expression

$$\chi_{nn}(q,0) = \frac{\chi_0(q,0)}{1 - v_q\,[1 - G(q)]\,\chi_0(q,0)}; \tag{1.5.3}$$

$G(q)$ is commonly referred to as a (static) *many-body local field factor*. The reader should notice that, by modifying χ_{nn}, the inclusion of the exchange term will lead to a change in both the electrostatic and the kinetic energy stiffness via a modification of the magnitude of the induced density modulations $n_{\pm q}$.

It is also possible to extend this simple picture to the dynamic case, where

$$-v_q G(q,\omega) n_{\mathbf{q}}(\omega)$$

is easily seen to be the Fourier transform of the exchange-correlation potential created by a density fluctuation of amplitude $n_{\mathbf{q}}(\omega)$.

We have seen it is possible to generalize RPA, which fails in accounting the correlations existing between fermions in a many body system, in a simple and elegant way, by introducing the concept of *local effective potential*.

It is of some interest to precisely know what is missing when not considering the correct correlation effects:

- $\rightsquigarrow$ the electrostatic field seen by the test-fermion should not include the field of that very same fermion;
- $\rightsquigarrow$ the fermionic many-body wave function is antisymmetric: the presence of a dipole in a certain place excludes the presence of an identical dipole in the same place and even in the very proximity. This is called "exchange-hole", and it is present in non interacting system, too (*see* § 1.3.2);
- $\rightsquigarrow$ the further decrease of the probability of finding a fermion in the proximities of another one is generally due to the additional repulsion term of the Coulomb interaction. This term redistributes the system's density and is referred to as "correlation-hole".

The correlation-hole is mainly important between non identical fermions, i.e., between fermions with opposite spin, while exchange-holes act in case of parallel spins. So this is why it is important to make a distinguish and introduce a spin dependence in the local field factor, which we take in account precisely in order to correct the total amount of the hole, overestimated in RPA. Spin effects are handled by introducing the local field factors $G_{\sigma\sigma'}(q,\omega)$.

It is quite natural to try and replace the average electrostatic potential by a *local effective potential* $V^{\text{eff}}_{\sigma}(\vec{r},t)$, where σ is the spin of the fermion that feels such a local potential. In the linear response regime, the Fourier amplitude $V^{\text{eff}}_{\sigma}(\vec{q},\omega)$ is a linear function of the numeric $n_{\sigma'}(\vec{q},\omega)$ and of $\uparrow$-spin and $\downarrow$-spin densities. Thus we can write

$$V^{\text{eff}}_{\sigma}(\vec{q},\omega) = V^{\text{eff}}_{\text{ext}\sigma}(\mathbf{q},\omega) + \sum_{\sigma'} v_q n_{\sigma'}(\mathbf{q},\omega) - \sum_{\sigma'} v_q G_{\sigma\sigma'}(q,\omega) n_{\sigma'}(\mathbf{q},\omega) \tag{1.5.4}$$

where the last term is the one containing the local field factors.[2] Actually the real interest of including the spin in the local field factors is the possibility to define the

[2] Notice that the G's always satisfy the symmetry relation $G_{\uparrow\downarrow} = G_{\downarrow\uparrow}$, while $G_{\uparrow\uparrow} = G_{\downarrow\downarrow}$ is satisfied only in paramagnetic systems.

spin symmetric and anti-symmetric combinations

$$G_{\pm}(q,\omega) = \frac{G_{\uparrow\uparrow}(q,\omega) \pm G_{\uparrow\downarrow}(q,\omega)}{2}$$

which control respectively the density-density and spin-spin response function of a paramagnetic fermion liquid, as it can be shown. It is then G_+ which properly enters Eqn. (1.5.3). Thus, the random phase approximation is re-achieved by setting $G_{\uparrow\uparrow} = G_{\uparrow\downarrow} = 0$.

The reliability of (1.5.4) stands on the possibility to connect the $G_{\uparrow\downarrow}$ and $G_{\uparrow\uparrow}$ to the correlation-hole.

We conclude this section with a phenomenological example first argued by Hubbard, who originally made an hypotesis over the form the local field factor should take for a 3D electron liquid interacting via Coulomb potential:

$$G_{\uparrow\uparrow}(q,\omega) \approx G^{H}_{\uparrow\uparrow}(q) = \frac{q^2}{q^2 + k_F^2}; \qquad G_{\uparrow\downarrow}(q,\omega) \approx 0. \tag{1.5.5}$$

Notice that in this approximation the *correlation*-hole correction is completely forgotten. Might the reader guess if the approximation (1.5.5) is a physically reasonable one? Here we propose the Hubbard's original explanation for this.

(1) The correlation between weakly-coupled fermions principally pops up from Pauli principle. Hence we won't consider the correlation hole;
(2) The zone in which correlation disappears is a short ranged one, so that the exchange (local) potential should be short ranged too. This means that the local field factor must vanish over long distancies (small wavevectors) and therefore shoul have an appropriate evolution to compensate divergencies of the potential;
(3) Conversely, Pauli exclusion acts on short ranges in a similar way as a hard sphere potential does, making the interaction potential enterely negligible. Using the equation (1.5.3), this leads to the ansatz $G_{\uparrow\uparrow} \overset{q\to\infty}{\longrightarrow} 1$.

1.6. The Singwi-Tosi-Land-Sjölander approximation scheme

We are left with the problem of determining the local field factor $G(\mathbf{q})$. In 1968 four physicists, Singwi, Tosi, Land and Sjölander, developed an approch to calculate the local field factor based on the central idea that, if we know the response function, we can use it in order to calculate the exchange-correlation hole and then obtain $G(\mathbf{q})$. They move from the facts that the RPA fails to take account of short-range effects, and the correction proposed by Hubbard, seen in the previous section, on the one hand does include the local field correction, while on the other hand neglects corrections to the correlation hole which would have been expressed by $G_{\uparrow\downarrow}$.

A possible way to obtain the self-consistent form of the local field factor is briefly explained below as formulated in Ref. [8]. One begins by looking for a solution of the equation of motion, provided by the Liouville equation $\frac{\partial}{\partial t} f + \{f, H\} = 0$, of a classical space and momentum density distribution f, imposing the following *ansatz* in order to take account in a self-consistent manner of the short range correlations responsible for the local field factor corrections:

$$f(\mathbf{1},\mathbf{1}') = f(\mathbf{1}) f(\mathbf{1}') \mathbf{g}(\mathbf{x} - \mathbf{x}')$$

where $\mathbf{g}(\mathbf{x})$ is the pair correlation function. On the other hand, we know that $\mathscr{F}[\mathbf{g}(\mathbf{r})-1] = (1/n)[S(\mathbf{q})-1]$ is related to the dielectric function via

$$S(\mathbf{q}) = -\frac{q^2}{4\pi^2 n}\int_0^\infty \Im\left[\varepsilon(\mathbf{q},\omega)\right]^{-1} d\omega. \tag{1.6.1}$$

The latter equation requires the self-consistency on $S(\mathbf{q})$ and $\varepsilon(\mathbf{q},\omega)$, for the dielectric function is now a functional of the static structure factor.

Given an external potential $V_{\text{ext}}(\mathbf{x},t)$ and the interaction $\Phi(\mathbf{x})$, the Liouville equation explicitly reads as:

$$\left[\frac{\partial}{\partial t}+\mathbf{v}\cdot\nabla_{\mathbf{x}}\right] f(\mathbf{x},\mathbf{p};t) - \nabla_{\mathbf{x}}V_{\text{ext}}(\mathbf{x},t)\cdot\nabla_{\mathbf{p}}f(\mathbf{x},\mathbf{p};t) + \\ -\int \nabla_{\mathbf{x}}\Phi\left(\mathbf{x}-\mathbf{x}'\right)\cdot\nabla_{\mathbf{p}}f(\mathbf{x},\mathbf{p};\mathbf{x}',\mathbf{p}';t)\,d\mathbf{x}'d\mathbf{p}' = 0 \tag{1.6.2}$$

where $f(\mathbf{x},\mathbf{p};\mathbf{x}',\mathbf{p}';t)$ is the two-particle distribution function. We note that equation of motion is "nested": If we take the equation of motion of the two-particle distribution function, it will contain the three-particle distribution function, and so on. The infinite hierarchy is terminated by making use of the *ansatz*

$$f(\mathbf{x},\mathbf{p};\mathbf{x}',\mathbf{p}';t) = f(\mathbf{x},\mathbf{p};t)f(\mathbf{x}',\mathbf{p}';t)\mathbf{g}(\mathbf{x}-\mathbf{x}'),$$

and $\mathbf{g}(\mathbf{x})$ will be the equilibrium static pair correlation function.

Now, if we write the distribution function as a sum of an equilibrium distribution function f_0 and a fluctuation f_1, namely

$$f(\mathbf{x},\mathbf{p};t) = f_0(\mathbf{p}) + f_1(\mathbf{x},\mathbf{p};t),$$

by linearizing Eqn. (1.6.2) we get the following equation of motion for the fluctuation:

$$\left[\frac{\partial}{\partial t}+\mathbf{v}\cdot\nabla_{\mathbf{x}}\right] f_1(\mathbf{x},\mathbf{p};t) + \\ -\left(\nabla_{\mathbf{x}}V_{\text{ext}}(\mathbf{x},t)+\int\nabla_{\mathbf{x}}\psi\left(\mathbf{x}-\mathbf{x}'\right)\cdot\nabla_{\mathbf{p}}f_1(\mathbf{x}',\mathbf{p}';t)\,d\mathbf{x}'d\mathbf{p}'\right)\cdot\nabla_{\mathbf{p}}f_0(\mathbf{p}) = 0 \tag{1.6.3}$$

where

$$\nabla_{\mathbf{x}}\psi(\mathbf{x}) = \mathbf{g}(\mathbf{x})\nabla_{\mathbf{x}}\Phi(\mathbf{x}). \tag{1.6.4}$$

The first main result is the expression of the effective field felt by a particle:

$$\begin{aligned}\mathbf{E}_{\text{eff}}(\mathbf{x},t) \quad = \quad & -\nabla_{\mathbf{x}}V_{\text{ext}}(\mathbf{x},t) \\ & -\int\nabla_{\mathbf{x}}\Phi\left(\mathbf{x}-\mathbf{x}'\right)\cdot\nabla_{\mathbf{p}}f_1(\mathbf{x}',\mathbf{p}';t)\,d\mathbf{x}'d\mathbf{p}' \\ & -\int\left[\mathbf{g}(\mathbf{x}-\mathbf{x}')-1\right]\nabla_{\mathbf{x}}\Phi\left(\mathbf{x}-\mathbf{x}'\right)\cdot\nabla_{\mathbf{p}}f_1(\mathbf{x}',\mathbf{p}';t)\,d\mathbf{x}'d\mathbf{p}'\end{aligned} \tag{1.6.5}$$

it can be derived from an inspection of the equations (1.6.3) and (1.6.4). The first two terms correspond to the usual macroscopic field, while the third is new as it arises from the *ansatz* and represents the local field correction, completely absent in the random phase approximation.

In general one can express the density distribution as the density matrix, and then obtain from the equation of motion for $\langle \phi_\sigma^\dagger(\mathbf{x},t)\psi_\sigma(\mathbf{x}',t)\rangle$ the effective field (1.6.5).

A solution of Eqn. (1.6.3) is readily found by using standard methods, indeed one finds the induced density as

$$\begin{aligned} n_{\text{ind}}(\mathbf{q},\omega) &= \int f_1(\mathbf{q},\omega;\mathbf{p})\, d\mathbf{p} \\ &= -\frac{Q_0(\mathbf{q},\omega)}{\Phi(\mathbf{q}) + \psi(\mathbf{q})Q_0(\mathbf{q},\omega)} V_{\text{ext}}(\mathbf{q},\omega) \end{aligned}$$

where

$$\psi(\mathbf{q}) = \Phi(\mathbf{q}) + \frac{1}{n}\int \frac{\mathbf{q}\cdot\mathbf{q}'}{q^2}\Phi(\mathbf{q}')\left[S(\mathbf{q}-\mathbf{q}')-1\right]\frac{d\mathbf{q}'}{(2\pi)^d}$$

and

$$Q_0(\mathbf{q},\omega) = -\Phi(\mathbf{q})\chi_0(\mathbf{q},\omega)$$

have been used. Therefore the dielectric function writes

$$\varepsilon(\mathbf{q},\omega) = 1 + \frac{Q_0(\mathbf{q},\omega)}{1 - G(\mathbf{q})Q_0(\mathbf{q},\omega)} \tag{1.6.6}$$

where, at last, the local field factor has been found

$$G(\mathbf{q}) = -\frac{1}{n}\int \frac{\mathbf{q}\cdot\mathbf{q}'}{q^2}\Phi(\mathbf{q}')\left[S(\mathbf{q}-\mathbf{q}')-1\right]\frac{d\mathbf{q}'}{(2\pi)^d}. \tag{1.6.7}$$

The set of three equations (1.6.1), (1.6.6) and (1.6.7) is a set of self-consistent equations that allows to calculate the local field factor in a simple and physically motivated manner. Furthermore, from the expression of the effective field, one can obtain also the new term in the effective potential due to correlations. It has been shown [8] that such term can be made local.

Until now we have seen the classical case. The authors of this approximation scheme generalise to quantum mechanic the argument above by merely replacing χ_0 and $S(\mathbf{q})$ by their correspective quantum mechanical analogs. They also stress that the only difference with the RPA is that now the density show depletion regions around each particle due to the exchange-correlation hole.

A partial improvement of the above method, including adjustments for the pair correlation function and henceforth for the screening, is given in Ref. [9] by the same authors.

1.6.1. Electrons in 2D: STLS v/s other approximation schemes. The STLS scheme constitues an important and often very successful improvement to the RPA [1]. However, it does not represent the only possible scheme that includes short-range correlations corrections, so does also the Hubbard (HA) and the Hartree Fock (HF) approximations. In this section we are going to illustrate some important features of a 2D electron gas that results to be improved by STLS, while comparing them with other schemes. The discussion and all graphics in this section are from Ref. [10] (U. de Freitas & al.). Also, one has to take into account that "2D" is only an approximation, if fact a residual thickness w is always present and could modify results. So we will do in this section.

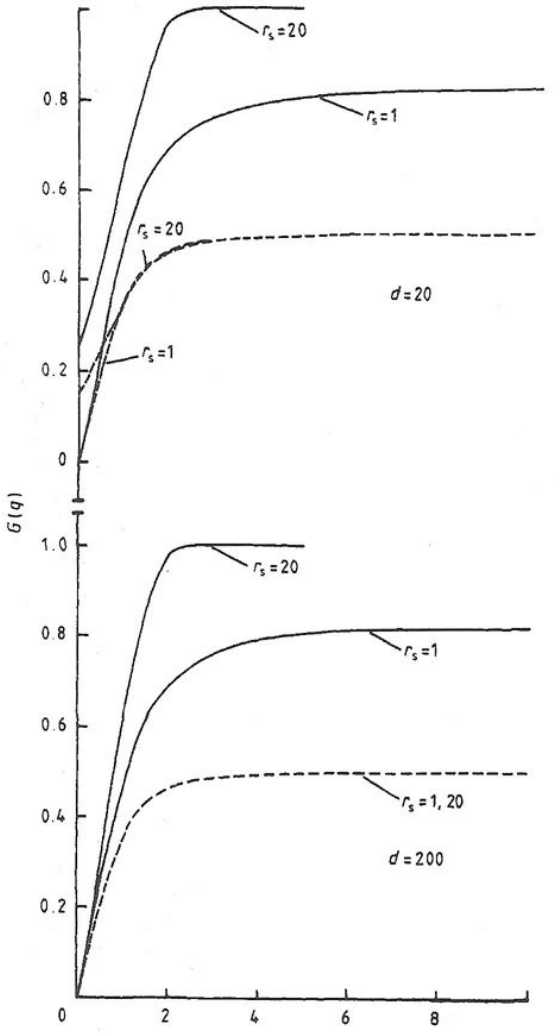

FIGURE 1.6.1. A comparison between $G(q)$ in the STLS (—) and in the HA ($- - -$) approximations, for $r_s = 1$ and 20 and $w = 20$ and 200 (Bohr radius units). Image from Ref. [10].

$G(q)$ and static structure factor. Some difference between G_{HA} (Eqn. (1.5.5)) and G_{STLS} has already been underlined previously, i.e. it is known that in HA only corrections to exchange are included. Corrections due to correlations, instead, may manifest through a dependence of the thickness w: In fact G_{STLS} varies significatively with w while G_{HA} does not, *see* Figures **1.6.1** and 1.6.2.

Correlation energy. Correlation energy can be written as

$$E^c(r_s) = -\frac{\sqrt{2}}{r_s^2}\int_0^{r_s} dr_s' \int_0^{\infty} F(qw;r)\left[S(q;r_s') - 1\right]\, dq$$

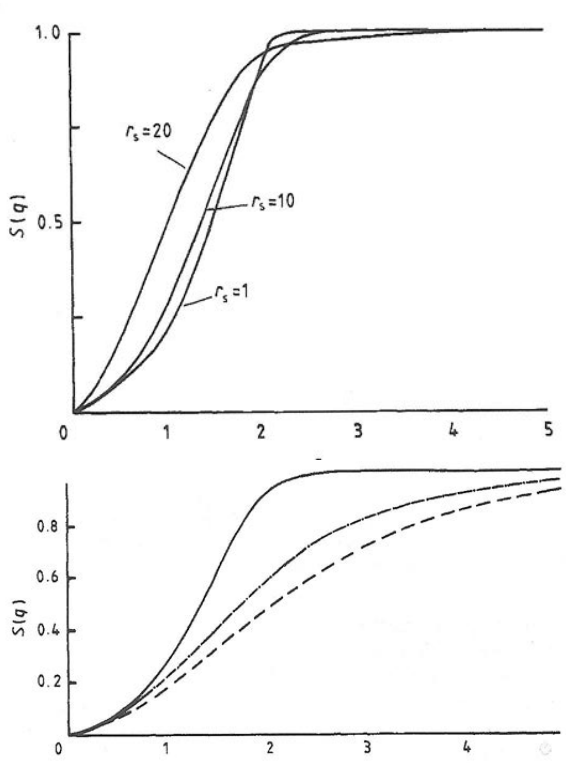

FIGURE 1.6.2. $S(q)$ behaviour in the STLS approximation for $w = 20$ and various values of r_s (top), and comparison of $S(q)$ in the STLS (—), in the HA $(- \cdot -)$ and in the RPA $(- - -)$ approximations for $w = 20$ and $r_s = 10$ (bottom). Image from Ref. [10].

where symbols have thier usual meaning and $F(qw; r_s') \sim 1/\varepsilon$ is the screening factor (ε is the dielectric function).

The RPA overestimates correlation energy (see for example [5, 1, 6]), as far as we expect HA does. In fact, numerical results confirm our expectations, and systematically $E^c_{STLS} < E^c_{HA} < E^c_{RPA}$.

Pair correlation function. The pair correlation function is a key element to evaluate how well an approximation scheme: For example, we have seen that the RPA pair correlation funtion takes unphysically negative values at tipical metallic electronic densities, that makes the approximation rather unsatisfactory. The STLS pair correlation function on the contrary is always positive till $r_s < 4$ and for higher r_s has only slighlty negative values at small particle separations. *See* Figure 1.6.3, in which diferent approximations are compared.

Dispersion relation. It is well known that the excitation spectrum of a electron gas can be found by studying the zeroes of the dielectric function

$$\varepsilon = 1 - v_{\mathbf{q}} \left[1 - G(\mathbf{q})\right] \chi_0(\mathbf{q}, \omega) = 0.$$

Clearly, different approximations of the local field factor yields different excitation spectra. Not only, but also the dimensionality of the system influences the spectrum,

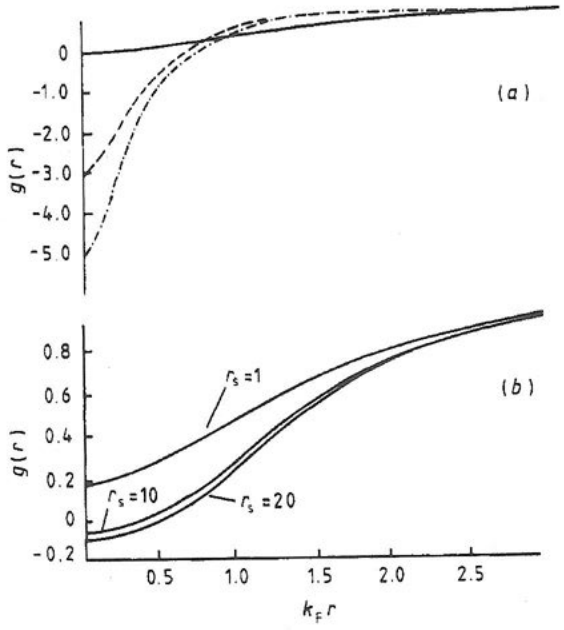

FIGURE 1.6.3. A $\mathbf{g}(r)$ comparison for $r_s = 10$, $w = 20$ in the STLS (—), the HA $(- - -)$ and the RPA $(- \cdot -)$ approximations (top). STLS scheme results for $w = 200$ and various r_s values (bottom). Image from Ref. [10].

and by the way, in quasi 2D systems the thickness w is expected to play a role in modifing excitations, even though it has lower effects. It is found that, for $\omega > q^2 + q$, the above equation can be rewritten

$$\sqrt{\nu_+^2 - 1} - \sqrt{\nu_-^2 - 1} = -q\,[qB(q) + 1]$$

where

$$B(q) = \frac{1}{\sqrt{2} r_s F(qw)\,[1 - G(q)]}, \qquad \nu_\pm = \frac{1}{2}\left(\pm\frac{\omega}{q} - q\right).$$

Thus the dispersion relation reads as:

$$\omega_p(q) = [1 + qB(q)] \sqrt{q \frac{4 + 2B(q)q^3 + B^2(q)q^4}{2B(q)\left[1 + \frac{1}{2}qB(q)\right]}}$$

and for very thick films in the long wave length limit one obtains

$$\omega_p(q) \simeq (2^{\frac{3}{2}} r_s q)^{\frac{1}{2}} \propto \sqrt{q},$$

the same relation found for a 2D electron gas with interactions like $1/r$ [12]. In Figure 1.6.4 we provide a comparison between the three approximations.

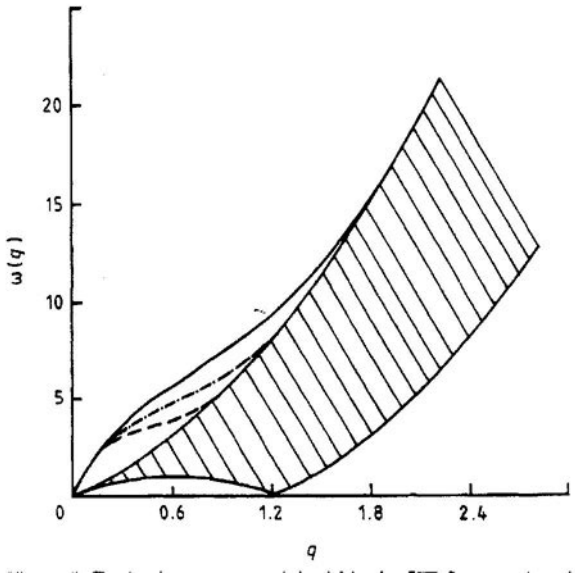

FIGURE 1.6.4. Here the excitation spectra are shown for the three approximations STLS ($- - -$), HA($- \cdot -$), and RPA (—), for $r_s = 10$, $w = 20$. Image from Ref. [10]

CHAPTER 2

DIPOLAR GASES

Most of the properties of systems like quantum gases are governed by the potentials acting between the gas components, and their scattering properties are of particular interest. Recently, new effective cooling methods both for bosonic and fermionic particle, has attracted huge interest in the study of new kind of quantum gases, whit richer interactions and new exotic phases. In particular, it is possible to cool down and trap molecules which exhibit also anisotropic interaction potential, such as the dipolar interaction. A gas of particles with permanent electric or equivalently magnetic dipoles, even in the weakly interacting limit, may lead to a new species of degenerate quantum gas. Specifically, the dipole-dipole interaction has recently attracted huge interest for two reasons: First, a significant experimental progress in trapping and handling ultracold gases, in particular of polar molecules and atoms with strong magnetic and electric dipolar moment, and second the peculiarities of the dipole-dipole interaction, strongly different from isotropic and/or contact interactions.

In this chapter we are going to present the most general features of the interactions in a quantum gas of dipoles.

2.1. Dipole-dipole interaction

One of the most relevant features in a many body system is the interaction between its components. In order to classify interactions, a first relevant distinction can be made on the basis of their range. Down to some details, a possible definition of the range of an interaction $U(r)$ comes with the finiteness of the integral

$$\int_{r_0}^{+\infty} U(r)\, d^d r,$$

where d stands for the dimensionality of the system: For $U(r)$ to have a long range it is necessary to decay as $1/r^{n \leq d}$, so whether the above integral is finite or not states, respectively, whether the interaction is short-range or long-range. Note that this definition strongly depends on the dimensionality of the system. Another important subdivision is based on the symmetry of the interaction potential, i.e. whether it is isotropic or not.

The peculiarity of the dipolar interaction potential is its anisotropy, in facts it has the same symmetry of the second order Legendre polynomial $P_2(\cos\vartheta)$, *see* Figure **2.1.1**. This anisotropy involves also the fact that the potential changes from being attractive if $\vartheta < \arccos(1/\sqrt{3})$ to being repulsive in the opposite case (the transition from attactive to repulsive is smooth). The dipolar interaction energy (as

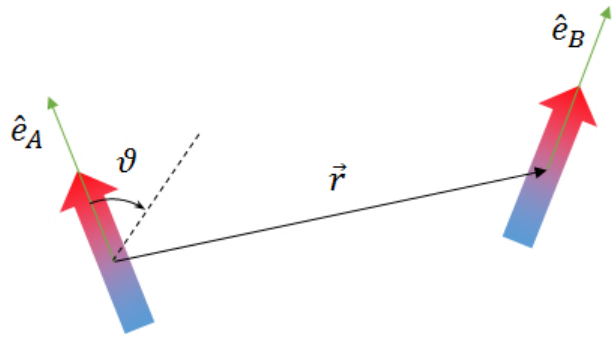

FIGURE 2.1.1. Dipole-dipole interaction. The angle ϑ is referred to one's dipole dipolar moment.

written for two dipoles A and B) reads

$$V_{dd}(\mathbf{r}) = \frac{C_{dd}}{4\pi}\frac{(\mathbf{e}_A \cdot \mathbf{e}_B)r^2 - 3(\mathbf{e}_A \cdot \mathbf{r})(\mathbf{e}_B \cdot \mathbf{r})}{r^5}, \tag{2.1.1}$$

where $\mathbf{r}$ represents the reciprocal position of the two dipoles, whose dipolar moments are oriented as $\mathbf{e}_X$. The dipole-dipole interaction is long-range only in three dimensions, and short-range at lower dimensions. The factor C_{dd} which appears in Eqn. (2.1.1) is a coupling constant: If we are considering identical dipoles, in the case of *magnetic* dipoles with magnetic dipole moment μ it reads as

$$C_{dd}^B = \mu_0 \mu^2$$

whereas its value when dealing with permanent *electric* dipoles of dipole moment D is given by

$$C_{dd}^E = \frac{D^2}{\epsilon_0}.$$

Thus the energy shows the same expression both for magnetic and electric dipoles, indeed the only difference stands in the coupling constant.

Incidentally we note that in the case of parallel dipoles, the interaction energy expression simplifies and can be rewritten

$$V_{dd}(r) = \frac{C_{dd}}{4\pi}\frac{1 - 3\cos^2\vartheta}{r^3}. \tag{2.1.2}$$

However, no matter the alignment between dipole moments, and no matter the dimensionality of the system, the dipolar potential not only controls distant interactions, but also influences the scattering properties due to *contact* interactions. This occurs because the dipolar potential does not conserve the angular momentum in scattering processes even though scattering between polarized dipoles conserves the projection of the angular momentum along the polarization axis. More precisely the dipolar potential $V_{dd}(r)$ mixes the angular momenta scattering channels, odd angular momenta scattering channels for fermions, and even angular momenta scattering channels for bosons. This coupling generates a short range contibution to the total effective potential in the s-wave channel, that adds to the contact interaction [18] + *bibliografia dello stesso articolo con ref. 20,27-33.* Thus it is possible to isolate two contributions in the interaction potential between dipoles: A slow

decaying potential, due to their electric or magnetic configuration, and a contact potential.

Contact interaction. All gases are in general composed of atoms or molecules, which interact via what we can call an *interparticle potential* $U(\mathbf{r})$, like the Van der Waals or the Lennard-Jones potential. Close to the particles, one can in general model the potentials as an hard-sphere isotropic potential, which constitutes the contact potential. When two particles interact, in general we can observe scattering.

Consider a system composed of a fixed target, which can be modeled as a central potential and stays in the origin of the coordinates axes, and of a particle in free motion along the z-axis toward the target; the central (interparticle) potential is assumed to vanish rapidly. We can cast an adecuate wavefunction for our central scattering problem: A good choice is

$$\psi_k(\mathbf{r}) = e^{ikz} + f(\theta)\frac{e^{ikr}}{r}$$

where $r = |\mathbf{r}|$ is the norm of the position vector, and θ the angle of $\mathbf{r}$ with respect to the z-axis. The above choice is justified if we think at the complexive wavefunction of the incident particle as the sum of an asymptotically free plane wave and a spherical wave, result of the scattering process, and then has cylindrical symmetry, so we can expand it in series of Legendre polynomial: From the coefficients of this expansion we get the required scattering amplitude $f(\theta)$ which squared modulus corresponds to the differential scattering section of the system $\frac{d\sigma}{d\Omega} = |f(\theta)|^2$. Moreover in the long wavelength limit

$$\lim_{k\to 0} \psi_k(\mathbf{r}) \propto 1 - \frac{a}{r}$$

and we can define the s-wave scattering length

$$a := -\lim_{k\to 0} f(\theta)$$

which determines whether the interaction is attractive ($a < 0$) or repulsive ($a > 0$), as can be proved e.g. within the Born approximation

$$a_{Born} = \frac{m}{2\pi}\int U(\mathbf{r})\, d\mathbf{r}.$$

In general then scattering properties depends of the potential, and in particular:

(1) A scattering potential which is not deep enough to hold a bound state, exhibits $a < 0$ and the attractive properties, whereas
(2) if one can modulate the potential parameters like depth such that it can eventually hold a bound state, then the scattering length becomes positive, $a > 0$, and the potential repulsive.

At this point we must account for the fermionic nature of the particles, that implies that the global wavefunction must be antisymmetric and hence that $f(\theta) + f(\theta + \pi) = 0$. Thus for a one-component Fermi gas, skew-symmetry directly leads to $\sigma = 0$, i.e. for such a system at zero temperature there is no s-wave scattering between identical particles, and their wave function is simply given by the plane wave $\psi(\mathbf{r}) = e^{ikz}$.

Feshbach resonances. We have seen that different potentials shows, obviously, different scattering properties: At the same time, if one can *tune* the parameters of the potential, it is possible to control scattering processes. However, we have seen that the only parameter which actually controls scattering processes between fermions is the scattering length a. Consider then an interatomic Van der Waals-like potential which also depends of spin $U_w(r,s)$. Hence we may raise or lower U_w by mean of an external magnetic field B, somewhat similar to the Zeeman effect, by removing the possible degeneracy in the energy, thus splitting the energy levels. In the most simple case, two new *channels* will originate from that splitting , each with its own bound state energy levels. We call $U_{bg}(r)$ the potential connecting two free atoms corresponding to the *open channel*, and $U_c(r)$ the raised potential, called *closed channel*. By varying B, a bound state E_c hold by the closed channel may coincide with the threshold state of the open channel, and therefore even a weak coupling can lead to strongly mixed channels. If this is the case, then two atoms collides at an energy E close to the crossing, they can resonantly couple: This phenomenon is known as Fesbach resonance [22]. Feshbach resonances are characterised by a magnetic field dependent scattering length

$$a(B) = a_{bg}\left(1 - \frac{\Delta}{B - B_0}\right),$$

where Δ is the resonance width and B_0 is the resonance position: Crossing the resonance a varies from $-\infty$ (tightly bound molecule) to $+\infty$ (loosely bound molecule), the phenomenon is clearly visible in BEC-BCS crossover. Incidentally, the binding energy of near-threshold states depends of the scattering length $E_t \sim 1/a^2$.

We can conclude that it is possible to regard the dipole-dipole interactions as a pseudopotential, sum of a short range part and a long range part. The short range term will be characterized by a scattering length a, it can be written like a delta function:

$$V_{\text{contact}}(\mathbf{r}) = \frac{4\pi\hbar^2 a}{m}\delta(\mathbf{r}) = g\delta(\mathbf{r}). \tag{2.1.3}$$

Explicitly, the more general expression for the total (pseudo)potential which we are dealing with reads as:

$$V(\mathbf{r}) = g\delta(\mathbf{r}) + \frac{C_{dd}}{4\pi}\frac{(\mathbf{e}_A\cdot\mathbf{e}_B)r^2 - 3(\mathbf{e}_A\cdot\mathbf{r})(\mathbf{e}_B\cdot\mathbf{r})}{r^5}. \tag{2.1.4}$$

Tuning of the interaction. Purely contact interactions at low energies, as already seen, are characterised by an unique parameter, the s-wave scattering length a, which can be modified e.g. via Fesbach resonances. But more complicated interactions, such as the anisotropic dipolar interaction, can modify, as previously cited, the scattering properties of particles.

Also the dipolar interaction exhibits tunability properties, that makes the dipolar quantum gases particularly interesting and versatile objects in experimental contests. The tunability is represented in the expression of the interaction by the coefficient C_{dd} (Eqn. (2.1.1) and (2.1.4)), trough its dependence of the dipole moment. Because of the scattering properties of the dipolar interaction the tuning of the long range part of the interaction modifies the properties of the short range part, too, as discussed previously and in the cited articles. Precisely, the scattering length is

modified, due to its dependence of the interaction strength. Then it is convenient to define the following "dipolar length":

$$a_{dd} \equiv \frac{C_{dd} m}{12\pi\hbar^2}.$$

It represents the absolute strength of the *dipolar* interaction. Thus it can be shown *[EXACT REFERENCE NEEDED]* that a_{dd} is in relation with the s-wave scattering length (due to *contact* interactions):

$$a = \frac{3g}{C_{dd}} a_{dd}$$

where g is the same as in V_{contact} (2.1.3). In some circumstances the ratio between the two lengths determines the physics of the system: It compares the strength of dipolar and contact interactions; if one wants to observe dipolar effects, the ratio must be non negligible.

But how can one *tune* the interaction strength? Dipole moment can be induced, in the case of neutral molecules without intrinsic dipole moment, by applying an external field (a DC electric field in the case of elecrtic dipoles). However, even in dipolar gases the external field is necessary in order to create a permanent dipole moment: It induces a coupling between spherically symmetric rotational ground state and anisotropic excited state with different spatial parity, reducing quantum and thermal disorder. Once saturation has been reached and disorder is at its minimum, further increasing the intensity of the external field will make the atomic and molecular orbitals polarize, but it is a lower effect.

An external static field is a possible solution to tune the dipolar strength, but it is not the only one. Namely it is possible to decrease by time averaging the dipole-dipole interaction, or even to invert its sign, via a fast rotating external field.

For example, let us consider a gas of magnetic dipoles trapped in somewhat optical trap with low density and temperature. Suppose then to apply a fast rotating external magnetic field

$$\mathbf{B}(t) = B\mathbf{e}(t),$$

where

$$\mathbf{e}(t) = \cos\phi\,\mathbf{e}_z + \sin\phi\,\left[\cos(\Omega t)\mathbf{e}_x + \sin(\Omega t)\mathbf{e}_y\right]$$

and where Ω is the rotation frequency, which we choose simultaneously much greater than the trapping frequency and much smaller than the Larmor frequency. Then the dipolar moment of the dipoles will rotate with the applied field, defining a cone of aperture 2ϕ. The appropriate choice of Ω allows one to average the dipole-dipole interaction over the rotation period $\tau = 2\pi/\Omega$ so that the obtained effective interaction becomes

$$\langle V_{dd}(\mathbf{r})\rangle = \frac{C_{dd}}{4\pi}\frac{1-3\cos^2\vartheta}{r^3}\alpha(\phi).$$

The factor $\alpha(\phi) = (3\cos^2\phi - 1)/2$, result of the time averaging, can be varied in a continuous manner from 1 to $-1/2$ if ϕ is changed, tuning the interactiong strength.

2.2. Dipolar interactions in 2D

2.2.1. 2D confinement. Optical lattices are to some extent the "Petri dishes" of condensed matter physics: They are intended to reproduce the crystalline structure of a solid, with the advantage of only very few or no unknown parameters, and

absence of defects. In optical lattices experiments, the cold atoms plays the role as elecrons in a crystal. The optical lattices are obtained using pairs of counterpropagating lasers, whose intensity and direction can be controlled thus creating almost any kind of lattice. In particular, the lasers can be arranged in order to create a 1D or 2D lattice.

This is the case also for the dipolar Fermi gas, which can be cooled down (e.g. via *sympathetic* cooling, where fermions, in a mixture of fermions and bosons, are cooled down by mean of their interactions with bosons, which adsorbe and then lower, by evaporating, the momentum of the fermions) and the trapped in a 1D lattice of layers, whose lattice parameter and layer thickness can be modulated.

1D lattices of layers of dipolar gases constitue the model we are going to study. The parameters one controls in this model are the dipolar strenght U of particles, which also include the density of the gas (*see* below), the dipolar tilting angle ϑ — by mean of an external field —, and the lattice parameter d. The thickness of the layers, instead, is always assumed to be $w \ll d$, as explained in the following paragraphs.

2.2.2. Intra-layer interaction. Once trapped the gas in layers, we ought to know what the interactions between dipoles of the same layer are. Our system is composed by parallel dipoles, so we consider the following form of the dipole-dipole interaction

$$V_{dd}(\mathbf{r}) = \frac{C_{dd}}{4\pi}\frac{1-3\cos^2\vartheta}{r^3}.$$

The expression for the 2D interaction in the case $\vartheta = 0$ can be recovered [30] by using

$$E_{dd} = \frac{1}{2}\int \tilde{\rho}(\mathbf{r})V_{dd}(\mathbf{r}-\mathbf{r}')\tilde{\rho}(\mathbf{r}')\,d\mathbf{r}d\mathbf{r}' = \frac{1}{2}\int \rho_{\mathbf{q}}\tilde{V}_{dd}(\mathbf{q})\rho_{-\mathbf{q}}\,d\mathbf{q}$$

where, thanks to the optical trapping, we can assume that the density is uniform in the plane and gaussian in the z-direction:

$$\tilde{\rho}(\mathbf{r}) = \frac{1}{\sqrt{\pi w^2}}\exp\left(-\frac{z^2}{w^2}\right)\tilde{n}(x,y) \qquad \rho_{\mathbf{q}} = \exp\left(-\frac{(q_z w)^2}{4}\right)n_{q_x}n_{q_y}$$

with w the width of the gaussian, and

$$\tilde{V}_{dd}(\mathbf{q}) = \mathscr{F}\left[V_{dd}(\mathbf{r})\right] = \frac{4\pi D^2}{3}(3\cos^2\vartheta_q - 1),$$

being $\cos\vartheta_q = \hat{\mathbf{q}}\cdot\hat{\mathbf{z}}$. Including the latter formulae in E_{dd}, one gets, in polar coordinates (q,ϕ) on the xy-plane

$$v_{\vartheta=0}(q) = \frac{8\pi D^2}{3\sqrt{2\pi}w}\left[1 - \frac{3}{2}\sqrt{\frac{\pi}{2}}\mathrm{erfc}\left(\frac{qw}{\sqrt{2}}\right)qwe^{\frac{(qw)^2}{2}}\right],$$

here clearly $q = \sqrt{q_x^2+q_y^2}$. Notice the absence of the azimuthal angle ϕ.

In the general case $\vartheta \neq 0$ a completely analogous derivation yields

$$v_\vartheta(q,\phi) = \frac{2D^2}{3w}\left(\sqrt{2\pi}(3\cos^2\vartheta - 1) - 3\pi qwe^{\frac{(qw)^2}{2}}\mathrm{erfc}\left(\frac{qw}{\sqrt{2}}\right)(\cos^2\vartheta - \cos^2\phi\sin^2\vartheta)\right)$$

which in the limit $qw \ll 1$ (the supposed regime of experiments) reduces to

$$v_\vartheta(q,\phi) = \frac{2\sqrt{2\pi}D^2}{3w}\left(3\cos^2\vartheta - 1\right) - 2\pi D^2 q\left(\cos^2\vartheta - \cos^2\phi\sin^2\vartheta\right).$$

In the following we will drop the subscript ϑ and write only $v(q,\phi)$.

In our calculations we will use the dimensionless quantity $U = mD^2k_F/\hbar^2$ to parametrize the dipolar interaction, where m is the fermion mass and $k_F = \sqrt{4\pi n}$ for a density n of fermions is the modulus of the Fermi wave vector. The constant term in v corresponds to the contact interactions we have described in previous paragraphs.

Then we can define and use the simplified dipolar interaction:

$$v(q,\phi) = 2\pi U\left[V_0 - q\left(\cos^2\vartheta - \sin^2\vartheta\cos^2\phi\right)\right].$$

As already stressed, V_0 is strongly connected to the scattering properties of the dipole-dipole interaction, furthermore V_0 depends of the confinement w, and provides a cut-off for high values of the wave vectors $\Lambda \gg k_F$. [23]

2.2.3. Bilayers: inter-layer interaction. Dipoles in different layers can interact via the inter-layer potential that writes

$$V_{12}(\mathbf{r}_{3D}) = \frac{D^2}{r_{3D}^3}\left(1 - 3\cos^2\vartheta_{r,3D}\right) = \frac{D^2}{(r^2+d^2)^{\frac{3}{2}}}\left(1 - 3\frac{(r\sin\vartheta\cos\phi_r + d\cos\vartheta)^2}{r^2+d^2}\right),$$

here r and ϕ_r are the polar coordinates of the proiection of r_{3D} in the xy-plane. In the very same way we have Fourier-transformed the intra-layer interaction, this can be Fourier transformed too, with the only change in the density distribution that now is given by

$$\rho_1(q_z) = \frac{e^{-\frac{(q_z w)^2}{4}}}{\sqrt{2\pi}} \qquad \rho_2(q_z) = \frac{e^{-\frac{(q_z w)^2}{4}}}{\sqrt{2\pi}}e^{-iq_z d}$$

therefore

$$v_{12}(\mathbf{q}) = \int_{\mathbb{R}} \rho_1(q_z)\tilde{V}_{12}(\mathbf{q})\rho_2(q_z)\,dq_z$$

where $\tilde{V}_{12}(\mathbf{q}) = \mathscr{F}\left[V_{12}(\mathbf{r}_{3D})\right]$. After some algebra, in the limit $w \ll d$ we get the following expression for the inter-layer potential in the space of momenta:

$$v_{12}(\mathbf{q}) = -2\pi U q e^{-qd}\left[\left(\cos^2\vartheta - \sin^2\vartheta\cos^2\phi\right) + i\sin 2\vartheta\cos\phi\right].$$

Notice that the potential is complex in this space. About the analytical aspect, the fact that it is complex originates from the parity properties in the real space, in fact if $\mathbf{r}$ is the projection of $\mathbf{r}_{3D}$ in the xy-plane, then $V_{12}(-\mathbf{r}) \neq V_{12}(\mathbf{r})$ unless $\vartheta = 0$. In the following this will result more clearly.

The complex nature of this potential, besides having a mathematical origin, has a slightly curious physical interpretation. It emerges simply re-writing the angular-dependent part of the potential as follow:

$$v_{12}(\mathbf{q}) = -2\pi U q e^{-qd}\left(\cos\vartheta + i\cos\phi\sin\vartheta\right)^2.$$

The argument into the brackets can be viewed as an ellipse in the complex plane. To change the sense of percurrence of the ellipse, namely the sign of $\cos\phi$, is not distinguishable from to change the orientation from ϑ to $-\vartheta$ for the dipoles in the plane, or equivalently to apply a parity operator.

$$\nearrow\ \nearrow\ \nearrow \qquad \longrightarrow \qquad \nwarrow\ \nwarrow\ \nwarrow$$

$$\begin{cases} \cos\phi > 0,\ \vartheta > 0 \\ \text{or} \\ \cos\phi < 0,\ \vartheta < 0 \end{cases} \quad \overset{\mathbf{r}\mapsto -\mathbf{r}}{\longrightarrow} \quad \begin{cases} \cos\phi < 0,\ \vartheta > 0 \\ \text{or} \\ \cos\phi > 0,\ \vartheta < 0 \end{cases}$$

Moreover, the change in sign of $\cos\phi$ consists in an inversion of the direction of the moment of the interaction propagator, and this finally might be interpreted as we are switching the two layers for each others. Indeed, the parity conjugation in the real space corresponds to the complex conjugation in the reciprocal space; this yelds to

$$v_{12}^{\star}(\mathbf{q}) = v_{21}(\mathbf{q}) \tag{2.2.1}$$

and then straightforwardly to

$$v_{12}^{\star}(\mathbf{q}) = v_{12}(-\mathbf{q}) \quad \Leftrightarrow \quad v_{12}(-\mathbf{q}) = v_{21}(\mathbf{q}). \tag{2.2.2}$$

CHAPTER 3

DENSITY INSTABILITIES IN DIPOLAR FERMI GASES: SINGLE- AND BI-LAYERS GEOMETRIES

The anisotropic nature of dipolar interactions makes dipolar gases be interesting and quite curious systems from a physical point of view. They exhibit a rich phase diagram where exotic phases like stripes emerge from density instabilities. The study and the realisation of such phase transitions are still object of debate, while what seems to be clear is that the random phase approximation, by neglecting exchange correlations, is never sufficiently accurate to describe dipolar gases, giving fallacious and incomplete phase diagrams.

In this chapter we are going to apply the STLS scheme in order to obtain the phase diagram of a quasi-2D dipolar Fermi gas in two different configurations: At first we analyse a single layer geometry, and later we will add a second layer. This two simple models are examinated in order to put in evidence the behaviours tipically due to the intra-layer interaction and separate them from other behaviours induced by the inter-layer interaction. In particular, we attempt here to reproduce results from Ref. [23] and [24], where the full STLS have been applied, for the transition toward the collapse (in the case of a single layer) or toward the $\phi = 0$ stripe phase. In fact, in these cases a simplified STLS scheme can be applied, nevertheless obtaining good results if compared with the complete theory.

Finally, a new calculation is explained that demonstrate how the phase shift in the density modulation (in the bi-layer geometry) may only be due to the dipolar interaction.

3.1. RPA for dipolar fermions: What to do?

What is the limit of validity and what the reliability for a perturbation theory in the study of dipolar Fermi gases? In order to make a comparison we refer to a neutral jellium model of electrons on a positive background; so that we can address the question by a semi-quantitative reasoning, i.e. considering the ratio between the interaction, which we think to as the perturbation, and the mean kinetic energy of a particle. We must account for the following arguments:

- $\rightsquigarrow$ because of the indetermination principle, the kinetic energy is of the order of $\hbar^2/mr_0^2$, with r_0 the radius of the specific volume (volume per particle);
- $\rightsquigarrow$ the Coulomb interaction, instead, within the first neighbours approximation is proportional to $-e^2/r_0$;
- $\rightsquigarrow$ thus the ratio is $\sim r_0$.

The perturbative expansion is valid when the ratio is small, then in the case of electron gas the limit of validity of the perturbational approach is the high-density limit.

An analogue calculation, if developed for a dipolar interaction, yields to a ratio of the order of

$$\sim \frac{1}{a(\phi) r_0}$$

where $a(\phi)$ is a sort of Bohr radius which modulus strongly depends of the direction, mean, of the angle between the one dipole moment and the relative position of the second one with respect to the first. Notice that such a "dipolar length" can assume negative values, too. Nevertheless, the proportionality to r_0^{-1} leads to the conclusion that the perturbation theory is valid when the gas density is small enough.

3.1.1. Why not RPA for dipolar Fermions. We have shown how to improve the RPA method via the so called Singwi-Tosi-Land-Sjölander scheme in Chapter 1, and in Chapter 2 some of the most important features of dipole-dipole interaction have been described.

Now the important question we have to answer is: How much is it important to care about the corrections to the correlations? STLS introduce them by the local field factor $G(\mathbf{q})$: We can show the entity of these corrections through the calculations that follow.

In RPA the system response to a perturbation is that of a non-interacting system to an external potential, which is regarded as the sum of the actual external potential plus an effective potential due to the density perturbation, so that in the expression

$$\delta n(\mathbf{q}, \omega) = \chi(\mathbf{q}, \omega) V_{\text{ext}}(\mathbf{q}, \omega)$$

we replace

$$V_{\text{ext}}(\mathbf{q}, \omega) \mapsto V_{\text{ext}}(\mathbf{q}, \omega) + v(\mathbf{q}) \delta n(\mathbf{q}, \omega)$$

giving

$$\chi^{-1}_{\text{RPA}}(\mathbf{q}, \omega) = \Pi^{-1}(\mathbf{q}, \omega) - v(\mathbf{q}).$$

As already said in previous paragraphs RPA overestimates correlation effects between fermions, then we introduced the local field factor (in fact from a physical point of view it is a correction to the RPA effective potential that stems for correlations), and we included it into the susceptibility:

$$\chi(\mathbf{q}, \omega) = \frac{\Pi(\mathbf{q}, \omega)}{1 - v(\mathbf{q}) \left[1 - G(\mathbf{q})\right] \Pi(\mathbf{q}, \omega)}.$$

We actually take the static limit $\omega = 0$ in our study.

As we have seen, the interaction between the single dipolar molecules can be written as the sum of a contact potential (a δ potential) and the long ranged dipole-dipole interaction:

$$V(\mathbf{r}) = g\delta(\mathbf{r}) + \frac{d^2}{r^3}(1 - 3\cos^2\vartheta)$$

with symbols as in Chapter 2.

If we consider the $r \to 0$, or equivalently the $q \to \infty$ limit, the contact interaction will suppress the long range interaction. As explained extensively later in this chapter, this implies $G(\mathbf{q}) = 1$, thus it arises clearly that exchange correlations uniquely due to the Pauli exclusion are totally neglected in RPA. In the $q \to \infty$ limit then RPA completely fails.

Even in the opposite ($q \to 0$) limit it will be shown that, for a dipolar gas, the RPA is not a good approximation.

Below we will further examine this aspect and then use the STLS formalism to make prediction over the phase transitions of the dipolar Fermi gas.

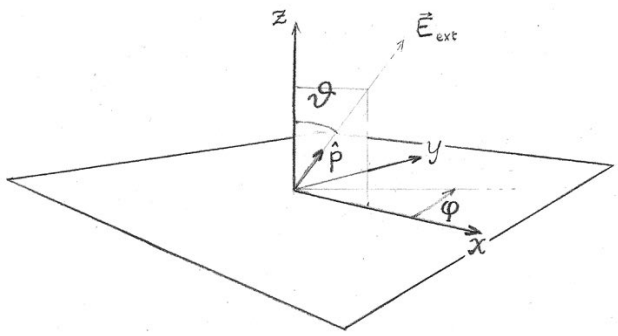

FIGURE 3.2.1. Coordinates frame on a monolayer. The dipole moment $\mathbf{p}$ is aligned to the external field $\mathbf{E}_{ext}$, tilted with an angle ϑ in the zx-plane.

3.2. Single layer geometry

Geometry of the system. The dipole gas is reduced to a 2D system through an harmonic potential in the z direction, which works as a confining potential. By mean of this potential we can infer that the wavefunction along the z-axis is the one of an harmonic oscillator, and we and we make the assumption, being at zero temperature, that the gas is in its ground state. So the denisty of dipoles in the direction transversal to the plane has a gaussian distribution, as explained in § 2.2.

We furthermore assume that the gas is initially homogeneus, and that we can make use of an external constant and uniform electrostatic potential, in order to keep the dipoles all aligned along a unique direction: We define ϑ as the tilting angle of the dipoles with respect to the normal to the layer, the z-axis. The projection of the dipole moment on the plane will define the x coordinates axis, and we can eventually define a polar coordinates system (ρ, ϕ) on the plane such that the x-axis will coincide with the direction $\phi = 0$. Notice that the ϕ coordinate will be preserved by the Fourier transform. In this manner, we have a well defined coordinate system on our layer (*see* Figure 3.2.1).

Finally, in order to isolate the significant quantities of this problem it is useful to define dimensionless units, by renormalizing the moment with respect to k_F and by using $m = \hbar = 1$. In this way the dipolar system is parametrized solely by the angle ϑ and by the interaction strength $U = mD^2k_F/\hbar^2$.

3.2.1. Recalls on STLS. Moving from the background of the first chapter it is possible to start analyze our system, constitued by a flat layer of fermionic dipoles. We begin by reminding the self-consistent equations of the STLS scheme, for a system of a single species of fermions:

$$G(\mathbf{q}) = -\frac{1}{n}\int \frac{d\mathbf{k}}{(2\pi)^2}\frac{\mathbf{q}\cdot\mathbf{k}}{q^2}\frac{v(\mathbf{k})}{v(\mathbf{q})}[S(\mathbf{q}-\mathbf{k})-1] \tag{3.2.1}$$

$$S(\mathbf{q}) = -\frac{\hbar}{n\pi}\int_{-\infty}^{\infty}\Im[\chi(\mathbf{q},\omega)]d\omega = -\frac{\hbar}{n\pi}\int_{0}^{\infty}\chi(\mathbf{q},i\omega)d\omega \tag{3.2.2}$$

$$\chi(\mathbf{q},\omega) = \frac{\Pi(\mathbf{q},\omega)}{1-v(\mathbf{q})\left[1-G(\mathbf{q})\right]\Pi(\mathbf{q},\omega)}. \tag{3.2.3}$$

The first step is to consider a 0^{th}-order approximation i.e. to start with a non interacting system, and then stop at the first recursion, that is: As we are dealing with a 2D system the susceptibility is at first recovered as the following Lindhard function (*see* § 1.3.1), relative to a non-interacting system:

$$\Pi_i(\mathbf{q}, i\omega) = \frac{m_i^2}{2\pi q^2}\left\{\sqrt{2}\sqrt{a_i + \sqrt{a_i^2 + \left(\frac{\omega q^2}{m_i}\right)^2} - \frac{q^2}{m_i}}\right\} \qquad a_i = \frac{q^4}{4m_i^2} - \frac{q^2 k_{F,i}^2}{m_i^2} - \omega^2,$$

then the static structure factor writes

$$S_{ij}^{(0)}(\mathbf{q}) = -\frac{\delta_{ij}}{n\pi}\int_0^\infty \Pi_i(\mathbf{q}, i\omega)d\omega$$

(where the indices i, j indicate the layers or, eventually different species of fermions) and it is possible to demonstrate [11] that in this case it takes the following analytical expression:

$$S_{ij}^{(0)}(\mathbf{q}) = \delta_{ij}\begin{cases} \frac{2}{\pi}\arcsin\left(\frac{q}{2k_{F,i}}\right) + \frac{q}{\pi k_{F,i}}\sqrt{1 - \left(\frac{q}{2k_{F,i}}\right)^2} & q < 2k_{F,i} \\ 1 & q \geq 2k_{F,i}. \end{cases}$$

The interacting potential must be now included into the STLS equations. The Fourier transform for the interaction between dipoles in a plane can be calculated, giving as seen previously (§ 2.2)

$$v(q, \phi) = 2\pi U\left(V_0 - q\left(\cos^2\vartheta - \sin^2\vartheta\cos^2\phi\right)\right). \tag{3.2.4}$$

The latter is the dipole-dipole interaction for parallely aligned dipoles. Notice that D represents the dipole moment, whereas the term V_0 in (3.2.4) is a constant representing the contact interaction, and we recall it is related to the thickness of the layer, so $\Lambda \sim 1/w \gg k_F$ provides a natural cut-off for high q.

In order to find the density instabilities of the system we must study its dielectric function. It is useful then to explore the limit behaviours of the local field factor, which we are going to estimate within the STLS scheme for a system of dipoles. As we will see, STLS will represents great improvement of the RPA, which on the contrary turns out to be always unaccurate for dipolar interactions.

First: retrieving RPA. Working within the RPA scheme, in which exchange correlations are completely neglected, essentially means to impose $G(\mathbf{q}) = 0$.

Then it is necessary to understand the meaning of $G(\mathbf{q}) = 0$ in the STLS picture, and show its relationship with the pair correlation function. Let us move from equation (3.2.1), after notice the evident fact that G is actually independent of $\mathbf{q}$, indeed it is a constant. In this case we impose:

$$0 = -\frac{1}{n}\int \frac{1}{(2\pi)^2}\frac{\mathbf{q}\cdot\mathbf{k}}{q^2}\frac{v(\mathbf{k})}{v(\mathbf{q})}[S(\mathbf{q} - \mathbf{k}) - 1]\, d\mathbf{k};$$

it is always possible to eliminate the dependence of $\mathbf{q}$ in $S(\mathbf{q} - \mathbf{k})$ by mean of the substitution $\mathbf{k} \mapsto \mathbf{p} + \mathbf{q}$, obtaining

$$0 = \int \frac{\mathbf{q}\cdot(\mathbf{p} + \mathbf{q})}{q^2}\frac{v(\mathbf{p} + \mathbf{q})}{v(\mathbf{q})}[S(\mathbf{p}) - 1]\, d\mathbf{p}.$$

We are left with the problem of how to eliminate the dependence of $\mathbf{q}$ in the right side of the equation. Imposing $q^2 v(\mathbf{q}) \neq 0$, we obviously recover

$$\int \left(q + p\cos(\phi_p - \phi_q)\right) v(\mathbf{p}+\mathbf{q}) \left[S(\mathbf{p}) - 1\right] \, d\mathbf{p} = 0.$$

There are only two possibilities: the first is to choose $\mathbf{q} = \mathbf{q}(\mathbf{p})$, but it does not make sense, because $\mathbf{q}$ and $\mathbf{p}$ are two independent variables. Then it clearly results that the only possibility to get the equality is for $S(\mathbf{p})$ to be identically 1.

Finally, the following relationship stands:

$$\mathbf{g}(r) = 1 + \frac{1}{n}\mathscr{F}[S(\mathbf{q}) - 1],$$

leading to $\mathbf{g}(r) = 1$, that is: $G(q) = 0$ is equivalent to neglect any correlation in the system.

Second: purely contact interaction. At very short distancies the dipolar interaction becomes negligible, and we are left with an extremely strong (δ-like) central contact potential, due to Pauli exclusion. Then the study of the scattering properties at low energies ($T = 0$) can be treated as the scattering from a central potential, excluding anisotropies arising from the dipole-dipole interaction.

So consider the expression of $G(\mathbf{q})$ in the case of a constant potential $v(\mathbf{q}) = V_0$:

$$G(\mathbf{q}) = -\frac{1}{n}\int \frac{d\mathbf{p}}{(2\pi)^2} \frac{q^2 + \mathbf{q}\cdot\mathbf{p}}{q^2} [S(\mathbf{p}) - 1];$$

in polar coordinates, imposing $k_F = 1$

$$\begin{aligned} G(q,\phi_q) &= -\frac{1}{\pi}\int_0^{2\pi} d\phi_p \int_0^{+\infty} \frac{q^2 + qp\cos\left(\phi_p - \phi_q\right)}{q^2} [S(p,\phi_p) - 1] p\, dp \\ &= -\frac{1}{\pi}\int_0^{2\pi} d\phi_p \int_0^{+\infty} [S(p,\phi_p) - 1] p\, dp + \\ &\quad -\frac{1}{\pi}\int_0^{2\pi} d\phi_p \int_0^{+\infty} \frac{p^2\cos\left(\phi_p - \phi_q\right)}{q} [S(p,\phi_p) - 1]\, dp. \end{aligned}$$

It must be considered now that the static structure factor, in the case of constant potential, does not depend at all of the angle: In fact $S^{(0)}$ does not, and at higher orders of iterations an angular dependence could enter the structure factor only via the potential, which in turn is constant. Therefore the second term is zero by integrating over ϕ_p and we are left with

$$\begin{aligned} G(q,\phi_q) &= -\frac{1}{\pi}\int_0^{2\pi} d\phi_p \int_0^{+\infty} [S(p) - 1] p\, dp \\ &= 1 - \left(1 + \frac{1}{\pi}\int_0^{2\pi} d\phi_p \int_0^{+\infty} [S(p) - 1] p\, dp\right) \end{aligned}$$

where the argument between parenthesis is

$$\mathbf{g}(r = 0) = 1 + \frac{1}{\pi}\int_0^{2\pi} d\phi_p \int_0^{+\infty} [S(p) - 1] p\, dp.$$

From previous discussion we know that (*see* also § 1.3.2) $\mathbf{g}(0) = 0$, henceforth

$$G(q,\phi_q) = 1 - \mathbf{g}(0) = 1.$$

What has been achieved is that being the potential a merely contact interaction the local field factor reaches the value $G = 1$, meaning that we are in presence of an isotropic non-interacting system.

In the specific case of the dipolar potential, we have already seen it is possible to divide the potential in two contribution: a constant term leading to a constant contribute to G, and a second term depending of $\mathbf{q}$. By imposing the physical constraint $\mathbf{g}(0) = 0$, one can see that the local field factor makes the suceptibility independent of the constant term, for by defining $G(\mathbf{q}) = \breve{G}(\mathbf{q}, v(\mathbf{q}))/v(\mathbf{q})$, and by using the short notation $v(\mathbf{q}) = 2\pi U(V_0 - qA(\phi_q))$ where $A(\phi_q) = \cos^2\vartheta - \sin^2\vartheta\cos^2\phi_q$, the dielectric function writes:

$$\begin{aligned} 1 - v(q)\,(1 - G(q))\,\Pi_0 &= 1 - v(q)\left(1 - \frac{\breve{G}(\mathbf{q}, v(\mathbf{q}))}{v(\mathbf{q})}\right)\Pi_0 \\ &= 1 - \left(2\pi U(V_0 - qA(\phi_q)) - \breve{G}(\mathbf{q}, v(\mathbf{q}))\right)\Pi_0 \\ &= 1 + 2\pi U\left(qA(\phi_q) - \breve{G}(\mathbf{q}, qA(\phi_q))\right)\Pi_0 \end{aligned}$$

so there is not dependence of V_0 at all thanks to $\mathbf{g}(0) = 0$. The unphysical dependence of V_0 can be removed at each order of iteration by imposing the constraint $\mathbf{g}(0) = 0$.

Third: $q \to 0$ limit behaviour for a weakly interacting system. For an electron gas in the $q \to 0$ limit the RPA is a good approximation, as it can be shown. On the contrary for dipolar system this is not true: In order to demonstrate it, one can estimate $G(q \to 0)$, that can be done by using the compressibility sum rule

$$\lim_{q\to 0} \chi^{-1}(q, \omega = 0) = -\frac{\partial^2}{\partial n^2}(n\varepsilon),$$

which can be rewritten

$$\lim_{q\to 0} G(q) = 1 - \frac{1}{V_0}\left(\frac{\partial^2}{\partial n^2}(n\varepsilon) - 1\right).$$

Thus it is sufficient to calculate the fundamental state energy ε of the system and include it in the latter equation. A good choice for ε is the Hartree Fock mean field approximation, which is expected to work fine at least for weakly interacting systems ($U \ll 1$). The ε_{HF} writes

$$\varepsilon_{HF} = \frac{1}{2}nv(0) + \frac{1}{2V}\sum_{\mathbf{q}} v(\mathbf{q})\,(S_0(\mathbf{q}) - 1)$$

where the continuous limit can be taken, that is identical to the 0^{th}-order STLS interaction energy, and gives

$$\varepsilon_{HF} = \frac{4\pi n\hbar^2}{m}\left[\frac{1}{4} + \frac{16}{45\pi}U\,(3\cos 2\vartheta - 1)\right].$$

For the sake of simplicity and without loss of generality we choose $\vartheta = 0$. Now, by using the compressibility sum rule we can extract informations about the local field factor:

$$G(0) = 1 - 32\hbar^2\frac{U}{3mV_0}.$$

Because we are in the weak interaction limit, the interaction strength U is small, and $G(0) \simeq 1$ so that RPA fails one more time.

In conclusion, it is now clear that RPA can never be a satisfying approximation when dealing with dipole gases.

3.2.2. Applying STLS: study of the phase diagram. In Figure 3.2.2 the complete phase diagram of the single-layer geometry of a dipolar Fermi gas is shown. In this chapter we are only interested in the transition toward the collapsed phase, as it is well reproduced also by a one-iteration STLS scheme.

Starting from low tilting angles, we note the improvement of predictions by the RPA: the stripe phase boundary is shown that results to be shifted at higher U with respect to the RPA boundary, this is because in the STLS includes corrections to interaction correlations that were overestimated otherwise. The stripe phase exhibit a density instability whose wave vector is oriented like the y-axis, i.e. orthogonally to the direction of the dipole alignment.

At higher ϑ a p-wave superfluid phase is found, due to correlations between fermions with anisotropic interaction.

Finally, the collapsed phase is encountered for sufficiently strong interactions ($U > 1$) and high dipoles tilting. The RPA does not predict this phase at all, whereas HF partially does (HF underestimates U at which transition occurs): this is simply because this transition is led by exchange correlation and attractive interactions overwhelm Pauli exclusion. This is also the cause for which one iteration of the STLS scheme is enough to describe rather correctly the collapse boundary, as explained later on. A fundamental aspect of this intability is that the compressibility goes to infinity in the collapsed phase boundary. Actually it is anisotropic, i.e., goes to infinity only for $\phi = 0$ [23]. The soundness of this transition is that of a BCS-BEC crossover: The system goes from a p-wave Cooper pairing to a three body bound state, like in a Feshbach resonance. A last important remark must be done for the $\vartheta = \pi/2$ case.

Full v/s zeroth order. Our aim is to estimate the local field factor. The first step in the STLS scheme is to consider the non interacting susceptibility Π_0 and insert the obtained $S_0(\mathbf{q})$ in the expression for $G(\mathbf{q})$, which can be called $G^{(1)}(\mathbf{q})$; to take $S(\mathbf{q}) = S_0(\mathbf{q})$ is equivalent to the choice $G^{(0)}(\mathbf{q}) = 1$. Then $G^{(1)}(\mathbf{q})$ includes exchange correlations only. We can call the first iteration step the 0^{th}-order STLS. The so-called full STLS, instead, consists of repeated iterations till the convergence of the self-consistent method. Note that the STLS scheme does not assure $\mathbf{g}(0) = 0$ at each iteration step, so an improved version of the scheme may be applied [23]: $\mathbf{g}(0) = 0$ is used as a constraint, and a corrective term $\delta S(\mathbf{q})$ is added to $S(\mathbf{q})$ then substituing $S \to S + \delta S$ in the scheme, similarly to Ref. [29]. In particular, the *ansatz*

$$\delta S(\mathbf{q}) = \left(S_0(\mathbf{q}) - S(\mathbf{q}) + A e^{-q^{2/(2k_F)^2}} \right) \left(1 - e^{-q^{2/(2k_F)^2}} \right)$$

is used to interpolate S for $q < 2k_F$ and the non interacting one S_0 for $q \gg 2k_F$.

However, here we are interested only in the 0^{th}-order, as it provides good results for the transition at $\phi = 0$ and high ϑ.

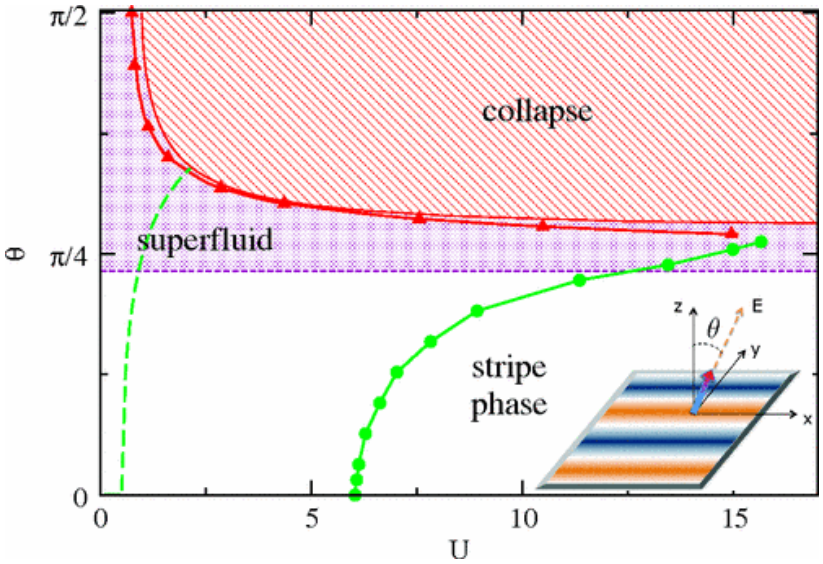

FIGURE 3.2.2. Complete phase diagram of the 2D dipolar gas. Here the collapse boundary calculated with full STLS (red triangles) approximation is compared with 0^{th}-order STLS (red solid line). At small ϑ another phase is present, that is the $\phi = \pi/2$ stripe phase (green circles), which boundary has been calculated with full STLS approximation and RPA (dashed green line). In this case the boundary is noticeably shifted, because RPA underestimate interaction correlations. A superfluid phase is visible, too, which at the moment we are not interested in. Image from Ref. [*CITAZIONE*]

3.2.3. System's instabilities. We proceed with our analysis by looking at the density-density response function of the system, taking the static limit, i.e.:

$$\chi(\mathbf{q}, \omega = 0) = \frac{\Pi(\mathbf{q})}{1 - v(\mathbf{q})\,[1 - G(\mathbf{q})]\,\Pi(\mathbf{q})}$$

and in this case the polarization takes (in our dimensinless units) the simpler form

$$\Pi(\mathbf{q}, \omega = 0) = \Pi(q) = \frac{1}{2\pi}\left[\frac{\sqrt{q^2 - 4}}{q}\Theta(q - 2) - 1\right].$$

The density-density response function gives a lot of information about the system, and, as an example, we can search for phase transition. Some property of the phases are provided by the compressibility sum rule (1.2.3).

First of all, we examinate the conditions under which the system undergoes density intabilities. Operatively, it means that we must find a divergence in the susceptibility, but it is clearly convenient to look for zeros of the inverse of the (renormalized) susceptibility, instead:

$$\Pi\chi^{-1}(\mathbf{q}) = 2\pi U(V_0 - q(\cos^2\vartheta + \sin^2\vartheta\cos^2\phi))(1 - G(\mathbf{q}))\Pi(q). \tag{3.2.5}$$

So, intabilities manifest when $\Pi\chi^{-1}(\mathbf{q};\vartheta) = 0$; it is a function of $\mathbf{q}$ and the tilting angle ϑ is considered as a parameter, in particular, for each fixed U, the higer is ϑ the lower values the curve $\Pi\chi^{-1}$ gets.

The new phase, at least in the proximities of the transition point, will show a density modulation which is periodic with $\underline{\mathbf{q}}$, where we understand that it is the wave vector at which instability occurs.

Minimum of $\Pi\chi^{-1}$. This function does not evolve smoothly in each variables (think at the polarization or at the static structure factor), implying we cannot find minima by a simple derivative with respect to each of this variable. Even more, sometimes it will be not possible at all, because we need a numerical evaluation of the static structure factor.

Briefly, we look for minima in q and ϕ and evaluate if these minima are affected by the system's paremeters U and ϑ.

U and ϑ effects. It follows immediately from derivation with respect to ϕ that U will not modify at all the position of the minima in (3.2.5):

$$\frac{\partial}{\partial\phi}\Pi\chi^{-1} = \frac{\partial v}{\partial\phi}(1-G) + v\left[\frac{\partial G}{\partial\phi}\right] = 0$$

where U simply has eliminated indeed.

More complicated is the case of the parameter ϑ. The most direct way to evaluate this peculiarity is to trace some graphic numerically. It emerges that effectively $\Pi\chi^{-1}$ changes with ϑ, as described above, but for large values of this - which we are interested in - the position of minimum does not vary. Precisely, we find that the minimum in q is not a stationary point, and it take place at $q = 0$ (see Figure 3.2.3).

Minima in ϕ. We have already demonstrate that the minimum of the rinormalized inverse of the susceptivity is indipendent of ϑ and U, it would be great now to find out if there are convenient conditions in which caluculate, if it exists, the boundary of a phase with infinite compressibility. We know that the system is non-isotropic, and this suggests that maybe it would be a preferred direction where our layer might manifest its instabilities. This would be the case if the quantity $\Pi\chi^{-1}(q,\phi)$ had a minimum along a certain direction, determined by ϕ.

Let us assume first that $\Pi\chi^{-1}$ is a smooth function of ϕ:

$$\Pi\chi^{-1}(q,\phi) = 1 - 2\pi U(V_0 - q(\cos^2\vartheta + \sin^2\vartheta\cos^2\phi))(1-G(q,\phi))\Pi(q).$$

Now we look for stationary points by imposing the condition $\frac{\partial\Pi\chi^{-1}}{\partial\phi} \stackrel{!}{=} 0$, i.e. we must find the roots of

$$q\left(\sin^2\vartheta\sin 2\phi\right)(1-G(q,\phi))\,\Pi(q) + \\ + \left(V_0 - q\left(\cos^2\vartheta + \sin^2\vartheta\cos^2\phi\right)\right)\left(\frac{\partial G}{\partial\phi}(q,\phi)\right)\Pi(q) = 0.$$

At this point of the discussion we do not know whether the stationary point is a saddle, a maximum or a minimum point, and in order to obtain a complete information we should consider the gradient $\nabla\left(\Pi\chi^{-1}(q,\phi)\right)$. But we have already seen, numerically, that the minimum is always in $q = 0$, hence we can try and ignore the dependence of q to outdraw a sort of equation of motion of G as a function of ϕ

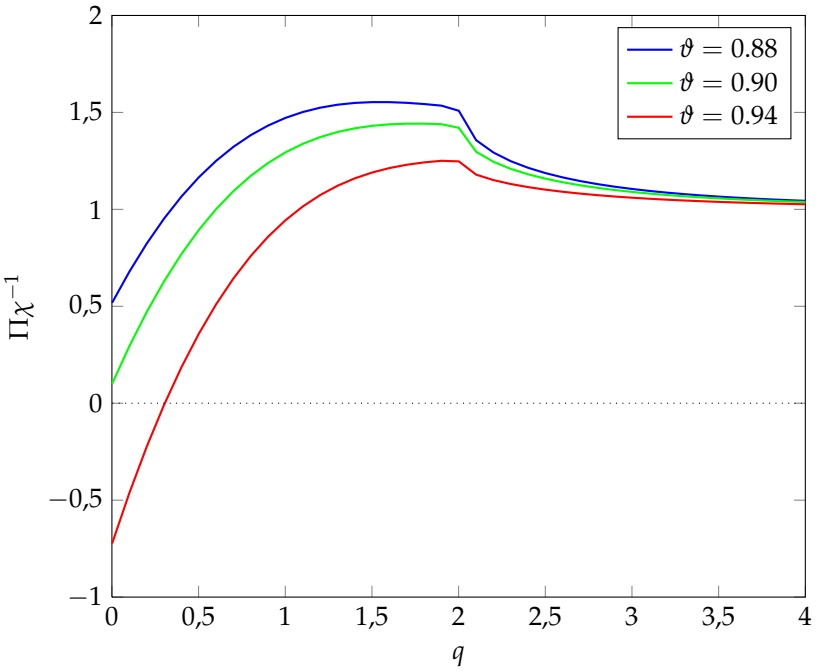

FIGURE 3.2.3. Behaviour of $\Pi\chi^{-1}$ varying ϑ: minimum in $q = 0$ does not move. We are observing the susceptibility behaviour for a fixed $U \simeq 3$ and fixed $\phi = 0$.

only, then looking at q as a parameter. After a trivial algebraic passage, this is the new form of the latter equation:

$$\frac{1}{1 - G_q}\frac{dG_q}{d\phi} = \frac{-q \sin^2\vartheta \sin 2\phi}{V_0 - q\left(\cos^2\vartheta + \sin^2\vartheta\cos^2\phi\right)},$$

that can be straightforwardly solved via variable sparation. From integration we get:

$$\frac{1 - G_q(0)}{1 - G_q(\phi)} = \frac{-2q + 8V_0 - 6q\cos 2\vartheta + 4q\cos 2\phi \sin^2\vartheta}{-2q + 8V_0 - 6q\cos 2\vartheta + 4q\sin^2\vartheta}. \tag{3.2.6}$$

We can now impose the constrain $q = 0$.

$$G_0(0) = G_0(\phi), \tag{3.2.7}$$

meaning that the direction $\phi = 0$ is a good candidate.

The minimum condition is verified if $\lim_{q\to 0}\Pi\chi^{-1}(q,\delta) - \Pi\chi^{-1}(q,0) > 0$ for small δ at least. The latter condition is completely equivalent to $\lim_{q\to 0} G_q(\delta) - G_q(0) < 0$, which can be verified numerically. Then the direction $\phi = 0$ is the one minimizing $\Pi\chi^{-1}$, even not necessarily the only one: In (3.2.6), in fact, one can see a periodic dependence on 2ϕ. Actually both in RPA (analitically) and in STLS (numerically) a minimum is encountered in $\phi = \pi/2$.

3.2.4. Phase transition. We are able to find a phase transition boudary, by looking for the values of the two system's parameters ϑ and U within the constraint $\min_q \{\Pi\chi^{-1}\} = 0$.

The most direct way to find the boundary is to find a relation between ϑ and U. We could glimpse what results from the constraint:

$$\min_q \left\{\Pi\chi^{-1}\right\} \quad = \quad \min_q \left\{1 - 2\pi U(V_0 - q(\cos^2\vartheta + \sin^2\vartheta\cos^2\phi))(1 - G(q,\phi))\Pi(q)\right\}$$

that, once imposed $\min_q \{\Pi\chi^{-1}\} = 0$, leads to the conclusion

$$U = \frac{1}{2\pi \max_q \{(V_0 - q(\cos^2\vartheta + \sin^2\vartheta\cos^2\phi))(1 - G(q,\phi))\Pi(q)\}}.$$

Then one can equivalently search the maximum of the denominator or imposing the values of the variables that have been found to minimize the normalized susceptibility. In this case we already know, from previous paragraphs, what these values are, than we simply impose them and find the curve as a function of ϑ.

Evaluation of the points of the curve must be done numerically. The phase boundary obtained with the STLS scheme for $\phi = 0$ is visible in Figure 3.2.2: One immediatly notice that an asymptote of the boundary emerges in the limit $U \to \infty$. We define the value of the angle corresponding to the asymptote as the critical tilting angle ϑ_c. Equivalently it is possible to introduce the critical interaction strength U_c as the value of U at which transition occurs for $\vartheta = \pi/2$.

In the monolayer case $\vartheta_c \simeq 0.88$ is recovered.

An important consideration must be done: For sufficiently strong dipoles (large U) and large dipole tilting, the system of one layer undergoes a collapse. It is known from the compressibility sum rule (1.2.3), which tells us that the compressibility goes to infinity being $q \to 0$. Furthermore, the value of the momentum q at which the system gets the instability allows to catch the term of the Fourier transform of the density fluctuations that is dominating in the phase transition. In this case the term is that describing the $\lambda \to \infty$ wavelength, i.e. the density fluctuations involving the whole layer.

3.3. Bilayer geometry

Thanks to the study of the one-layer system, it has been possible to classify behaviours and peculiarities exclusively due to the intra-layer interaction, such as the collapse of the dipolar Fermi gas. But in general, real systems are composed by a great number of layers. The our simple model can be made more complex if a second layer is added at a distance d to the first one. This is a first step in the direction of a multi-layer system. What is new, in this case, is the presence of an interlayer potential, i.e. the interaction between the fermions confined in two distinct layers. It would be conceptually the same if we were treating a mixture of two distinguishable fermions. More precisely the system is constitued by two layers, the first lies in the xy-plane and the second, parallel to the first, overlies at a distance $z = d$.

Multiple coupling and susceptibility. In these systems a multiple coupling density-density response function has to be considered (see § 1.1.3) instead, as explained below.As for the case of the monolayer, we are interested in the density properties of the system; now the layers are two, and each of them will respond to external perturbations and to the interlayer interactions showing density fluctuations. In this system, the susceptibility is described by a matrix, and the fluctuations of the density in the two layers are coupled as cast by the law

$$\left\langle \hat{A}_k(\mathbf{r},t)\right\rangle = 2i\sum_j \int_{-\infty}^{t} dt' \int \chi''_{A_kA_j}(\mathbf{r},\mathbf{r}',t-t')f_j(\mathbf{r}',t')\,d\mathbf{r}'$$

as already explained in § 1.1.3 ($\hat{A}_i = \delta n_i$ is the density fluctuation of the i-th layer).

Actually the susceptibility matrix is hermitic, then it can be diagonalized and its eigenvalues are real.

Each distinct eigenvector gives informations about a distinct configuration of the system. Precisely, each talks about the relationships between the density fluctuations in the various layers. it is well known that to each eigenvector is associated an eigenvalue. Then, as we are studying the density-density response function, we can associate to each configuration of the system its susceptibility. Furthermore, as the matrix has been diagonalized, we can order the eigenvalues and then the possible configurations from the more stable to the less stable. Let us suppose that the system undergoes a transition if some parameter varies: The configuration assumed from the system after the transition is the one that was less stable, i.e. the one which susceptibility eigenvalue would have reached a singularity first. The other configurations will not realize at all, and are not physical.

It is clear that we are only interested in the state which susceptibility is the very next to a singularity.

3.3.1. RPA approximation for a system of two layers. Even though we already know that the RPA is never a good approximation, it can be useful, before to proceed and apply STLS, to very breifly present some calculations within the RPA approximation that we can use as to make a comparison.

All evaluations in this approximation can be done analytically, first of all because we are neglecting both intra and inter-layer exchange correlations, and this

traduces in $G_{ij} = 0$. Then the $\hat{\chi}^{-1}$ matrix simplifies and takes the form

$$\hat{\chi}^{-1} = \begin{pmatrix} \frac{1}{\Pi} - v_{11} & -v_{12} \\ -v_{12}^{\star} & \frac{1}{\Pi} - v_{11} \end{pmatrix}.$$

Its inverse matrix, the susceptibility, has two distinct eigenvalues:

$$\chi_{\mp} = \frac{\left(\chi^{-1}\right)_{\mp}}{\det\left(\hat{\chi}^{-1}\right)} = \frac{1}{\left(\chi^{-1}\right)_{\pm}} \tag{3.3.1}$$

where the eigenvalues of the inverse susceptivity are

$$\left(\chi^{-1}\right)_{\pm} = \chi_{11}^{-1} \pm \left|\chi_{12}^{-1}\right|;$$

here χ_{11}^{-1} and χ_{12}^{-1} are the corresponding matrix elements of $\hat{\chi}^{-1}$. Clearly the eigenvalues of $\hat{\chi}$ are the opposit of those of $\hat{\chi}^{-1}$.

Now in order to find the "directions" in the system, namely sets of variables and parameters, along which instabilities are favoured, we look for the minor between the two quantities $\Pi\left(\chi^{-1}\right)_{+}$ and $\Pi\left(\chi^{-1}\right)_{-}$, and then for its minimum. It is the very same procedure we followed in the monolayer case, but for the fact that susceptibility was a scalar. Back to the bilayers, we must operate a choice between the eigenvalues: being the Lindhard function a negative function, we immediately choose the eigenvalue $\left(\chi^{-1}\right)_{+}$.

In the RPA approximation the direction (in the sense specified above) minimizing the normalized susceptibility is still independent of the tilting of the dipoles, as one can promptly verify: $\phi = \frac{\pi}{2}$ must be choosen. Then, but in reality independently of ϕ, as in the monolayer case, it is found to be $q_c = 2k_F$ the critical value of the momentum. In this way, the phase transition boundary is

$$U = \frac{1}{2\cos^2\vartheta\left(1 + e^{-2d}\right)}$$

and we are not in presence of a collapse, in this case as well as in the monolayer case within the same approximation.

What if $G_{ii} = 1$? An improved RPA for two layers. As alredy pointed out, the limit $G = 1$ means that there are only contact interactions in the system we are considering. It is a quite interesting exercise to isolate the inter-layer interaction by supposing for a while to kill intra-layer interactions. We are watching at what would be going on if the transition were led by inter-layer potentials, indeed. This already constitues an improvement of the RPA, because, at least for intra-layer interactions, by imposing $G_{11} = G_{22} = 1$ we are including corrections to the correlation.

Let's begin directly considering the eigenvalues matrix of susceptibility

$$\hat{\tilde{\chi}} = \frac{1}{\det(\hat{\tilde{\chi}}^{-1})} \begin{pmatrix} \lambda_{+} & 0 \\ 0 & \lambda_{-} \end{pmatrix}$$

where in this particular case $\lambda_{\pm} = \frac{1}{\Pi} \mp |v_{12}|$ and then the eigenvalues writes $\tilde{\chi}_{\pm} = \left(\frac{1}{\Pi} \pm |v_{12}|\right)^{-1}$. This time too we will choose the $\tilde{\chi}_{+}$ value for our pourposes,

as $\Pi\tilde{\chi}_+^{-1} < \Pi\tilde{\chi}_-^{-1}$. Now the minimum of $\Pi\tilde{\chi}_+^{-1}$ occurs at

$$\begin{cases} q = \frac{1}{d} & \text{if } d \geq 2 \\ q = 2 & \text{if } d < 2 \end{cases} \quad \text{and} \quad \begin{cases} \phi = 0 + 2k\pi & \text{or} \\ \phi = \frac{\pi}{2} + k\pi, & k \in \mathbb{Z} \end{cases}$$

and we can see two important things: The first is the *stabilization* of the system *exactly via the inter-layer potential*, because the minimum of q will never occur at $q = 0$. Well, it could occur for $d = \infty$, but clearly we are not interested in this. Second: RPA-like behaviours appers once more if the two layers are close enough to each other, so we could imagine that things go almost as there was an intra-layer interaction without exchange correlation effects.

As a final consideration, we write the phase boundary expression:

$$U = \frac{1}{2\pi q_c e^{-q_c d}\left(\left(\cos^2\vartheta - \mathfrak{f}\sin^2\vartheta\right)^2 + \mathfrak{f}\sin^2 2\vartheta\right)^{\frac{1}{2}}}$$

where the symbolic expression $\mathfrak{f}$ stands for 1 if $\phi = 0$ and for 0 if $\phi = \frac{\pi}{2}$.

3.3.2. Bilayer within the STLS scheme. It is then necessary to update the STLS equation by including the peculiarities of two differents layers.

Briefly, we write the new set of self-consistent equations of the STLS scheme for the bi-layer system.

$$S_{ij}(\mathbf{q}) = -\frac{\hbar}{n\pi}\int_0^\infty \chi_{ij}(\mathbf{q}, i\omega)d\omega$$

$$G_{ij}(\mathbf{q}) = -\frac{n}{n_i n_j}\int \frac{d\mathbf{k}}{(2\pi)^2}\frac{\mathbf{q}\cdot\mathbf{k}}{q^2}\frac{v_{ij}(\mathbf{k})}{v_{ij}(\mathbf{q})}\left[S_{ij}(\mathbf{q}-\mathbf{k}) - \frac{n_i}{n}\delta_{ij}\right]$$

and finally now the response function is a 2×2 matrix:

$$\chi_{ij}^{-1} = \frac{\delta_{ij}}{\Pi_i} - v_{ij}(1 - G_{ij}).$$

Beyond to ensure the reality of the potential in the direct space, the relations (2.2.1) and (2.2.2) will simplify the susceptibility matrix, which is expected to be hermitic. His inverse writes

$$\hat{\chi}^{-1} = \begin{pmatrix} \frac{1}{\Pi_1} - v_{11}(1 - G_{11}) & -v_{12}(1 - G_{12}) \\ -v_{12}^\star(1 - G_{12}^\star) & \frac{1}{\Pi_2} - v_{11}(1 - G_{11}) \end{pmatrix}$$

and assuming the same *species* of molecules (then with the same *mass*) and the same numeric density in the two layers we can impose $\Pi_1 = \Pi_2 = \Pi$: in fact the only properties of the system that could affect the validity of this assumption are these two we mentioned, but effectively we are here considering identical layers.

The symmetry properties of the relations (2.2.1) and (2.2.2), transfer to the whole set of STLS equation via the self-consistency of the equations themselves, as it will be skatched below.

(1) $G_{12}(-\mathbf{q}) = G^{\star}_{12}(\mathbf{q}) \;\rightarrow\; S_{12}(-\mathbf{q}) = S^{\star}_{12}(\mathbf{q})$: this is readily demonstrated starting to the definitions of G and S:

$$\begin{aligned} G_{12}(\mathbf{q} \mapsto -\mathbf{q}) \quad &= \quad +\frac{n}{n_1 n_2}\int \frac{d\mathbf{k}}{(2\pi)^2}\frac{\mathbf{q}\cdot\mathbf{k}}{q^2}\frac{v_{12}(\mathbf{k})}{v_{12}(-\mathbf{q})}S_{12}(-\mathbf{q}-\mathbf{k}) \\ &\overset{\mathbf{k}'=-\mathbf{k}}{=} \quad -\frac{n}{n_1 n_2}\int \frac{d\mathbf{k}'}{(2\pi)^2}\frac{\mathbf{q}\cdot\mathbf{k}'}{q^2}\frac{v^{\star}_{12}(\mathbf{k}')}{v^{\star}_{12}(\mathbf{q})}S_{12}(\mathbf{k}'-\mathbf{q}) \overset{!}{=} G^{\star}_{12}(\mathbf{q}) \end{aligned}$$

and the only way this request can be satisfied is through the validity of the relation $S_{12}(-\mathbf{q}) = S^{\star}_{12}(\mathbf{q})$.

(2) $v_{12}(-\mathbf{q}) = v^{\star}_{12}(\mathbf{q}) \;\rightarrow\; G_{12}(-\mathbf{q}) = G^{\star}_{12}(\mathbf{q})$: now here the self-consistency plays his role. Starting from the 0$^{\text{th}}$-order approximation, we can write $\chi^{-1}_{12} = -v_{12}$, and immediately $\chi_{12} = \frac{v_{12}}{\det(\hat{\chi}^{-1})}$. Given that $\det(\hat{\chi}^{-1})$ is real, from the definition of S and G we get the conclusion, clearly valid at each order.

As a matter of facts, the relation (1) above is the sufficient and necessary condition to ensure the reality of the pair-correlation function $\mathbf{g}_{12}(\mathbf{r})$ and now it will be shown as easily as the previous statements, let's see:

From the definition of the static structure factor for a multiple coupled system

$$S_{ij}(\mathbf{q}) = \frac{n_i}{n}\delta_{ij} + \frac{n_i n_j}{n}\int d\mathbf{r}\, e^{-i\mathbf{r}\cdot\mathbf{q}}(\mathbf{g}_{ij}(\mathbf{r}) - 1),$$

we can see that a Fourier transform relates the pair-correlation function and the static structure factor. Then the relation (1) is enough to ensure the reality of $\mathbf{g}_{12}(\mathbf{r})$.

We have at last obtained a 2×2 hermitic susceptibility matrix for a coupled double layer system in the self-consistent STLS scheme.

0$^{\text{th}}$-order approximation. In which, as previously done for the monolayer, we initially impose $G^{(0)}_{ij} = 1$ for all i, j. This is equivalent to assume that the system is non interacting (eventually *see* § 3.2.1), or rather, that we are assuming that only exchange interaction is relevant; then we will introduce the correlation due to the dipolar interactions, by using the first step of the STLS scheme. This step will be called 0$^{\text{th}}$-order approximation.

In this rough zero-approximation the susceptibility matrix is diagonal:

$$\hat{\chi}^{(0)} = \begin{pmatrix} \Pi & 0 \\ 0 & \Pi \end{pmatrix}.$$

This implies that at the initial stage of the calculations there are only the intra-layer static structure factors, namely S_{11} and S_{22}, with $S_{11} = S_{22}$. It directly follows that the off diagonal local field factors S_{12} and S_{21} are zero in this approximation. So we need no further calculations to write the first order susceptibility, because we already know all the necessary to trace the formal expression

$$\left[\hat{\chi}^{-1}\right]^{(1)} = \begin{pmatrix} \frac{1}{\Pi} - v_{11}(1 - G^{(1)}_{11}) & -v_{12} \\ -v^{\star}_{12} & \frac{1}{\Pi} - v_{11}(1 - G^{(1)}_{11}) \end{pmatrix}.$$

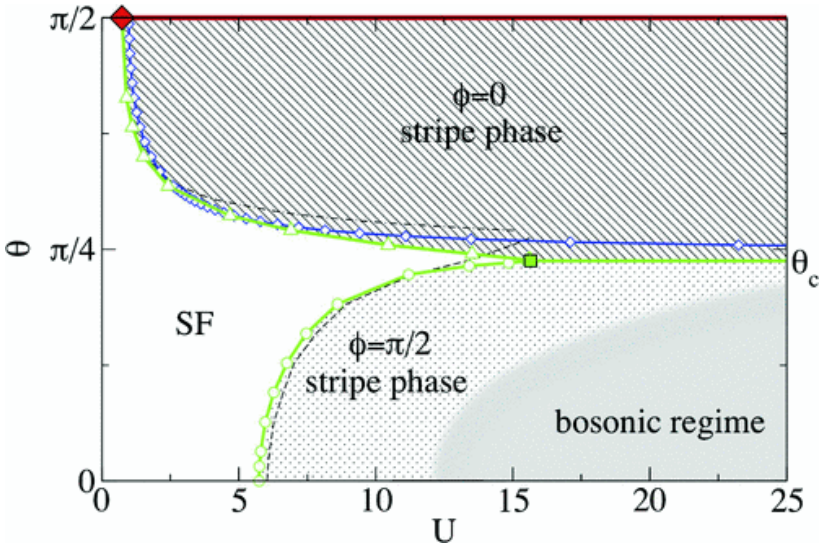

FIGURE 3.3.1. Bilayers' complete phase diagram at fixed interlayer distance, $k_F d = 2$, as a function of ϑ and interaction U. The liquid phase is superfluid (SF). The (green) open triangles [circles] set the boundary of the stripe phase oriented along $\phi = 0$ [$\phi = \pi/2$], derived from a self-consistent STLS calculation. The filled (green) square at $\vartheta_c \simeq 0.75$ and $U \simeq 15.65$ is a quantum critical point beyond which there is a phase transition between the two stripe phases. The (blue) open diamonds for the $\phi = 0$ stripe phase are instead determined including exchange correlations only (see text). These boundaries can be compared to the $\phi = \pi/2$ stripe transition (dashed line) and the collapse instability (dashed-dotted line) for the single-layer case (see Figure 3.2.2). The shaded "bosonic" region is where the system can be described in terms of interlayer bosonic dimers. The (red) filled diamond and thick (red) line at $\vartheta = \pi/2$ indicate collapse in the bilayer. Image from Ref. [24].

The complete phase diagram. The complete phase diagram [24] of a bilayer system looks very similar to the one of a single-layer system. What is completely new is the stripe phase in the same region where before there was the collapsed phase. It arises from the stabilization of the system via the inter-later interaction, as explained above. Identically as in the monolayer case, we note an instability toward the $\phi = \pi/2$ stripe phase at small ϑ, whereas in the strong interaction region ($U > 10$), if the two layers are close enough, we note the instauration of a bosonic coupling between the two layers (not object of this thesis). At higher tilting angles, the $\phi = 0$ occupies most of the phase diagram. It is also noticeable the presence of a new phase boundary between the two (orthogonally oriented) stripe phases: A critical angle exists at which the switch from $\phi = \pi/2$ to $\phi = 0$ occurs. Again, we note that the zeroth order STLS represents a good approximation of the full STLS if we look for a description of the instability toward the $\phi = 0$.

Finally, for $\vartheta = \pi/2$ we note the onset of a collapsed phase: There, intra-layer interactions are not softened by inter-layer interactions, and the surplus of exchange

correlation toghether with the absence of correlation hole make the system undergo a collapse, as in the monolayer geometry.

Eigenvalues... What we have to do now is to find as in previous cases the eigenvalues, and find out the one that takes the lowest values. The eigenvalues have the same formal expression as in Eqn. (3.3.1), even if the local field factor makes numerical calculation necessary. Then the pourpose to minimize it will be achieved numerically, except for the dependence of the angle ϕ, of which the minima at the two values $\phi = 0, \frac{\pi}{2}$ can be found analitically.

We will focus on the $\phi = 0$ minimum: Why? Because the $\phi = \frac{\pi}{2}$ transition is driven by interaction induced correlations, whereas the $\phi = 0$ one is well described by Hartree-Fock like approximations: Our firts order STLS approximation in fact is basically a sort of HF approximation at this iteration order. The $\phi = \frac{\pi}{2}$ can be otherwise be described by full STLS calculation, but this is not in our poureposes. A rough estimation can nevertheless be studied in the RPA approximation, even if it yields a shifted transition, i. e. by RPA the transition could have place at lower interaction strength U with respect to the full STLS prediction: In fact RPA overestimates the interaction correlations.

So the eigenvalues of the susceptibility take the form of the expressions (3.3.1) and we immediately obtain

$$\left[\chi_{\pm}^{-1}\right]^{(1)} = \chi_{11}^{-1} \pm \left|\chi_{12}^{-1}\right| = \frac{1}{\Pi} - v_{11}(1 - G_{11}^{(1)}) \pm |v_{12}|$$

at the first of iteration, but the expression can be straightforwardly updated for each number of iterations n, and in full generality results

$$\left[\chi_{\pm}^{-1}\right]^{(n)} = \frac{1}{\Pi} - v_{11}(1 - G_{11}^{(n)}) \pm \left|v_{12}(1 - G_{12}^{(n)})\right| \qquad \forall n;$$

clearly from now on we consider only the first iteration, then we can omit the order between parenthesis.

The first observation that can be done once chosen the appropriate eigenvalue χ_{min}^{-1} is that now the position of the minimum of $\Pi\chi_{\text{min}}^{-1}(q)$ is not constant, but varies in the range included between $q = 0$ and $q = 2k_F$. This results from the presence of the inter-layer potential, as underlined in the previous section, but the position of q_c is influenced also by the intra-layer local field factor. At higher orders the off-diagonal local field fators will influence its position, too. Thus, we cannot include the critical values of the quantities directly in the constraint $\Pi\chi_{\text{min}}^{-1} = 0$ to find the phase boundary, but we can find out numerically the maximum of $\frac{1}{U}$. Note that the system is characterized by the further parameter d, that might not only influence the minimum behavior, as we already know, but also modify the value of the critical tilting angle of the dipoles.

For the sake of order, we choose here first to fix the inter-layer distance whereas the tilting varies, and then to observe the behavior of an eventual critical angle ϑ when d varies. The critical value of ϑ is expected to tend at the value it had in the one-layer system $\vartheta_{c,\text{mono}} \simeq 0.88$ when the interlayer distance grows to infinity. This is verified, as shown in Figure 3.3.2. Thus the phase boundary varies with d.

...and eigenvectors. At this point of the analisys, we recall the foundamental expression of the density reponse:

$$\delta n_i(\mathbf{q}, \omega) = \chi_{ij}(\mathbf{q}, \omega) V_j^{\text{ext}}(\mathbf{q}, \omega),$$

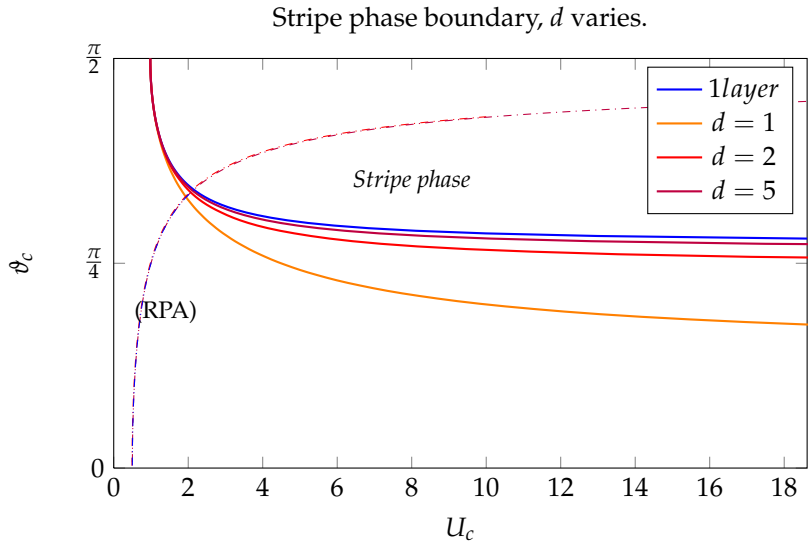

FIGURE 3.3.2. Phase boundaries obtained in the 0^{th}-order STLS and in the RPA. We have reproduced the boundaries for various values of the distance d. It clearly appears that the $\phi = \pi/2$ phase RPA boundary remains substantially unvaried, while more evidently the spacing between the layers influence the $\phi = 0$ stripe phase boundary, obtained with STLS at the first reiteration. The monolayer behaviour ("1layer" in the graphic) is approximated as d becomes sufficiently great.

here the indices indicate the layer which we are referring to.

Let $\mathbf{a}_\pm = \mathbf{a}\left(\chi_\pm^{-1}\right)$ be the two eigenvectors of $\hat{\chi}$: they reflect the evolution of one layer density with respect to the other.

The general expression for the ratio between the two components of the eigenvectors, valid at each order, is:

$$\frac{\mathbf{a}_1^\pm}{\mathbf{a}_2^\pm} = \mp \frac{v_{12}(1 - G_{12})}{|v_{12}(1 - G_{12})|}.$$

Then two eigenvectors of the susuceptibility writes

$$\mathbf{a}_\pm = \begin{pmatrix} 1 \\ \mp \frac{|\chi_{12}|}{\chi_{12}} \end{pmatrix}$$

from which we choose the one relative to the $+$ eigenvalue, for it is the physically relevant one.

Being χ_{12} a complex quantity, the second component of both eigenvectors are two (identical and opposite) phases, thus it indicates that the system is having a phase shift between the two layers, and a density wave modulation.

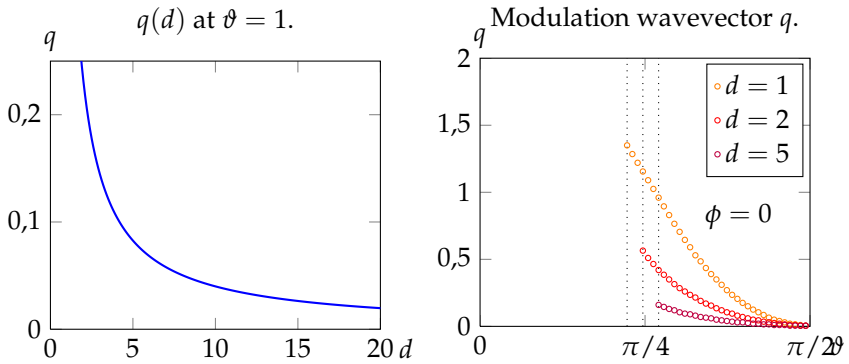

FIGURE 3.3.3. Values assumed by the wavevector of the density modulation as a function of the distance between the layers (left) and as a function of ϑ (right).

It is easily found that (η has been explicited for the 1st-order STLS):

$$\frac{|\chi_{12}|}{\chi_{12}} = e^{-i\eta}, \quad \eta = \begin{cases} 2\vartheta & \text{if } \phi_c = 0 \\ 0 & \text{if } \phi_c = \frac{\pi}{2} \end{cases}.$$

On the other hand, not only the density in the second layer reproduces the first layer's one, but also there is a wave-modulation of the density response, which wave length is $\bar{\lambda}_c = \frac{2\pi}{q_c}$; here the adimensional quantity $\lambda_c \equiv \bar{\lambda}_c k_F$ has been used.

As we have already said studying the limit case in which we considered $G_{11} = 1$ and $G_{12} = 0$, the second layer is expected to stabilise the system: Now we can see that effectively this was true not only in the limit case, but in this first order approximation too. In Figure 3.3.3 it is possible to see the wavevector as a function of the dipole tilting angle.

Calculations show that the wave length becomes infinite for $\vartheta = \frac{\pi}{2}$, reminding a collective phenomenon, involving the whole layer in a uniform shift of density. In facts, it is what happens for a single layer, in which there is not a further layer which would stabilise the system, as we have seen in a previous paragraph. single layer behaviour re-obtained for large d's.

The relationship between d and q_c. In the small d limit, the critical q tends to saturate at $q_c = 2$ (in units of k_F, of course). In the opposite limits of $d \to \infty$, instead, the stabilising effect of the second layer becomes weaker and weaker, till it disappears: This will make the q_c to tends to the values assumed in a monolayers system: $q_c \overset{d\to\infty}{\longrightarrow} 0$.

In order to verify this behaviour we fitted the numerical data with a power series. Before the fitting, in order to choose the appropriate powers we verified the behaviour of the integrated curve: this has been integrated between $d = 1$ and $d = 20$ by mean of the rectangle method.

The best fit of this curve has been find to be

$$f(d) = a \log^b(d),$$

where $b \to 1^-$ and $a \sim 0.73$. Notice that the integral function could be *underestimated* at each point by mean of

$$\delta f(d_i) \sim [\log(d_i + \delta d) - \log d_i] \frac{\delta d}{2} = [\log d_{i+1} - \log d_i] \frac{\delta d}{2},$$

giving a complexive uncertainty over the integration interval $[D_1, D_2]$ of length D

$$\Delta f(D) = \sum_{i=0}^{N} \delta f(d_i) \sim \frac{\log(D_2/D_1)}{2D} (\delta d)^2.$$

Then the derivative

$$\begin{aligned} f'(d) &= ab \log^{b-1}(d) \frac{1}{d} - \mathcal{O}\left(\frac{(\delta d)^2}{d}\right) \\ &\sim \frac{a}{d} - \mathcal{O}\left((\delta d)^2\right) \end{aligned}$$

represents the fitting we were looking for.

3.4. A classic comparison: a dipole in a dipolar ribbons field.

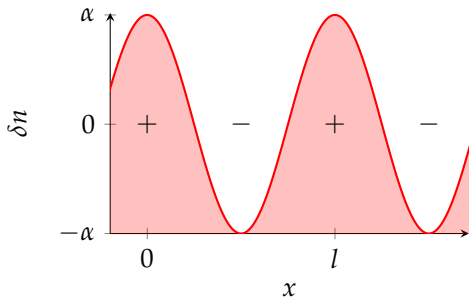

FIGURE 3.4.1. Introduced density modulation.

How would a classical dipole merged in a field of dipolar ribbons behave? This question arises in order to make a comparison between our system in the stripe phase and a more simple classical model, in order to highlight the stable equilibrium conditions.

The model: We take an isolate dipole floating over a 2D density of a gas of dipoles. We choose the plane to be perpendicular to the z axis.

In order to reproduce the stripe phase on the (x, y) plane where the dipolar gas lies, we need to introduce a dipolar density modulation: e.g. we can choose a periodic cosinusoidal density modulation, namely a plane wave, constitued of ϑ_E-tilted dipoles

$$\delta n(x) = D\alpha \cos(kx);$$

this must be summed to the uniform background of ϑ_E-tilted dipoles whose density is n_P. If $\alpha = 0$ the density is uniform, and it is possible to demonstrate that the interaction of the floating dipole with the uniform dipolar layer is identically zero: The angle ϑ_r between the relative position vector ${}^t(x, 0, d)$ of the floating dipole and the dipolar tilting direction is defined by

$$\cos^2 \vartheta_r = \frac{(x \sin \vartheta_E + d \cos \vartheta_E)^2}{r^2}$$

whereas the dipole-dipole interaction writes

$$V(\mathbf{r}) = D^2 \frac{1 - 3\cos^2 \vartheta_r}{r^3}.$$

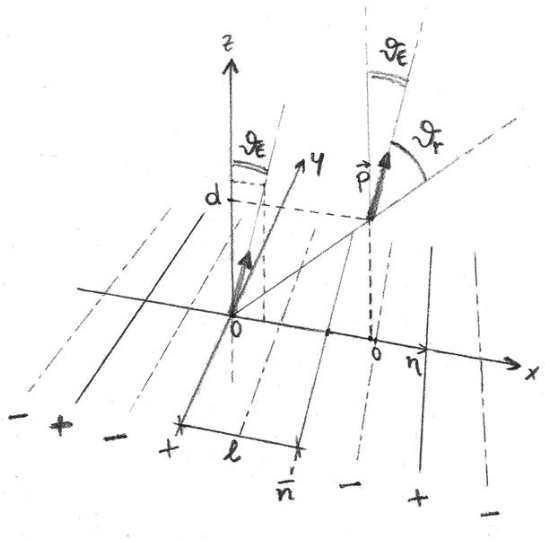

FIGURE 3.4.2. Scheme of the classic model. Note the relative coordinate η and the relative position of the dipole moment of the floating dipole $\mathbf{p}$ and of the dipolar distribution of the ribbon in the origin. The motion of the floating dipole is restricted to the plane $z = d$.

The interaction energy between the floating dipole and the planar uniform distribution is given by

$$\begin{aligned} E_{dP} &= D^2 n_P \int_0^\infty \rho\, d\rho \int_0^{2\pi} \left(\frac{1}{(\rho^2 + d^2)^{3/2}} - 3\frac{(\rho\cos\phi\sin\vartheta_E + d\cos\vartheta_E)^2}{(\rho^2 + d^2)^{5/2}} \right) d\phi \\ &= 0, \end{aligned}$$

thus we can neglect any uniform background and restict our study to the interactions with density fluctuations.

Including the $\delta n(x)$ modulation reproduce the series of "peaks" and "graves" in the density due to the stripes.

We can simplify the model by mean of the substitution of the plane waves with a 1D lattice of dipolar wires: at each maximum we place a "ribbon" of dipolar linear density γ and dipole moment $\hat{\mathbf{p}}$ oriented along the ϑ_E direction. In the calculation we will account for the interaction of the floating test-dipole with those wires and with the graves, too, but for the graves the sign of the interaction is changed, because they are the results of "digging" into the uniform dipolar density.

The simplified model, in sum, consists in the system of $N \to \infty$ wires in the xy-plane, aligned along the x-axis at a distance l to each other and parallel to the y-axis, as schematized in Figure 3.4.2. In order to describe the position of the floating dipole we usefully defines the new coordinate η relative to the middle point among two consecutive ribbons in the following way:

$$x = \left(\nu(n) + \frac{1}{2}\right) l + \eta, \qquad \eta \in \left[-\frac{l}{2}, \frac{l}{2}\right],$$

where $\nu(n) = \bar{n} - n$ if the ribbon-dipole distance is referred to a $+$-ribbon, whereas $\nu(n) = \bar{n} - (n + \frac{1}{2})$ if referred to a $-$-ribbon. In our expressions $\bar{n}$ represents the $+$-ribbon closest to the test-dipole with the lower index. In the name of the discrete traslational symmetry we are always free to choose $\bar{n} = 0$.

The dipoles energy writes as usually:

$$E_{Sd} = \int \rho_S(\mathbf{r}) V_{Sd}(\mathbf{r} - \mathbf{r}') \rho_d(\mathbf{r}') \, d\mathbf{r} d\mathbf{r}' \tag{3.4.1}$$

with

$$\begin{aligned} \rho_S(\mathbf{r}) &= \sum_{n=-\infty}^{\infty} \delta(x - nl)\delta(z)\gamma, \\ \rho_d(\mathbf{r}') &= D\delta\left(x' - \left(\frac{1}{2}l + \eta\right)\right) \delta\left(y'\right) \delta\left(z' - d\right) \end{aligned}$$

where γ is the dipoles density of the ribbons whereas D is the dipole moment of the test-dipole.

We underline that $\rho_d(\mathbf{r}')$ means that the position of the test-dipole is $\mathbf{r}' = (\frac{1}{2}l + \eta,\, 0,\, d)$.

In particular we are considering the case in which the dipoles are *all* aligned in the zx-plane, tilted with an angle ϑ_E whit respect to the z-direction, and γ is a constant. In such a way the dipole moment is oriented like $\hat{\mathbf{p}} = (\sin\vartheta_E,\, 0,\, \cos\vartheta_E)$.

The final interaction potential V_{Sd} is the sum over all the ribbons of the interaction V_{dd} between aligned dipoles.

Once called $\vartheta_{\mathbf{r}_n}$ the angle formed by the dipole tilting direction and the position of the test-dipole with respect to the n^{th} $\pm$-ribbon, we can write

$$V_{Sd}(\mathbf{r}_n - \mathbf{r}') = \frac{1 - 3\cos^2(\vartheta_{\mathbf{r}_n})}{|\mathbf{r}_n - \mathbf{r}'|^3}.$$

Now we can substitute the cosine with the expression

$$\cos^2(\vartheta_{\mathbf{r}_n}) \equiv \frac{(\hat{\mathbf{p}} \cdot \mathbf{r}_n)^2}{\mathbf{r}_n^2}$$

where the position vector is $\mathbf{r}_n = (\left(\nu(n) + \frac{1}{2}\right) l + \eta,\, 0,\, d)$.

So

$$\hat{\mathbf{p}} \cdot \mathbf{r}_n = d\cos\vartheta_E + \left[\left(\nu(n) + \frac{1}{2}\right) l + \eta\right] \sin\vartheta_E.$$

Finally for the sake of brevity we define

$$\alpha_n^2 = d^2 + \left[\left(\nu(n) + \frac{1}{2}\right) + \eta\right]^2.$$

Performing the integration after including the previous expression in (3.4.1), the interaction energy results to be

$$E_{Sd}^{+} = 2\gamma D \sum_n \frac{1}{\alpha_n^2} - \frac{2}{\alpha_n^4}\left(d\cos\vartheta_E + \left[\eta + \left(-n + \frac{1}{2}\right) l\right] \sin\vartheta_E\right)^2$$

for the interaction with the $+$-ribbons and

$$E_{Sd}^{-} = -2\gamma D \sum_n \frac{1}{\alpha_n^2} - \frac{2}{\alpha_n^4}\left(d\cos\vartheta_E + [\eta - nl]\sin\vartheta_E\right)^2$$

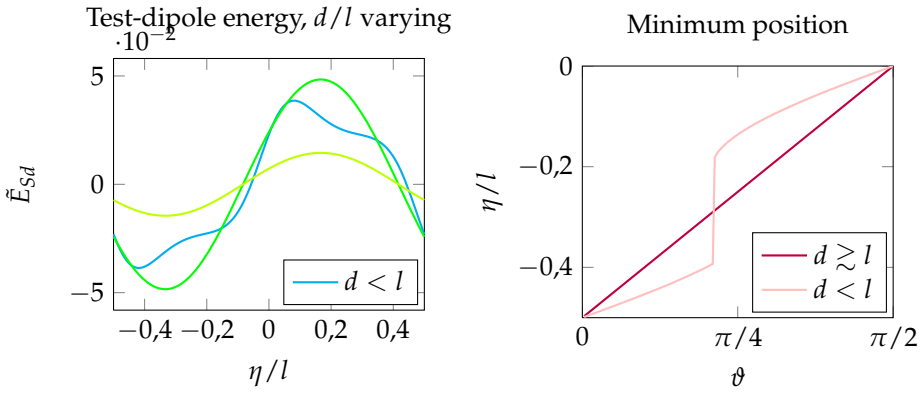

FIGURE 3.4.3. Energy minimum behaviour. Left: Energy profile (energy has been rescaled: $\tilde{E}_{Sd} = E_{Sd}\left(\cosh\left(d^2\right) - 1\right)$) varying the ratio d/l; note that for if $d/l \ll 1$ two minima may appear. The arrow indicates the direction to which the minimum moves towards when ϑ increases. Right: Position of the minimum as a function of ϑ. The behaviour for $d/l < 1$ is due to the presence of two local minima.

for the $-$-ribbons.

It is now necessary to perform the two sums, from which result: 1) a periodic dependence on the angle ϑ_E and on the coordinate η and 2) a more-than-exponential decay of the interaction with the distance:

$$E^{+}_{Sd} = 2\gamma D\frac{\pi^2}{l^2}\left\{\cos\left(2\vartheta_E\right)\Re\left[\operatorname{sech}^2\left(\frac{\pi}{l}\left(d+i\eta\right)\right)\right] - \sin\left(2\vartheta_E\right)\Im\left[\operatorname{sech}^2\left(\frac{\pi}{l}\left(d+i\eta\right)\right)\right]\right\},$$

$$E^{-}_{Sd} = 2\gamma D\frac{\pi^2}{l^2}\left\{\cos\left(2\vartheta_E\right)\Re\left[\operatorname{csch}^2\left(\frac{\pi}{l}\left(d+i\eta\right)\right)\right] - \sin\left(2\vartheta_E\right)\Im\left[\operatorname{csch}^2\left(\frac{\pi}{l}\left(d+i\eta\right)\right)\right]\right\}.$$

To get the whole interaction energy results from the sum $E_{Sd} = E^{+}_{Sd} + E^{-}_{Sd}$.

Now let $z \in \mathbb{C}$: then from the hyperbolic functions properties it is true that

$$\operatorname{csch}^2 z + \operatorname{sech}^2 z = 4\coth(2z)\operatorname{csch}(2z).$$

So we define $f(\eta) = 4\coth\left(\frac{2\pi}{l}(d+i\eta)\right)\operatorname{csch}\left(\frac{2\pi}{l}(d+i\eta)\right)$ giving

$$E_{Sd} = 2\gamma D\frac{\pi^2}{l^2}\left\{\cos\left(2\vartheta_E\right)\Re\left[f(\eta)\right] - \sin\left(2\vartheta_E\right)\Im\left[f(\eta)\right]\right\}.$$

The pourpose was to find the stable equilibria of the test-dipole. Clearly it can be done by simply derivating with respect to η and imposing the stationary point condition. Then the equation that should be resolved is

$$\frac{\partial_\eta \Re}{\partial_\eta \Im} = \tan(2\vartheta_E),$$

that must be done numerically, because it is a trascendental equation. In the limit $d \gtrsim l$ it is obtained (see Figure 3.4.3) a linear dependence of the type

$$\eta_{eq} \propto 2\vartheta_E$$

as expected.

Change of perspective. Nevertheless, we do not actually know if the distortion from the linear dependence in the opposit limit $d < l$ is only due to the higher spatial resolution of the lattice of ribbons as viewed from the test dipole, or to other proximity effects.

We can try and *rest* the previous ribbon approximation together with the *relative* coordinate η.

The new coordinates of the test dipole are simply the coordinates *in the frame* fixed with the layer; we will nevertheless indicate the (fixed) x-coordinate of the test dipole with the symbol η, which recalls us the phase-shift introduced before in the chapter.

We definitely remove the ribbons, and assume a *uniform* plane density of dipoles in the layer instead; consequentely the calculation of the interaction energy will be performed through a "per-wires" integration, wires that are parallel to $\hat{y}$. The density modulation effects will be re-obtained with the assumpion that those wires have a linear density of dipolar moment modulus which is a function of the x-coordinate: If we look at the integration-wire in the position $x = \xi$, its linear dipolar density will be $\gamma(\xi) = \gamma_0 \cos\left(\frac{2\pi}{l}\xi\right)$, with l the wavelength of the modulation. Clearly, as in the previous treatment, the dipoles in the xy-plane and the floating dipole are all aligned along the same direction which tilting is ϑ_E.

After this change, the densities of dipolar "charge" read as:

$$\rho_d(\mathbf{r}') = D\delta\left(x' - \eta\right)\delta\left(y'\right)\delta\left(z' - d\right)$$

for the floating dipole and

$$\rho_w(\mathbf{r}) = \gamma(\xi)\delta(x - \xi)\delta(z)$$

for the integration-wire.

The choice of the so called per-wires integration makes sense because, once written the expression for the interaction between the integration-wire in ξ and the test dipole, it is sufficent to sum over all the wires in the layer.

We do not need further calculations to extract the two quantities

$$\hat{\mathbf{p}} \cdot \mathbf{r} = d\cos\vartheta_E + [\eta - \xi]\sin\vartheta_E$$

$$\alpha_\xi^2 = d^2 + [\eta - \xi]^2$$

and include them in E_{Sd} that now writes

$$E_{Sd} = \frac{1}{L}\int_{-\infty}^{+\infty} 2\gamma(\xi)D\left\{\frac{1}{\alpha_\xi^2} - \frac{2}{\alpha_\xi^4}\left[d\cos\vartheta_E + (\eta - \xi)\sin\vartheta_E\right]^2\right\}d\xi.$$

The explicit calculation of this integral makes use of residues: The trick stands in rewrite the cosine in its exponential form, and then replace $\eta - \xi \mapsto X$. The renormalization constant $\frac{1}{L}$ can be absorbed in γ_0 that becomes the dipolar *surface* density Γ_0. Some tedious calculation yields

$$E_{Sd}(\eta, d, \vartheta_E) = -4\pi D\Gamma_0 \frac{e^{-\frac{2\pi}{l}d}}{l}\cos\left(\frac{2\pi}{l}\eta - 2\vartheta_E\right)$$

and it is clear that now the position of the minimum does not depend on d:

$$\frac{\partial}{\partial\eta}E_{Sd} = 0$$

if and only if

$$\frac{2\pi}{l}\eta = 2\vartheta_E + (2\pi z)\,, \qquad z \in \mathbb{Z}.$$

We can faithfully conclude that also in the quantum bilayer system the phase shift is a purely classical effect.

CHAPTER 4

MULTILAYERS SYSTEMS

By using previously developed techniques, we proceed in the analysis of system composed by an increasing number of layers. While the presence of more layers is expected to stabilize the dipole gas, preventing it to collapse, at the same time it furthers the arise of the stripe phase. This is suggested from the fact that the critical dipole tilting angle is lower in the case of two layers with respect to the monolayer case. Is this trend confirmed if the number N of layers increases? The very next pourpose is to examinate the properties of systems with low N, as to find out some peculiar behaviour.

At first, we will focus on the 3 and 4 layers systems, then some numerical analysis result for systems with an increasing number of layer will be presented. Later, we will present an attempt to simplify the interactions and make predictions in an approximate fashion, i.e. we will consider a first neighbours approximation. After a numerical study of this approximation, a diagonalising method will be proposed and its results will be shown.

Some preliminar discussion. Our study starts from the (inverse) susceptibility matrix, the real core of phase transitions. The general formula for the matrix elements is already known, then we directly writes down the inverse of the susceptibility in the 0^{th}-order of approximation:

$$\hat{\chi}^{-1} = \begin{pmatrix} \frac{1}{\Pi} - v_{11}(1-G_{11}) & -v_{12} & -v_{13} & \cdots \\ -v_{12}^{\star} & \frac{1}{\Pi} - v_{11}(1-G_{11}) & -v_{12} & \cdots \\ -v_{13}^{\star} & -v_{12}^{\star} & \frac{1}{\Pi} - v_{11}(1-G_{11}) & \\ \vdots & \vdots & & \ddots \end{pmatrix}$$

where

$$v_{jk} = -2\pi U q e^{-|j-k|qd} \left(\cos\vartheta - i\,\mathrm{sgn}\,(j-k)\cos\phi\sin\vartheta\right)^2,$$

which can be rewritten as $v_{jk} = U u_{jk}$.

In order to extract eigenvalues and eigenvectors we separate its diagonal part from its off-diagonal part.

Precisely, we are interested in the minimum eigenvalue χ_x^{-1} of the matrix in rder to get the level set $\Pi\chi_x^{-1}(q,\vartheta) = 0$ for some q and fixed ϑ, as well as we did in previous chapters. Observe that $\hat{\chi}^{-1}$ can be written

$$\hat{\chi}^{-1} = \chi_{11}\mathbb{1} + U\hat{u}$$

where $U\hat{u}$ is the matrix of the off-diagonal elements. Now, let $\hat{\omega}$ be the matrix of the eigenvalues of $\hat{u}$, and let $\hat{A}$ be the respective matrix of the eigenvectors. Then

the action of $\hat{\chi}^{-1}$ on a vector $\vec{v}$ whatever reads as:

$$\begin{aligned}\hat{\chi}^{-1}\vec{v} &= \left(\chi_{11}^{-1}\mathbb{1} + U\hat{A}\hat{\omega}\hat{A}^{-1}\right)\vec{v} \\ &= \hat{A}\left(\chi_{11}^{-1}\mathbb{1} + U\hat{\omega}\right)\hat{A}^{-1}\vec{v}.\end{aligned}$$

Let now $\vec{v} = \vec{a}_{min} = \vec{a}(u_{min})$ be the eigenvector associated with the minimum eigenvalue u_{min} of $\hat{u}$, then it is true that

$$\begin{aligned}\hat{\chi}^{-1}\vec{a}_{min} &\equiv \hat{A}\left(\chi_{11}^{-1}\mathbb{1} + Uu_{min}\mathbb{1}\right)\hat{A}^{-1}\vec{a}_{min} \\ &= \left(\chi_{11}^{-1} + Uu_{min}\right)\mathbb{1}\vec{a}_{min} \\ &= \chi_x^{-1}\vec{a}_{min},\end{aligned}$$

namely that the separation into diagolal and off-diagonal part of a matrix shaped as $\hat{\chi}^{-1}$ will not modify the eigenvectors of the complete susceptibility matrix with respect to the ones of $\hat{u}$. So the $\hat{\chi}^{-1}$ minimum eigenvalues is $\chi_x^{-1} = \chi_{11}^{-1} + Uu_{min}$.

Hence we only have to evaluate the eigenvalues and eigenvector of $\hat{u}$ to obtain all the informations about the system.

In particular, for a three layers system it can be proved that

$$\vec{a}(u_{min}) = {}^t\left(x(u_{min}),\ 1,\ x^\star(u_{min})\right)$$

where

$$x(u_{min}) = \frac{v_{12}u_{min} - v_{12}^\star v_{13}}{u_{min}^2 - |v_{13}|^2}.$$

The hermiticity of the matrix $\hat{u}$ ensures the reality of its eigenvalues; nevertheless they cannot be obtained analitically if $N \geq 3$, then numerical solution will be used.

Quantities of interest. Significant quantities can be extracted from the phase diagram, first of all the critical angle which we are going to define as follows:

The critical angle. The critical tilting angle is defined as

$$\vartheta_c = \min\left\{\vartheta \,|\, U \to \infty,\ \delta n \neq 0\right\}$$

and δn is the stripe phase density modulation. This is the definition we have implicity used until now. The request for $U \to \infty$ is necessary, because if in the phase diagram $(U,\ \vartheta)$ the boundary has no asymptotes, "criticity" of an angle makes no sense.

In fact we will see that if the layers are not spaced enough the phase boundary will not show any asymptote, so that for each values of the tilting of the dipoles we ca have a striped phase.

The critical distance. It is defined as

$$d_c = \left\{d \,|\, \vartheta_c = 0\right\};$$

clearly, if $d < d_c$ there is no critical angle.

We are looking for a relation between two parameters of the system, i.e. the number of layers, and the critical dipole tilting at which transition occurs. The search for a relationship should opportunely include the ϑ dependence of the distance d between layers. Such a relation is found in the phase boundary, which in

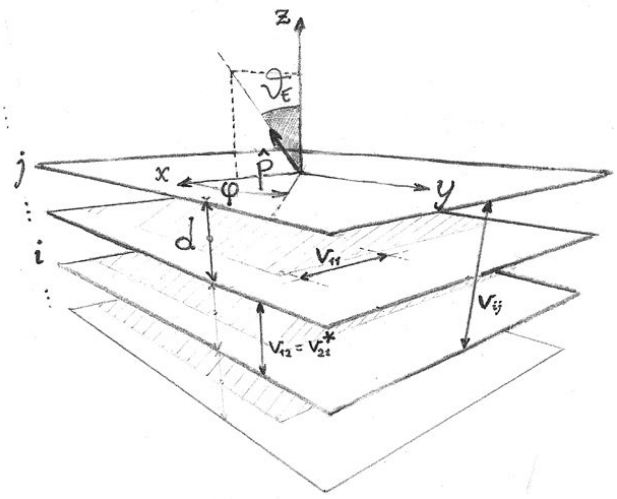

FIGURE 4.1.1. Schematic of a multi-layers system. Each quantity has been introduced in the text.

turn can be determined through the expression $\min_q \{\Pi \chi_x^{-1}\} = 0$. Including all the opportune substitutions in leads us to search for

$$\frac{1}{U} = \max_q \{\Pi \left((1 - G_{11}) \, v_{11} + u_{min} \right)\}$$

and then plot it against ϑ.

4.1. Three and four layers

We can begin by verifying that if the layers are quite far from each other we actually re-obtain a monolayer-like behaviour.

In Figure 4.1.2, in order to better appreciate the variations of the system parameters due to the interlayer separation, we have chosen to fix a large ϑ, $0.88 < \vartheta < \pi/2$: it emerges that (left graphic) the convergence toward the single layer behaviour slightly slows down as far as the number of layers increases, and it requires lower values of the interaction strength to realize the transition to stripe phase (shadowed area). In the graphic on the right, significant differences in the density modulation wavevector cannot be observed between the three systems of 3, 4 and 5 layers. However, this modulation tends to have an infinite wavelength when the inter-layer distance is very large, reproducing a tipical single-layer behaviour.

3 layers. Down to some details, we look now at the features of a three layers system. We will fix three values of d: a distance below d_c, d_c itself — calculated from the definition — and a distance above d_c. In the graphics, data relative to the critical distance d_c are always represented by red solid lines.

The first fact one could notice in the phase diagrams (U, ϑ) is that for values of the spacing $d \geq d_c$ the boundary exhibits a horizontal asymptote, whereas for $d \leq d_c$ the curve falls down vertically, i.e.

$$\left. \frac{\partial U}{\partial \vartheta} \right|_{\vartheta = 0} = 0 \qquad \forall d < d_c,$$

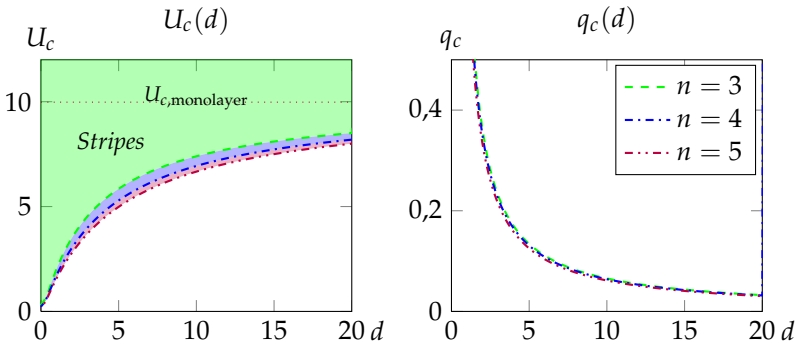

FIGURE 4.1.2. Values of q_c and U_c (critical) at a fixed tilting angle $\vartheta = 0,9$ as a function of the distance between layers. It can be seen that for large d's the monolayer behaviour is re-obtained.

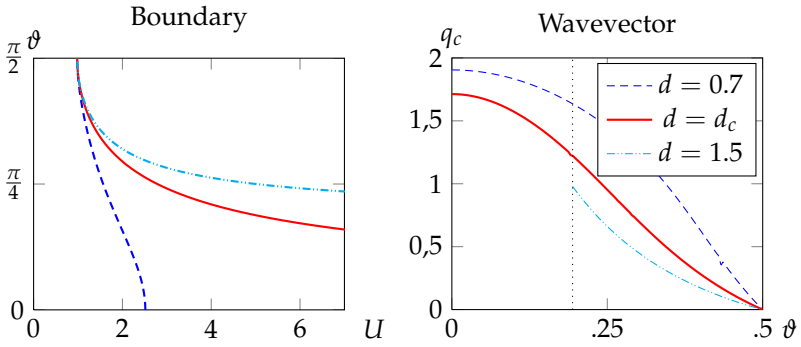

FIGURE 4.1.3. Boundary and critical wavevector for a 3 layer system. In red is visible the boundary and the $q_c(\vartheta)$ curve for the distance at which ϑ_c becomes zero.

clearly visible in Figure 4.1.3, in conjunction with the fact that the density modulation shows larger wave vectors at small d's rather than at larger distances. These are universal behaviours in multilayers systems. We observe also the onset of a collapsed phase at $\vartheta = \pi/2$, independently of d.

Another aspect of the critical angle dependence of the distance between layers is underlined in Figure 4.1.4. It is noticeable how suddenly the critical ϑ increases at $d = d_c$; the approach to the superior asymptote $\vartheta \simeq 0.88$ is appreciably fast, too: borrowing some terminology from signal theory, we can say that the "rise time" of the curve $\vartheta_c(d)$ is $\Delta d \simeq 2$, while the 70% of the "signal amplitude" is reached in just $\Delta d \simeq 0,5$. We do not need enormous distancies between layers to approximatively obtain a monolayer-like behaviour. Explicitly multi-layers behaviours are visible if the layers are not far from each other.

Now, looking at the eigenvectors of the susceptibility, it is possible to explore the properties of the density modulation that looms up in the gas. As it has been clarified in the study of a two layer system (§ 3.3) , one can read some information

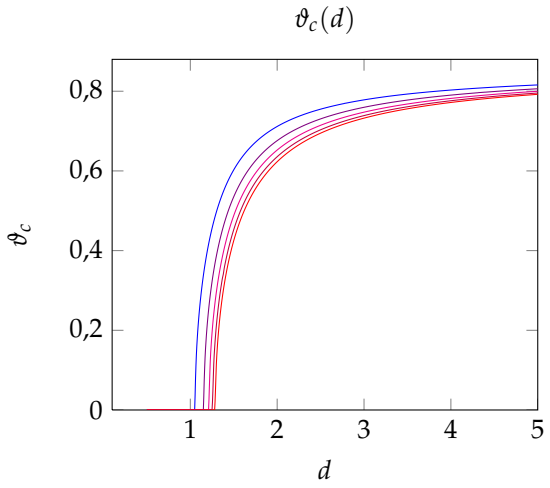

FIGURE 4.1.4. A graphic of how ϑ_c varies when the distance d between the layers varies. Notice the sharp edge where the change occurs.

about relative phase shift and relative modulation amplitude simply looking at the ratio between the various components of those eigenvectors.

In the following figures (Figures 4.1.5, 4.1.6 and4.1.7) the relative amplitude and phase shifts are drawn, calculated as the ratio between the components of the eigenvector relative to the minimum eigenvalue χ_x^{-1}. The two magnitudes have been evaluated for each the three values of d chosen, as a function of the dipole tilting angle.

In this case it is not clearly distingushable any particular behaviour in relation to the value of the distance, but a certain flatness in the relative amplitude if $d = d_c$, i.e. for that value of d the wave amplitude depends very weakly of the angle ϑ.

The phase shift, instead, varies linearly with the number of the layer, and almost linerly along almost the whole range in which ϑ varies.

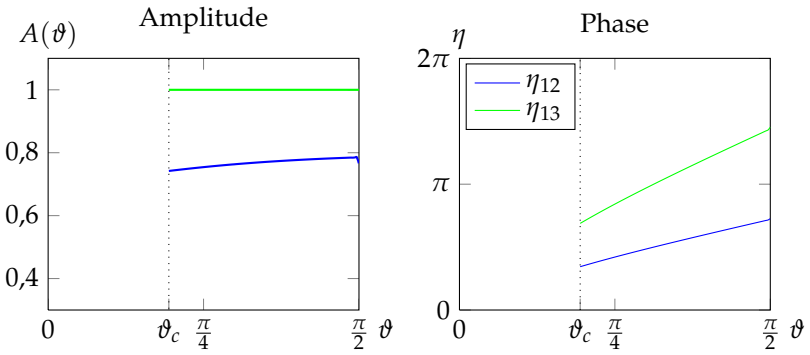

FIGURE 4.1.5. Relative amplitude (left) and phase shift (right) of the density modulation between the layers. Here the distance is taken to be $d = 1,5$.

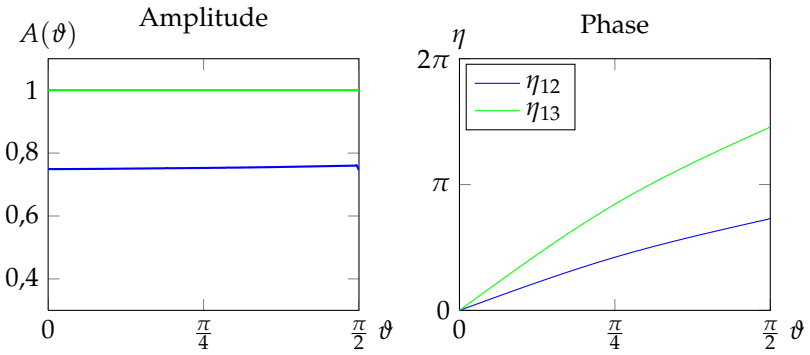

FIGURE 4.1.6. Relative amplitude and phase shift, $d = d_c$.

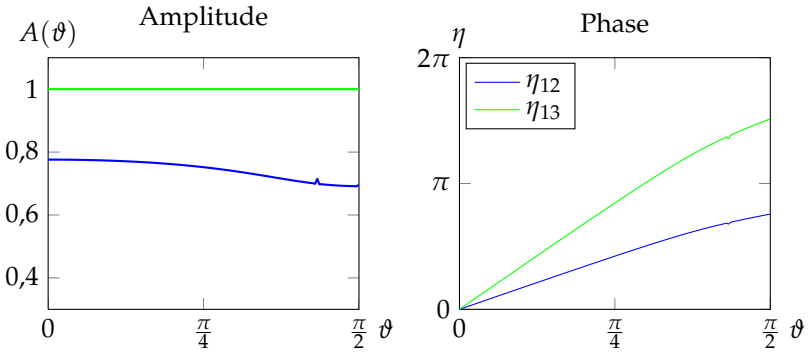

FIGURE 4.1.7. Relative amplitude and phase shift, $d = 0,7$.

4 layers. The same considerations as for the three layers system are still valid for a system of four layers. If we make a comparison with the three layers system described above, we can observe:

- ⇝ slightly lower values of the modulus of the wave vector at all the angles and spacings, and
- ⇝ the same almost linear evolution with ϑ of the relative phase shift, as in the previous case.

The two central layers show equal amplitude of the density modulation, clearly because of the simmetry of the system; with respect to that of the central layer in the three layers system it is a little bigger. One can note also that the complexive variation of the amplitude between $\vartheta = 0$ and $\vartheta = \pi/2$ results greater that the one of the three layers system.

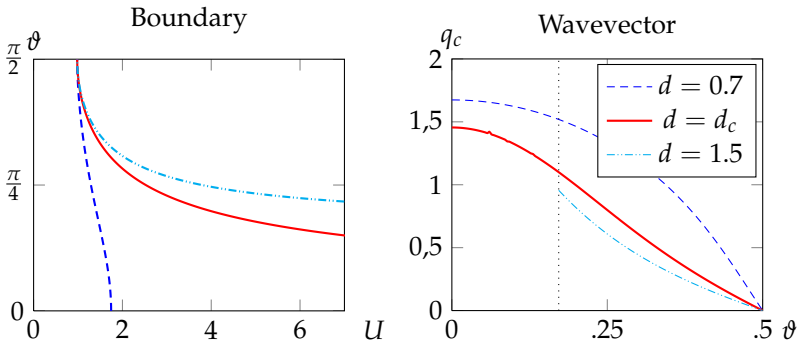

FIGURE 4.1.8. Boundary and critical wavevector for a 4 layer system. In red is visible the boundary and the $q_c(\vartheta)$ curve for the distance at which ϑ_c becomes zero.

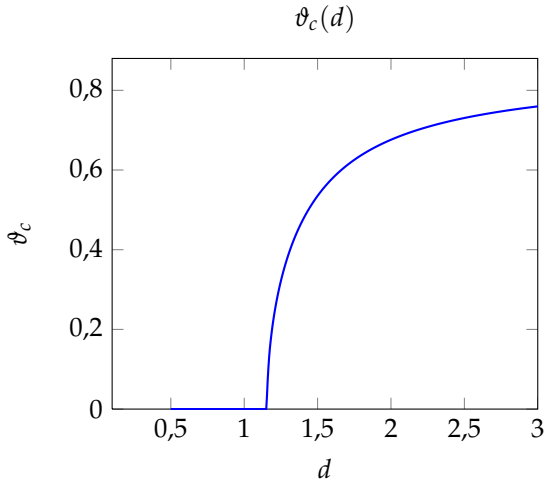

FIGURE 4.1.9. A graphic of how ϑ_c varies when the distance d between the layers varies. Notice the sharp edge where the change occurs.

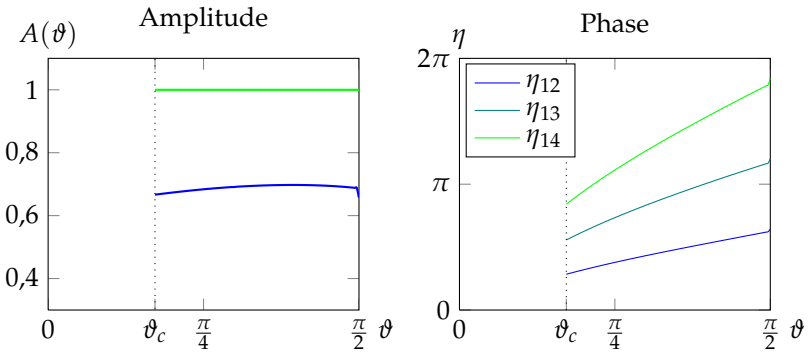

FIGURE 4.1.10. Relative phase shift (left) and amplitude (right) between the layers.

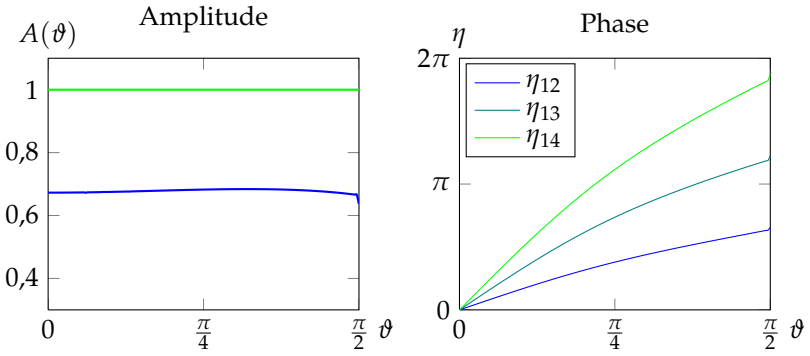

FIGURE 4.1.11. Relative phase shift (left) and amplitude (right) between the layers.

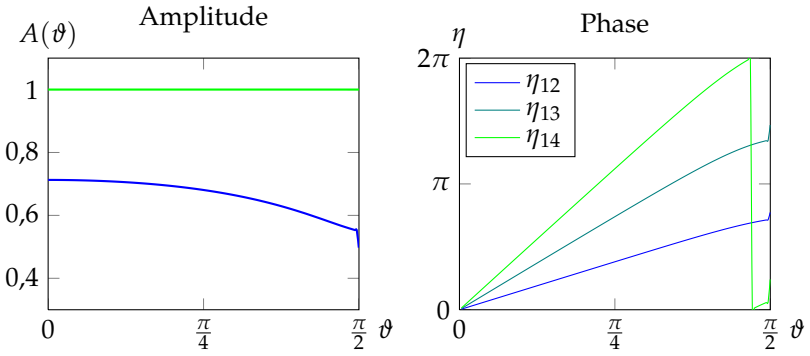

FIGURE 4.1.12. Relative phase shift (left) and amplitude (right) between the layers.

4.2. Asymptotic trends

If we consider each layer as a point of a 1D lattice, we can think of the interlayer potential as of a short-range potential. Strictly speaking, it is not a good argument, but it it provides the valid insight that the "relevant" interactions take place between nearest layers, then adding more points to the lattice will not, or it will only partially, modify the behaviour of the system. Therefore we can hypotise the onset of asysmptotic trends as the lattice growths.

Comments on asymptoticities. We have already observed that $\vartheta_c(N=3) < \vartheta_c(N=4)$, hence $\vartheta_c(N)$ can be cast as a non-decreasing function of the number of layers N, making the $\phi = 0$ stripe phase occupy the whole phase diagram for sufficiently large U, provided d sufficiently small. On the contrary, a great spacing between layers will make monolayer-like behaviours emerge, independently of the number of layers.

In Figure 4.2.1 seven series of critical angles are shown, each series associated with a distinct value of the interlayer distance. The upper series are concerned with more spaced layers.

A first qualitative conclusion is the critical angle dependence of the distance: ϑ_c increases as d increases, till the value of $\vartheta_{c,\text{mono}} \simeq 0.88$ of the monolayer system.

Second: for sufficiently close layers, and for a sufficient number of them, the case $\vartheta_c = 0$ can be realized.

Third, a critical distance d_c exists above which the stripe phase will not appear until a non-zero critical tilting angle $\vartheta_c > 0$ is reached. This last fact can be forecast from Figure 4.2.2, where the distance at which $\vartheta_c = 0$ is plotted against the number of layers. Furthermore, data suggest an asymptoticity of d_c to a finite and small value as the number of layers becomes larger (at $N = 100$ layers, $d_c \simeq 1.46$). Such an asymptote can be defined as the *limit distance*:

$$d_l := d_c(N \to \infty).$$

From previous paragraphs considerations we can also infer that for each N

$$d_c(N-1) < d_c(N).$$

By this way, once fixed the number of layers, if the distance between the layers is lower than d_c, a critical tilting angle cannot exist any more, because for each ϑ there will be a critical interaction strength U_c at which the phase transition will occur. Anyway, for any ϑ we can measure the wave length of the density modulation and make some comparison with other systems. In particular, one can choose $\vartheta = 0$.

So let us define q_c as a function $q_c = q_c(N, d, \vartheta)$ and let $\mathfrak{N}$ be the number of layers at which $\vartheta_c = 0$ and, obviously, $d = d_c$. It is a matter of fact that the following relation is valid within a very good approximation:

$$q_c\left(\mathfrak{N}, d_c(\mathfrak{N}-1), 0\right) = q_c\left(\mathfrak{N}, d_c(\mathfrak{N}), \vartheta_c\right).$$

Remind that $\vartheta_c(\mathfrak{N}, d_c(\mathfrak{N})) = 0$, then in the right side of the equation $\vartheta_c \equiv 0$.

In those points the "derivative" of the curve $q_c(N)$ varies quite abruptly; it coincides with the fact that the number of layers N becomes higher than $\mathfrak{N}$.

Finally, we stress that even for a fixed distance, the wave length slightly increases with the number of layers.

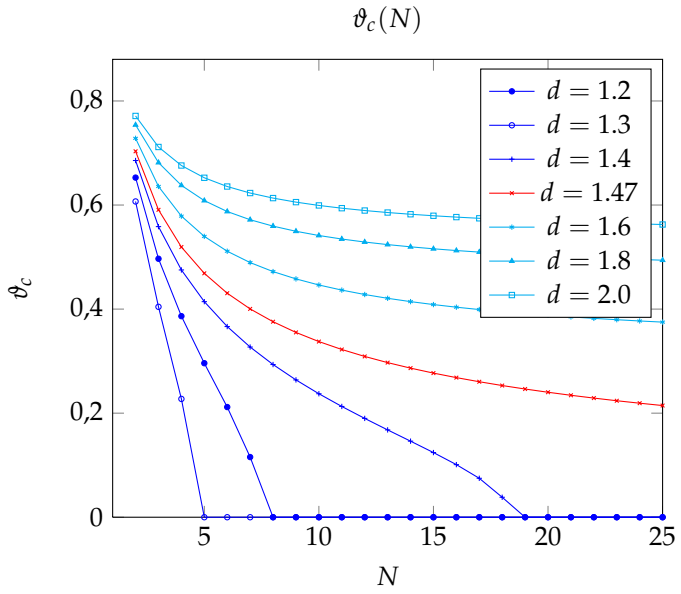

FIGURE 4.2.1. Critical tilting angle as the number of layers N increases, for some distance d fixed. We will *not* obtain a $\vartheta_c(N) = 0$ for any n if $d \gtrsim 1.5$.

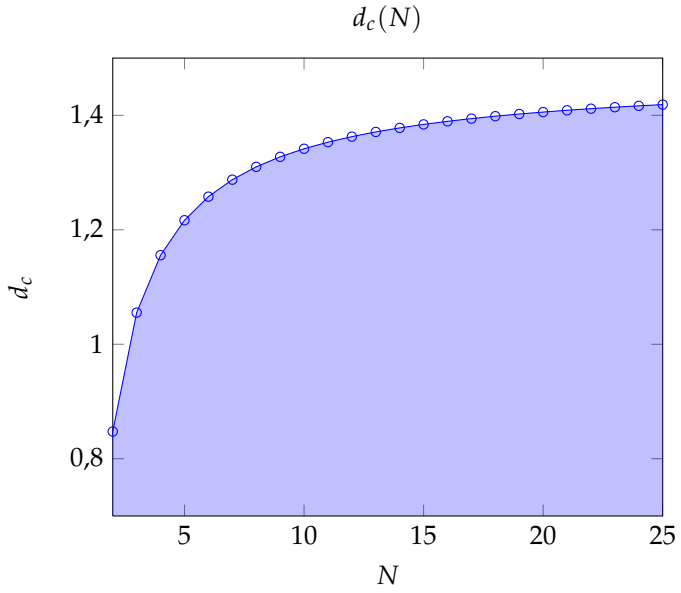

FIGURE 4.2.2. Distance at which $\vartheta_c = 0$. Below this distance, for a sufficiently big interaction strength U, the system will always assume the $\phi = 0$ stripe phase configuration.

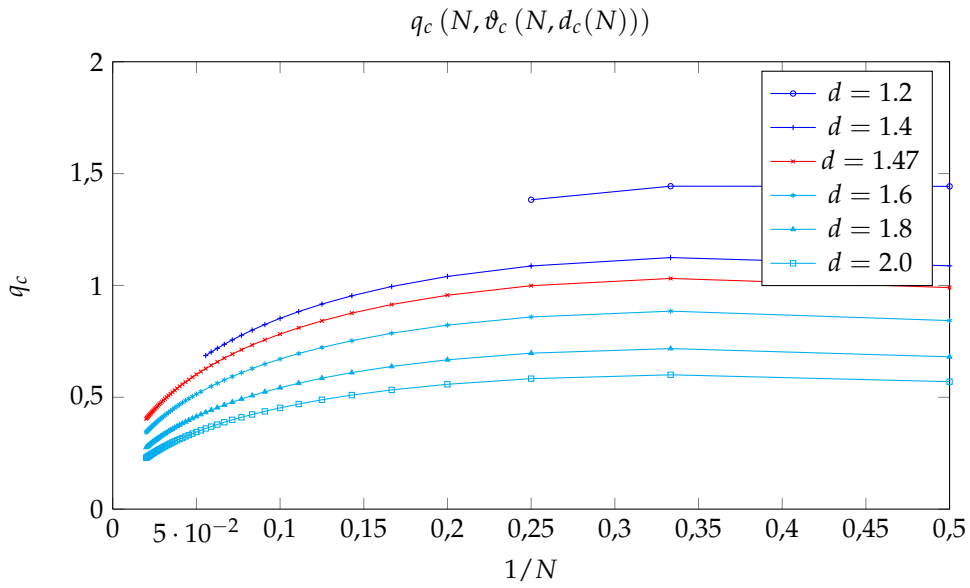

FIGURE 4.2.3. Module of the wavevector as the number of layers N increases, for some distance d fixed. For each point we choose the critical angle. The lines interrupt if d is too small to have a critical angle for that number of layers.

4.3. First neighbours approximation

We would like to extract the eigenvalues of $\hat{\chi}^{-1}$ in an analytic form. Such a formalism could enable us to find out the properties of a bulk system of layers, and determine the asymptotic behaviours we have roughly hypotised. One possible way is the first neighbours interaction approximation (FNA). Anyway, we should honestly evaluate the errors we made in calculations by forgetting the complete interaction, numerically, making a comparison with the previous calculations. Furthermore, we must take in account that the previous results come from a 0^{th}-order STLS approximation, which can also significatively differ from the full STLS approximation (as in the case of a wave density modulation along the $\phi = \pi/2$ direction). This approximation should therefore be carefully examinated.

How the results are expected to differ. All the results obtained in previous sections have been extracted numerically, so that we should settle for qualitative previsions of the expected results.

About the critical angle, being the interlayer interaction the one driving the system to the stripe phase, to reduce the coupling between layers will lead to larger critical angle; in the same way this will simulate a weaker interlayer interaction and the critical distancies will decrease.

We can also point out that the asymptotic behaviours related to a large number of layers will be reached more rapidly, because the layers beyond the very next one are invisible to each others. This also means that the module of wavevector of the coupling, and then of the density modulation, will be greater with respect to the complete interaction.

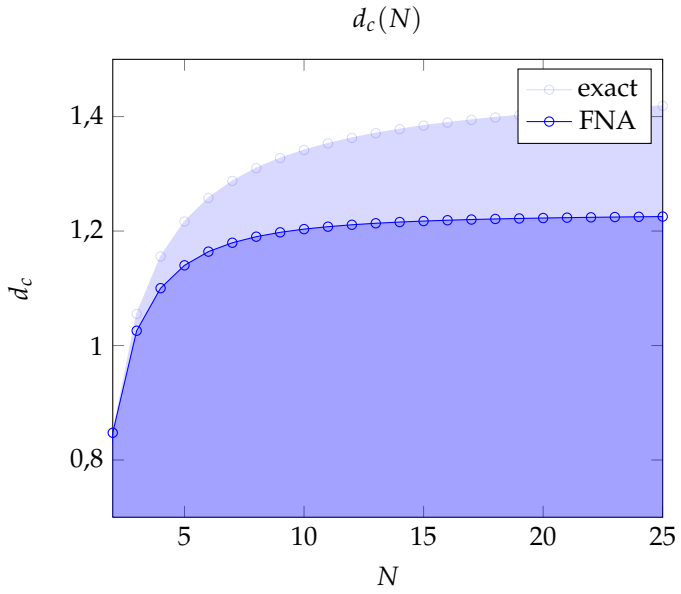

FIGURE 4.3.1. Distance at which $\vartheta_c = 0$: A comparison between exact interaction and first neighbours interaction approximation. It is manifest that the newly calculated limit distance is lower with respect to that of the complete interaction.

Figures 4.3.1 and 4.3.2 confirm the above reasoning; there, one can quickly realise that FNA gives qualitatively similar results to SLTS, but quantitatively bad results.

4.3.1. Diagonalization of susceptibility. The susceptibility matrix within the FNA results with evidence simplified, it is a tri-diagonal matrix, and along each diagonal the matrix entries are all the same:

$$\hat{\chi}^{-1}_{\text{FNA}} = \begin{pmatrix} \frac{1}{\Pi} - v_{11}(1-G_{11}) & -v_{12} & 0 & \cdots \\ -v^{\star}_{12} & \frac{1}{\Pi} - v_{11}(1-G_{11}) & -v_{12} & \cdots \\ 0 & -v^{\star}_{12} & \frac{1}{\Pi} - v_{11}(1-G_{11}) & \\ \vdots & \vdots & & \ddots \end{pmatrix}.$$

We are interested in the eigenvalues of this matrix for a system of an arbitrarily great number N of layers, so the problem is the diagonalization of a tri-diagonal $N \times N$ matrix. Fortunately, it can be shown that diagonalization is possible in the reciprocal space of the 1D lattice of layers.

First of all, diagonalization can be further simplified, as proved at the beginning of this chapter, by the reduction of $\hat{\chi}^{-1}_{\text{FNA}}$ in a diagonal plus an off-diagonal part:

$$\hat{\chi}^{-1}_{\text{FNA}} = \chi^{-1}_{11}\mathbb{1} - \hat{u}',$$

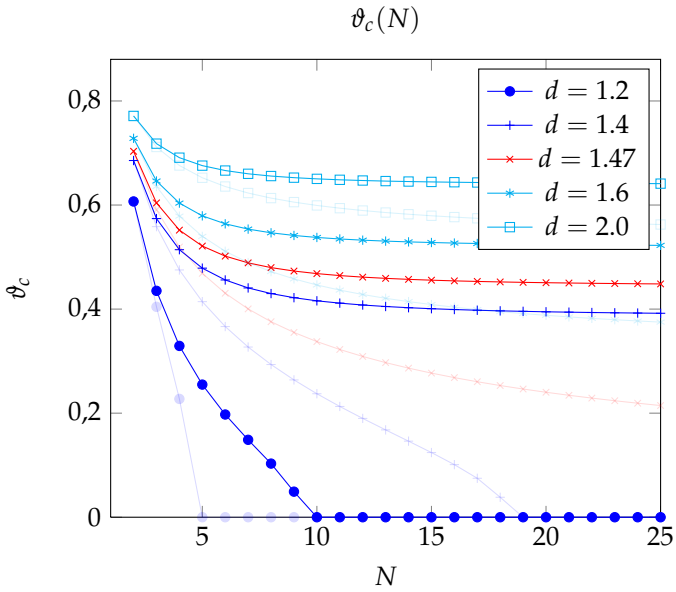

FIGURE 4.3.2. Critical tilting angle as the number of layers N increases, for some distance d fixed. Here the first neighbour approximation is compared with the exact interaction. Due to the approximate interaction, the systems behaves as the distance between the layers were major of what it is in reality. The effect is quite minor if the spacing is wide, indeed. In transparency, the exact results. The same marker correspond to the same layers spacing.

where

$$\hat{u}' = \begin{pmatrix} 0 & v_{12} & & & \\ v_{12}^\star & 0 & v_{12} & & \\ & v_{12}^\star & 0 & & \\ & & & & \\ & & & & \ddots \end{pmatrix}.$$

Hence we can diagonalise the mere off-diagonal part $\hat{u}'$; from its eigenvalues, we take only u'_{max}. Notice that with respect to the argument at the beginning of the chapter the sign has changed, namely $u_{min} = -u'_{max}$.

Imposing periodic boundary conditions, we define the lattice reciprocal space κ

$$\kappa = \frac{2\pi}{Nd} m, \qquad m \in \left]-\frac{N}{2}, \frac{N}{2}\right]$$

therefore we can also define the discrete Fourier transform for the inter-layer potential (the intra-layer potential does not need to be transformed, because it

appears uniquely in the diagonal part):

$$v_{jk}(\mathbf{q}) = \frac{1}{N} \sum_{m=-\frac{N}{2}+1}^{\frac{N}{2}} \exp\left(i\frac{2\pi m(j-k)}{N}\right) v_m(\mathbf{q}),$$

and its inverse

$$v_m(\mathbf{q}) = \sum_{j=1}^{N} \exp\left(-i\frac{2\pi m(j-k)}{N}\right) v_{jk}(\mathbf{q}).$$

The only terms that are non-zero in the sum are those for which $j-k=\pm 1$, so that explicitly:

$$v_m(\mathbf{q}) = e^{i\frac{2\pi}{N}m} v_{k-1,k}(\mathbf{q}) + e^{-i\frac{2\pi}{N}m} v_{k+1,k}(\mathbf{q}).$$

Actually, this expression is k-independent, in fact

$$v_{k+1,k}(\mathbf{q}) = v^{\star}_{k-1,k}(\mathbf{q}) = v^{\star}_{12}(\mathbf{q}) \qquad \forall k.$$

It is convenient to rewrite the potintial in the trigonometric form $v_{12}(\mathbf{q}) = \rho_\vartheta(q,\phi)\exp(i\eta_\vartheta(\phi))$, and its inclusion in the expression of $v_m(\mathbf{q})$ yields

$$v_m(\mathbf{q}) = \rho(e^{i\frac{2\pi}{N}m+i\eta} + c.c.) = 2\rho\cos\left(\frac{2\pi}{N}m+\eta\right).$$

For concreteness and simplicity, from now on we refer to the case $\phi = 0$. Thus the latter expression writes

$$v_m(\mathbf{q}) = -2\rho_\vartheta(q,0)\cos\left(\frac{2\pi}{N}m + 2\vartheta\right)$$

and it is now clear that the maximum eigenvalue we were looking for is the one for which the constrain

$$\frac{m}{N} = \frac{\vartheta}{\pi} + \frac{1}{2}$$

is valid. Clearly, in the case of a small N, it is difficult to strictly satisfy this relation, then the m closest to fulfill the constrain must be taken. Anyway, due to the periodic boundary condition, the obtained eigenvalues give a good description of the system only in the limit $L \gg d$, where $L = N-1$ is the total length of the 1D lattice. In this limit we can approximate the cosine up to a constant $\varepsilon = \mathcal{O}(N^{-2})$ by writing

$$\cos\left(\frac{2\pi}{N}m + 2\vartheta\right) = -1+\varepsilon, \qquad 0 < \varepsilon \ll 1$$

and

$$u'_{max}(q,\phi=0) = 2(1-\varepsilon)\rho_\vartheta(q,0).$$

Finally, the $(i+1)$-th component of the eigenvector relative to u'_{max} can be cast in the form

$$a_{i+1} = \frac{2\rho(1-\varepsilon)a_i - v^{\star}_{12}a_{i-1}}{v_{12}},$$

and the parameter ε vanishes in the $N\to\infty$ limit.

At this point, the boundary of the $\phi = 0$ stripe phase can be found by including u'_{max} in the susceptibility formula, and looking for the point of the set

$$\frac{1}{U} = \max_q \left\{\Pi\left(\left(1-G_{11}\right)v_{11} - u'_{max}\right)\right\}.$$

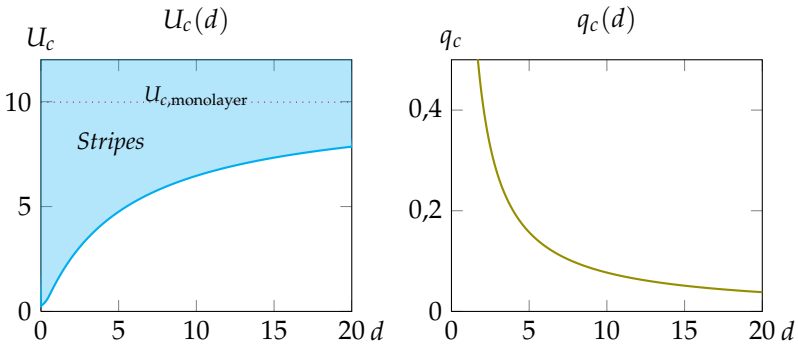

FIGURE 4.3.3. $U_c(d)$ and $q_c(d)$ at fixed $\vartheta = 0.9$, obtained from diagonalisation in the reciprocal space.

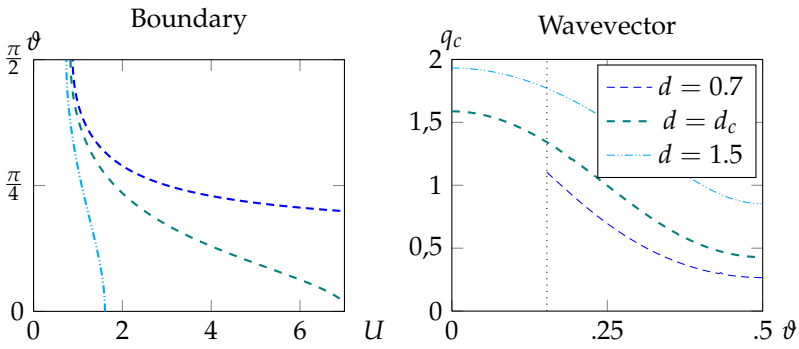

FIGURE 4.3.4. Boundaries and relative $q_c(\vartheta)$ curves for three values of d.

Results from this approximation are in good agreement with expectative, even though unfortunately this model does not predict the collapse expected for $\vartheta = \pi/2$, which in the exact model has been found, neither with numerical diagonalization nor by using the proposed method.

The application of the FNA to a $N \to \infty$ system gives the results in reported in Figures 4.3.3 - 4.3.5.

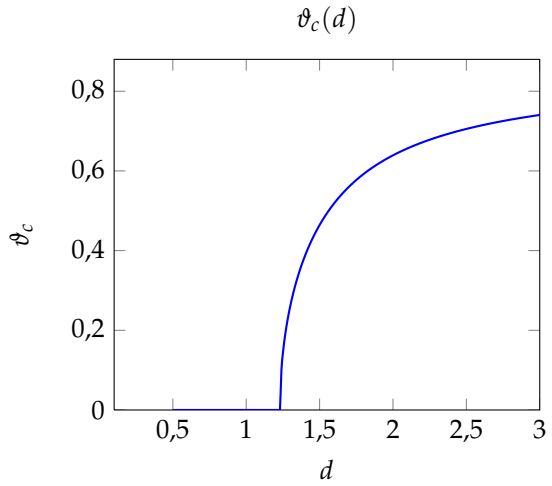

FIGURE 4.3.5. $\vartheta_c(d)$ curve, as obtained from diagonalisation in the reciprocal space. This more than other graphics confirms the validity of this diagonalisation method, as it predicts the same $d_l^{FNA} \simeq 1.23$ as from numerical diagonalisation of $\hat{\chi}_{\text{FNA}}^{-1}$.

CHAPTER 5

CONCLUSIONS

The introduction of the STLS self-consistent scheme has actually improved the description of quantum systems like dipolar Fermi gases: In fact, we have seen how the STLS scheme can reproduce both Hartree-Fock and RPA results in a unique, simple way, which furthermore refines their predictions. Its simplicity is given in the expression of the susceptibility, which results to be as simple as in the RPA and at the same time includes all the effects previously neglected. In fact, we have shown that the RPA is never a good approximation when applied to dipolar systems. Also, we have seen that the simplified 0^{th}-order STLS is similar to HF as it roughly takes into account — actually exaggerating a bit — the corrections necessary to include the exchange correlation in the system. Such a simplified scheme is a good approximation at least where the correlation hole is almost absent, namely for large tilting angles of the dipoles. In this way, simple calculations have allowed us to estimate the phase boundary between the superfluid phase and the collapsed regions in the single-layer geometry, and between the superfluid and a $\phi = 0$ density-wave phase in the bi-layer geometry: Those are exchange-driven instabilities, indeed.

We have seen that the inter-layer interaction stabilises the system preventing it to collapse, and at the same time it allows the onset of the already cited $\phi = 0$ stripe-phase. However, such a preventing action is not enough to ensure stability also for $\vartheta = \pi/2$: When the dipoles are aligned head-to-toe, in facts, the attractive nature of the dipole-dipole interaction simply overcomes correlations, and collapse is inevitable. We have shown that the eigenvectors of the susceptibility matrix let a phase shift emerge between the two layers. Such a phase shift seems to be uniquely due to classical effects, as it can be predicted by the simple model of a floating classical dipole over a planewave distribution of dipolar density.

We have focused on the wave vector q_c of the density modulation, studying, in particular, its dependence on the distance d between layers and finding $q_c \sim 1/d$. At the same time, we have observed that the $\phi = 0$ stripe phase boundary approximates, as obviously expected, the single-layer collapsed phase boundary for $d \to \infty$. On the contrary, the $\phi = 0$ stripe phase tends to enlarge its limits and occupies the whole phase diagram for sufficiently high interaction strength U, at least in the 0^{th}-order STLS scheme.

Encouraged by these results, we have applied the 0^{th}-order STLS scheme to systems composed of many layers: The cases of three and four layers has been studied extensively, highlighting in particular the existence of a critical distance d_c, slowly increasing with the number of layers N and almost constant after a sufficiently large $N \geq \bar{N}$, such that for lower values of the inter-layer separation the $\phi = 0$ stripe phase occupies the whole phase diagram. In turn, numerical calculations also suggest that over a certain limit distance d_l the $\phi = 0$ stripe phase

can never invade completely the phase diagram, neither in the limit $N \to \infty$. This limit distance is estimated in $d_l k_F \simeq 1.47$ or more.

In order to make predictions on the $N \to \infty$ case, we have attempted a first neighbour approximation, in which inter-layer interactions are considered not neglectable only between two consecutive layers. In this approximation, all quantities are expected to converge more rapidly to their eventual asymptotic value: So does the limit distance, whose value is given in $d_l^{FNA} k_F \simeq 1.23$. Hopefully one might find out the asymptotic value also for the relevant quantity $q_c(N \to \infty)$, unfortunately this approximation does not yields reliable results. In fact, we do not recover the result $q_c(\vartheta = \pi/2) = 0$, expected for each value of N because it is uniquely due to intra-layer interactions.

To do. The very next and quite obvious step to improve the multi-layers phase diagram is to apply the full STLS scheme, and then study the complete phase diagram. Then one can reconsider the FNA, and correct the wrong predictions about the wave vector, which, unphysically, never goes to zero.

Actually the complete phase diagram involves, for sufficiently large interaction strength and sufficiently small distances between layers, the possibility of a strong coupling between fermions of different layers as underlined in Ref. [24]. This coupling eventually leads to the formation of composite bosons, and their presence could describe the multi-layered system better than the fermionic behavior.

Finally (from the personal point of view of the author), perhaps it is possible to abandon the FNA and diagonalise the inverse susceptibility matrix via the Lanczos method, i.e., via the Lanczos method one can obtain, starting from the complete matrix, its equivalent tridiagonal form in an opportune basis (whose seed could be the unit vector $e^{i\eta}\hat{\mathrm{e}}_1$) and then get the eigenvalues of the tridiagonal form by diagonalising in the reciprocal space, as previously done.

Bibliography

[1] Giuliani G.F., Vignale G., *Quantum Theory of the Electron Liquid*, 2005, Cambridge University Press
[2] Orlandini E., Baldovin F., *Stochastic processes in statistical mechanics*, lecture notes
[3] Jensen J., Mackintosh A.R., *Rare earth magnetism: Structure and excitations*, 1991, Clarendon Press, Oxford
[4] Kubo R., Toda M., Hashitsume N., *Statistical Physics II*, 1985, Springer Verlag, Berling Heidelberg
[5] Fetter A., Walecka J., *Quantum theory of many-particle systems*, 2003, Dover publications, New York
[6] Atland A., Simons B., *Condensed Matter Field Theory*, 2010, Cambridge University Press
[7] Pitaevskii L., Stringari S., *Bose-Einstein Condensation*, 2003, Clarendon Press, Oxford
[8] Electron Correlations at Metallic Densities, Singwi, K. S. and Tosi, M. P. and Land, R. H. and Sjölander A., *Phys. Rev.* **176**, 589-599 (1968)
[9] Electron Correlations at Metallic Densities. IV, Singwi, K. S. and Sjölander, A. and Tosi, M. P. and Land, R. H., *Phys. Rev. B* **1**, 1044-1053 (1970)
[10] Theoretical study of a two dimensional quantum system: electrons on a helium film, de Freitas, U., Ioratti, L. C. and Studart, N., *J. Phys: Solid State Phys.* **20**, 5983-5997 (1987)
[11] Ioriatti, L. C. Jr and Ishiara A., *Z. Phys. B* **44** 1 (1981)
[12] Jonson, M., *J. Phys. C: Solid State Phys.* **9**, 3055 (1976)
[13] F. Stern, *Phys. Rev. Lett.* **18**, 546 (1967)
[14] Lian Zheng and A. H. MacDonald, *Phys. Rev. B* **49**, 5522 (1993)
[15] G. Grüner, *Rev. Mod. Phys.* **60**, 1129 (1988)
[16] C.-K. Chan, C.-J. Wu, W.-C. Lee, and S. Das Sarma, *Phys. Rev.* **A** 81, 023602 (2010)
[17] J. Zaanen, arXiv:cond-mat/9711009 (1997)
[18] Theoretical progress in many-body physics with ultracold dipolar gases, Baranov, M. A., *Phys. Rep.* **464**, 71-111 (2008)
[19] M. Marinescu and L. You, *Phys. Rev. Lett.* **81**, 4596 (1998)
[20] B. Deb and L. You, *Phys. Rev. A* **64**, 022717 (2001)
[21] The physics of dipolar bosonic quantum gases, T. Lahaye, C. Menotti, L. Santos, M. Lewenstein and T. Pfau, *Rep. Prog. Phys.* **72** 126401 (2009)
[22] Feshbach Resonances in Ultracold Gases, Cheng Chin, arXiv:0812.1496v2 (2009)
[23] Density Instabilities in a Two-Dimensional Dipolar Fermi Gas, Parish, M. M. and Marchetti, F. M., *Phys. Rev. Lett.* **108**, 145304 (2012)
[24] Density-wave phases of dipolar Fermions in a bilayer, Marchetti, F. M. and Parish, M. M., *Phys. Rev. B* **87**, 045110 (2013)
[25] Kai Sun, Congjun Wu and S. Das Sarma, *Phys. Rev. B* **82**, 075105 (2010)
[26] J. K. Block, N. T. Zinner, and G. M. Bruun, *New J. Phys.* **14**, 105006 (2012)
[27] N. Zinner and G. Bruun, *Eur. Phys. J. D* **65**, 133 (2011)
[28] J. K. Block and G. M. Bruun, arXiv:1404.5622v1 (2014)
[29] Yoshizawa, K., and Takada, Y., *J. Phys.: Condens. Matter* **21**, 064204 (2009)
[30] U. R. Fischer, Stability of quasi-two-dimensional Bose-Einstein condensates with dominant dipole-dipole interactions, *Phys. Rev. A* **73**, 031602(R) (2006)